DOKUZ EYLÜL UNIVERSITY
GRADUATE SCHOOL OF NATURAL AND APPLIED SCIENCES

DEVELOPMENT OF SPECTRUM SENSING METHODS FOR DYNAMIC SPECTRUM MANAGEMENT IN COGNITIVE RADIO

by
Timur DÜZENLİ

August, 2016
İZMİR

DEVELOPMENT OF SPECTRUM SENSING METHODS FOR DYNAMIC SPECTRUM MANAGEMENT IN COGNITIVE RADIO

A Thesis Submitted to the
Graduate School of Natural and Applied Sciences of Dokuz Eylül University
In Partial Fulfillment of the Requirements for the Degree of Doctor of Philosophy in Electrical and Electronics Engineering,
Electrical and Electronics Program

by
Timur DÜZENLİ

August, 2016
İZMİR

Ph.D. THESIS EXAMINATION RESULT FORM

We have read the thesis entitled **"DEVELOPMENT OF SPECTRUM SENSING METHODS FOR DYNAMIC SPECTRUM MANAGEMENT IN COGNITIVE RADIO"** completed by **TİMUR DÜZENLİ** under supervision of **ASSOC. PROF. DR. OLCAY AKAY** and we certify that in our opinion it is fully adequate, in scope and in quality, as a thesis for the degree of Doctor of Philosophy.

Assoc. Prof. Dr. Olcay AKAY

Supervisor

Prof. Dr. Esin FIRUZAN

Thesis Committee Member

Assoc. Prof. Dr. Damla KUNTALP

Thesis Committee Member

Prof. Dr. Aydın AKAN

Examining Committee Member

Assoc. Prof. Dr. Mustafa ALTINKAYA

Examining Committee Member

Prof. Dr. Ayşe OKUR
Director
Graduate School of Natural and Applied Sciences

ACKNOWLEDGEMENTS

I would like to express my deepest gratitude to my supervisor Assoc. Prof. Dr. Olcay Akay for his excellent guidance, endless patience, and for his contributions at every stage of this dissertation. I am grateful to him for his valuable advices that greatly contributed to my academic development.

I am thankful to Prof. Dr. Esin Firuzan and Assoc. Prof. Dr. Damla Kuntalp, my thesis committee members, who made this thesis better with their guiding suggestions and comments. I am also thankful to my former supervisor Assist. Prof. Dr. Nalan Özkurt for her encouragement and support to begin my Ph. D. education.

I would like to thank all my colleagues and friends in my department for their continuous support.

I wish to extend my appreciation to my family for their endless support and understanding. It would be very hard for me to get over the difficult times without their support and unconditional love.

Timur DÜZENLİ

DEVELOPMENT OF SPECTRUM SENSING METHODS FOR DYNAMIC SPECTRUM MANAGEMENT IN COGNITIVE RADIO

ABSTRACT

In cognitive radio (CR), traditional spectrum sensing methods usually assume that the primary user (PU) does not change its status within the sensing period. However, when the PU is assumed to be dynamic, detection performance of traditional techniques decreaeses. In this dissertation, three methods are proposed for sensing dynamic PUs and for prediction of channel status in the future sensing periods.

First of all, a novel approach based on estimation of the last status change point (LSCP) of the PU is proposed in this study. According to this scheme, the LSCP of the dynamic PU is estimated first. Then, the observed samples from the LSCP until the end of the sensing period are used in the decision process by being subjected to a cumulative sum based weighting scheme. An enhancement is achieved for traditional spectrum sensing methods in terms of probability of detection using this approach.

For detection of dynamic PUs, goodness of fit (GOF) tests are also considered in this dissertation. GOF test based spectrum sensing methods in the literature assume that the PU does not change its status during the sensing period and generally it is assumed that the PU signal is constant valued. A new GOF test based algorithm is proposed in this dissertation for dynamic PUs. According to the simulation results, the proposed algorithm outperforms other GOF test based methods in terms of probability of detection for different PU signalling schemes.

In CR, channel status prediction is as important as sensing of PU in the channel. In this dissertation, decisions taken in the past sensing periods are used to predict the status of the channel for the future sensing periods. Two different prediction algorithms are proposed and the performances of these proposed algorithms are compared against correlation based prediction techniques.

Keywords: Dynamic primary user (PU), PU traffic, spectrum sensing, last status change point (LSCP), goodness of fit (GOF) test, channel status prediction.

BİLİŞSEL RADYODA DİNAMİK SPEKTRUM YÖNETİMİ İÇİN SPEKTRUM ALGILAMA YÖNTEMLERİNİN GELİŞTİRİLMESİ

ÖZ

Bilişsel radyoda, geleneksel spektrum algılama yöntemleri genel olarak birincil kullanıcının algılama periyodu boyunca durumunu değiştirmediğini varsaymaktadır. Ancak, birincil kullanıcının dinamik olduğu varsayıldığında, geleneksel yöntemlerin algılama performansları düşmektedir. Bu tezde, dinamik birincil kullanıcıların algılanması ve kanalın gelecek periyotlardaki durumunun tahmini problemleri için üç farklı çözüm yolu önerilmektedir.

İlk olarak, bu çalışmada birincil kullanıcının son durum değişim noktasının kestirimine dayalı yeni bir yaklaşım önerilmektedir. Buna göre, önce dinamik birincil kullanıcının son değişim noktası kestirilmekte ve sonrasında, bu noktadan itibaren algılama periyodunun sonuna kadar olan gözlem örnekleri kümülatif toplama dayalı bir ağırlıklandırmaya tabi tutularak karar verme sürecine katılmaktadırlar. Bu yaklaşımla, geleneksel spektrum algılama yöntemleri için sezme performansında iyileştirme sağlanmaktadır.

Dinamik birincil kullanıcıların sezilmesi için uyum iyiliği testleri de tez kapsamında incelenmiştir. Literatürde yer alan uyum iyiliği testi tabanlı spektrum algılama yöntemleri, birincil kullanıcının algılama periyodu içerisinde durum değiştirmediğini varsaymakta ve genellikle birincil kullanıcıya ait işaretin sabit olduğu kabul edilmektedir. Bu tezde, dinamik birincil kullanıcıların sezilmesi için uyum iyiliği testi tabanlı yeni bir algoritma önerilmektedir. Simülasyon sonuçlarına göre; önerilen algoritma, farklı birincil kullanıcı işaret türleri için, diğer uyum iyiliği testi tabanlı yöntemlerden daha yüksek sezme performansı göstermektedir.

Bilişsel radyoda, kanal durum tahmini, kanaldaki birincil kullanıcının algılanması kadar önemlidir. Bu tezde, kanalın gelecek periyotlardaki durumunun tahmini için geçmiş sezme periyotlarında verilmiş olan kararlar kullanılmaktadır. İki farklı tahmin

algoritması önerilmekte ve önerilen bu algoritmaların performansı, ilinti tabanlı tahmin yöntemleriyle karşılaştırılmaktadır.

Anahtar kelimeler: Dinamik birincil kullanıcı (BK), BK trafiği, spektrum algılama, son durum değişim noktası (SDDN), uyum iyiliği (Uİ) testi, kanal durum tahmini.

CONTENTS

Page

LIST OF FIGURES

Page

LIST OF TABLES

Page

CHAPTER ONE
INTRODUCTION

Frequency spectrum is a limited resource which has existed in the nature from the beginning of time. Since the discovery of its existence, technology has greatly evolved and the number of devices that use this valuable resource has greatly increased. Today, it is possible to say that almost all electronic devices have the capability of wireless communication. However, this causes the inevitable problem of spectrum insufficiency which is also named as "spectral scarcity". Increasing number of wireless devices and growing population who use these technologies make it mandatory to use frequency spectrum more efficiently. Although several techniques have been proposed for efficient bandwidth usage (e.g. frequency division multiplexing), a much more radical solution is required to solve the problem fundamentally.

A revolutionary solution for this problem has been proposed in 1999 (Mitola & Maguire, 1999). Mitola and Maguire (1999) have introduced a new communication scheme which makes possible more efficient use of the frequency spectrum at any time and anywhere. According to the proposed scheme in Mitola & Maguire (1999), a communication system is designed such that it can adjust its parameters based on software rather than employing conventional pre-adjusted hardware equipments. The capability of changing communication parameters by using only software also allows the opportunistic use of the frequency spectrum. This new technology has been named as cognitive radio (CR) by Mitola, since it is intelligent as it can sense its environment and can rapidly change its parameters to adapt to current environmental conditions. A CR should continously sense its environment and should be able to adjust its functional operations in order to work in the most efficient way by changing its system parameters.

There are four functions of a communication system to define it as a CR. These functions are illustrated in Figure 1.1.

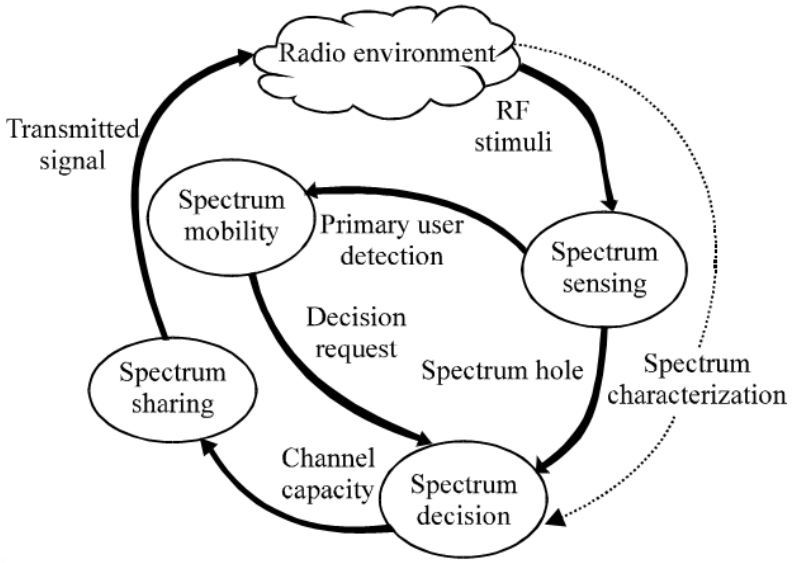

Figure 1.1 Workflow for a typical CR (Akyildiz, Lee, & Chowdhury, 2009).

In Figure 1.1, the cycle of workflow which is performed by a typical CR is shown. According to this workflow, wireless data is collected from wireless medium when the CR attempts to begin its transmission. This wireless data is analyzed by the CR to determine spectral holes, i.e. currently unused sections of the frequency spectrum. This step is named as spectrum sensing. It is a very crucial function of CR since the detection of primary (or licenced) user/users in the concerned frequency band is carried out in this step. A primary user (PU) has the licence of a particular frequency band and CR guarantees that it will leave the channel when the legal owner of the frequency band (in other words, the PU) is present in the channel. To make this possible, an accurate detection of the PU should be accomplished.

Possibility of the reappearence of the PU in the channel raises the question of how CR maintains its previously started transmission without interrupting the PU. The answer to this question is given by another function of CR which is named as spectrum mobility. As it is shown in Figure 1.1, CR performs a spectrum mobility function when a PU is detected in the current channel. Therefore, the CR system should have the capability of changing its parameters in a rapid way to carry out spectrum mobility.

The next step in the cognitive cycle is spectrum decision. At this point, CR has the knowledge of idle and busy slots in the spectrum. Using this knowledge and considering the required bandwidth, the most appropriate channel is selected for transmisson of data. At the end, CR should have a fair scheduling about the use of the spectrum since there are also other CR users in the spectrum. This is accomplished by the spectrum sharing function of the CR.

Each one of these four functions comprises broad research areas in themselves. As one of the most important functions of CR, the studies presented in this dissertation can be considered within the area of spectrum sensing.

Spectrum sensing is used in CR to obtain information about spectral opportunities which can be utilized by CR systems. As an example, Figure 1.2 shows the heavy, medium, and sparse uses of the frequency spectrum. According to Figure 1.2, it is possible to say that the content of spectral distribution is concentrated on particular frequency bands. In CRs, it is considered that the PU exists in those frequencies. The aim of secondary users (which are CRs themselves) is to detect the frequency bands where the PU does not exist.

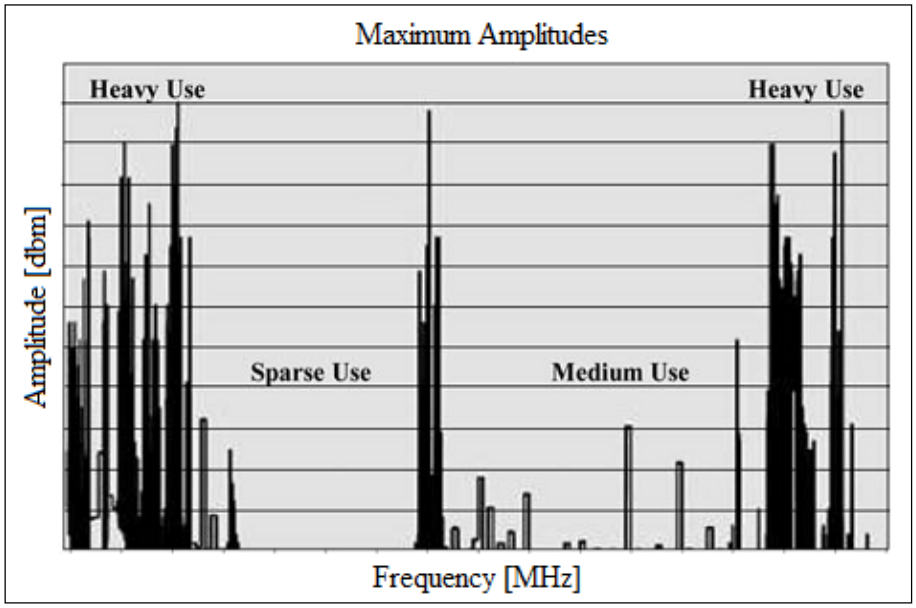

Figure 1.2 An illustration for spectrum utilization (Akyildiz, Lee, Vuran, & Mohanty, 2006).

Frequency spectrum has a dynamic structure such that the location and size of idle and busy slots may change with time. This makes periodic sensing of the spectrum mandatory since CR makes a decision for a short time and for a particular frequency band. A schematic diagram for dynamic spectrum access is given in Figure 1.3.

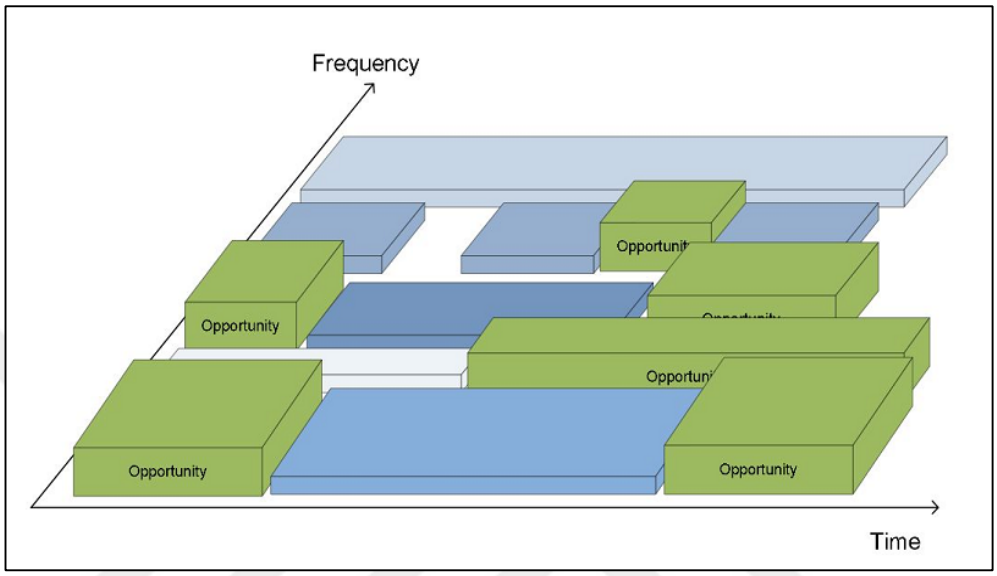

Figure 1.3 Dynamic spectrum access (Yücek & Arslan, 2009).

According to Figure 1.3, spectral utilization shows a varying characteristic according to both time and frequency. CRs aim to benefit from this varying structure to provide communication among secondary users (SUs). The green regions in Figure 1.3 show the spectral holes in the frequency spectrum and the other regions represent the presence of PUs with different power levels. In this manner, accurate sensing of the frequency spectrum should be accomplished in a short time and this should be carried out periodically since the shape of the spectrum changes dynamically as time progresses.

Various spectrum sensing techniques for detection of PUs in the channel have been recently proposed in the literature and most of them assume that the behavior of the PU is homogeneous, i.e. there is no PU status change in the channel during the sensing period. In contrast to this assumption, it is highly probable to encounter PU status changes (busy-to-idle or idle-to-busy transitions) during the sensing period

particularly when there exists high PU traffic in the channel or if a long sensing period is used to achieve better detection performance. Various forms of PU status changes in the channel are illustrated in Figure 1.4 where blue regions represent the time instances when the channel is used by the PU (or the channel is in busy status).

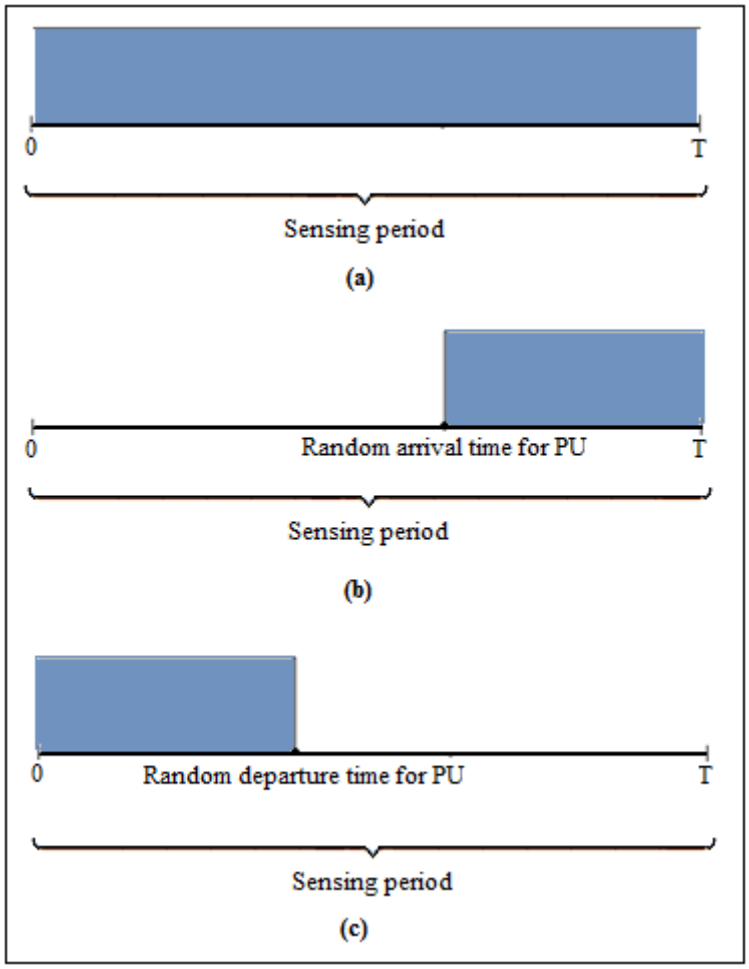

Figure 1.4 Different channel status change schemes: (a) no PU traffic (conventional assumption), (b) PU arrives at the channel, (c) PU departs from the channel.

In Figure 1.4(a), there are not any PU status changes in the channel since there is no PU traffic. However, a PU arrives at the channel within the sensing period in Figure 1.4(b) and it is expected from CR to notice this status change in the channel, or at least, it is expected from it to label the channel as busy at the end of the sensing period. Lastly in Figure 1.4(c), PU departs from the channel and CR should be able to accurately indicate that the channel is idle for the next sensing period.

Detection of dynamic PU is an important research topic for CR since the detection performances of conventional spectrum sensing techniques dramatically decrease when the PU status changes occur in the channel. Although various studies have been recently proposed on this problem, a robust sensing scheme has not yet been found. Motivated by this void in the literature, investigation and proposal of novel spectrum sensing methods and channel status prediction schemes for dynamic PUs have been aimed in this dissertation.

CHAPTER TWO
LITERATURE SURVEY AND CONTRIBUTIONS OF DISSERTATION

2.1 Literature Survey

Spectrum sensing is currently being developed for CR and several studies have been carried out on this topic. In general, it is possible to group all the studies in the literature under two titles:

- Local spectrum sensing
- Cooperative spectrum sensing

In local spectrum sensing, CRs decide individually whether the channel is in use or not based on their own observations. In this sensing scheme, it is possible to take quick decisions. On the other hand, two or more CRs may participate in the decision process in cooperative spectrum sensing allowing more reliable decisions. Cooperative spectrum sensing can be divided into two subclasses as central and distributed spectrum sensing.

In central cooperative spectrum sensing, CRs send their decisions to a fusion center (FC). The final decision is taken by this center and all CRs in the region are informed. In distributed spectrum sensing, there is not any FC; however, CRs share their sensing results with each other. After that, each CR decides individually whether the channel is in use or not based on these shared sensing results. In central cooperative sensing, CRs have to communicate with a FC, whereas in distributed sensing, each CR should be informed of other CRs' decisions. For both cases, an additional communication link is required (between CRs and FC or CRs and CRs). This can be considered as one of the disadvantages of cooperative sensing compared to local sensing.

Another issue in cooperative sensing is the sensing delay caused by additional communication requirements. A considerable time is wasted during communication between CRs and FC and CRs and CRs causing an increase in sensing duration. This delay is undesirable in CR since the system throughput and sensing duration are

inversely proportional. No matter which sensing scheme is used, a CR should have a robust and powerful sensing technique to accurately detect spectral holes in the frequency spectrum. Then, the result can be used by the CR itself (local spectrum sensing) or it can be shared with other CRs or a FC (cooperative spectrum sensing).

To achieve spectrum sensing with high accuracy, various methods have been proposed in the literature. Each of these techniques have their own pros and cons under different scenarios; e.g. different techniques show high detection performance depending on whether the PU signal waveform is known or unknown.

Energy detection is one of the most popular spectrum sensing techniques in the CR literature. First of all, it is easy to calculate the energy of a signal making the energy detector (ED) the appropriate choice for CR implementations. Also, it is the optimal detection technique when the PU signal is unknown (Urkowitz, 1967; Sahai et al., 2004). However, ED is sensitive to noise uncertainty and its performance degrades if the noise power is unknown by CR. Since only the energy of the signal is considered for analysis, CR cannot differentiate interference from noise by using an ED (Yücek & Arslan, 2009).

One of the pioneer works on ED was announced by Urkowitz (1967). In his study, Urkowitz proposed a technique to detect unknown deterministic PU signals. Mathematical derivations and closed form expressions were also presented in that work making it one of the milestones in signal detection literature. Although deterministic signals are considered in the study, Urkowitz states that the proposed detector can also be applied to random signals. Based on the simulation results, ED shows similar performance with the matched filter, the optimal technique for detection of known PU signals, under high SNR values.

After the work of Urkowitz, ED was used by several studies as a benchmark to determine the detection performance of newly proposed sensing techniques (Bhargavi & Murphy, 2010; H. Wang et al., 2009; Rostami et al., 2012; Wei & Tirkkonen, 2012; Yücek & Arslan, 2009; Zeng et al., 2008). Alternatively, various

modifications of ED have also been proposed in the CR literature (Chen, 2010; X. Chen et al., 2013; Eghbali et al., 2014; Guo et al., 2015; F. Wang et al., 2011; Xie & Hu, 2014).

Improved ED proposed in Chen (2010) can be given as a typical modification of the conventional ED. In this work, improvement of the detection performance of ED is targeted by changing the squaring operation with an arbitrary power operation. In this way, better performance results are obtained for detection of random signals in Gaussian noise. According to simulation results in Chen (2010), the power value in the proposed detector depends on the probability of false alarm, probability of detection, average signal-to-noise ratio, and the observation sample size.

Another modified ED is introduced in Eghbali, Hassani, Koohian, & Ahmadian-Attari (2014) where modification is carried out for wideband spectrum sensing. According to the introduced scheme in Eghbali et al. (2014), the frequency spectrum is divided into equal length non-overlapping sub-bands and a detection threshold for each sub-band is determined. In this way, authors find maximum aggregated opportunistic throughput of CR networks. As in Chen (2010), an optimal power value is searched for replacing squaring operation. According to the simulation results, aggregate opportunistic throughput is improved using optimal power values.

In some studies, ED is modified by weighting the signal samples before energy calculation (X. Chen et al., 2013; Guo et al., 2015; F. Wang et al., 2011; Xie & Hu, 2014). For example, a weighted sum of signal amplitude and its square are proposed as the decision statistic in Guo, Jiang, & Luo (2015). The optimal weight and power values are also determined by proposing a new parameter optimization method based on large deviation theory. The results of the study are compared against the improved ED in Chen (2010) and against conventional ED. According to simulation results, the proposed technique outperforms the other two detectors in terms of detection performance.

Optimization of system parameters (Liang et al., 2008; W. Zhang et al., 2009) and hardware implementation issues (Cabric et al., 2004; Li et al., 2012) are the other typical research topics related to ED. The studies on optimization basically aim to obtain optimal parameters to allow the system operate in the most efficient way.

To increase probability of detection, it is intuitive to increase the sensing duration. However, this will also shorten the time used for transmission of data, and therefore, the system throughput will inevitably be decreased. This problem is considered in Liang, Zeng, Peh, & Hoang (2008). In that study, the optimal sensing duration is obtained for a CR network where the ED is used in a cooperative sensing scheme. The frame structure which is attempted to be optimized in Liang et al. (2008) is shown in Figure 2.1 where τ is the duration for sensing slot and $T-\tau$ is the duration for data transmission slot. T denotes the overall frame length.

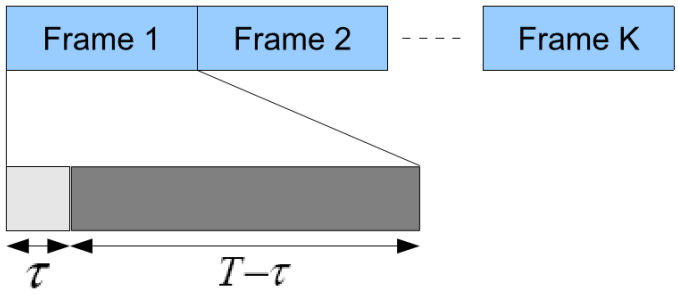

Figure 2.1 Sensing slot and transmission slot durations in one frame (Liang et al., 2008).

Optimization of cooperative sensing scheme using ED is considered for minimization of total error rate in Zhang, Mallik, & Letaief (2009). A new sensing scheme which needs fewer number of CRs in a cooperative CR network is also introduced in that work.

ED was introduced as the optimal detector when the PU signal is unknown by the CR and when the SNR value is adequately high. If the PU signal is known, matched filter is given as the optimal detector since the received SNR is maximized in this detection scheme (Cabric, Mishra, & Brodersen, 2004). According to this technique, decision about the channel is taken by analyzing the correlation between the

observed signal and the known PU signal pattern by CR. This method provides high detection performance under low SNR values. However, it requires knowledge of the PU signal and therefore it is impractical to use the matched filter in real life applications. Performance comparison of matched filter with other sensing techniques (Bhargavi & Murthy, 2010), experimental evaluation of matched filter (Eduardo & Caballero, 2015), PU detection in GSM bands (Mohamad, Wen, & Ismail, 2012) are some of the example works on matched filter.

In addition to ED and matched filter, there are various sensing techniques recently proposed in the literature. As an example, a feature analysis is made by cyclostationarity detectors to determine if the signal contains periodicity features. Cyclostationarity detectors decide whether the channel is busy or idle based on the existence of these features. They have higher detection performance than ED when there is high noise uncertainty in the channel (Satheesh, Aswini, Lekshmi, Sagar, & Kumar, 2013). Eigenvalue based spectrum sensing can be given as another technique which is based on feature detection. According to this technique, the differences in eigenvalues of the observed data are discriminative indicators of the PU in the channel (Nadler et al., 2011; Wei & Tirkkonen, 2009; Zeng & Liang, 2009).

Radio identification (RI) based sensing is also given as a feature analysis based signal detection technique. According to this sensing scheme, the observed signal samples are subjected to a feature extraction process and these extracted features are used to obtain the technology employed to generate the PU signal (Yücek & Arslan, 2009). The previously introduced techniques such as ED and cyclostationarity based methods can be used in RI based sensing. In addition, other features including channel bandwidth, instantaneous frequency, maximum duration of signal can also be used. It is possible to use different types of classifiers in the classification stage.

Generally, conventional spectrum sensing methods assume that the SUs have some knowledge about the PU. For example, the PU signal should be exactly known by a CR which use matched filter technique to fullfil its spectrum sensing task.

However, there are also blind spectrum sensing techniques which do not need any a priori knowledge (Wang, Yang, Zhao, & Zhang, 2009). Most of these techniques are based on goodness of fit (GOF) testing which is particularly used to determine if the observed data comes from a particular distribution or not. This approach can also be adapted to spectrum sensing as a hypothesis testing problem. Traditional GOF tests such as Anderson–Darling (Arshad & Moessner, 2013), Kolmogorov-Smirnov (Lei, Wang, & Shen, 2011), and Cramer-von Misses (Stephens, 1974) are the most popular GOF test based spectrum sensing techniques. However, there are also other GOF tests based on order statistics (OS) and log-likelihood ratio (LLR) in the literature (Rostami et al., 2012; Teguig et al., 2015; Zhang, 2002).

Previously discussed sensing techniques are performed in the time domain, and observed data is directly subjected to a test statistic without any transformation. On the other hand, there are also sensing techniques that are carried out in the frequency domain (Chiang et al., 2009; Gismalla & Elsusa, 2011, 2012; Haykin et al., 2009; Wang & Zhang, 2009). Periodogram based ED is one of the frequency domain based sensing methods (Gismalla & Elsusa, 2011). According to this technique, spectral density of the observed signal is obtained at first using periodogram. Then, an energy detection is performed in the frequency domain using this spectral density. It is stated by Gismalla and Elsusa (2011) that considered frequency domain based ED is superior to its conventional counterpart.

In another work performed by the same authors in Gismalla & Elsusa (2011), Bartlett spectral density estimation is used instead of periodogram for frequency domain transformation (Gismalla & Elsusa, 2012). Again, ED is used for comparison. According to simulation results, Bartlett spectral density based energy detection provides higher probability of detection compared to periodogram.

Multitaper spectral estimation (MTSE) is another frequency domain based detection scheme using multitaper method as spectral density estimator (Chiang, Lin, & Ma, 2009). As stated in Chiang et al. (2009), the decision statistic is represented as a function of frequency. There are also other studies which use MTSE to obtain

frequency domain based detectors in the literature (Haykin et al., 2009; Wang & Zhang, 2009).

The previously discussed sensing techniques have been developed using only one dimension which is either time or frequency. For example, ED, matched filter, and feature detector consider a particular frequency band to obtain whether the channel is in use or not. According to this scheme, other idle frequency bands cannot be detected and this possibly causes inefficient use of the frequency spectrum. Therefore, multidimensional spectrum sensing has become a hot research topic and the studies on techniques which use time and frequency dimensions simultaneously have drawn great interest in the literature (Guibene & Hayar, 2010; Javed & Mahmood, 2010).

Most of the proposed spectrum sensing methods in the literature assume that the channel is entirely busy or idle for the whole sensing period. However, this assumption is not realistic in today's world because there are millions of wireless device users that use the same spectrum. For example, a dynamic PU may leave the channel and another PU may arrive at the channel in the same sensing period, or alternatively, a PU may have dynamic properties which means it may be present at the beginning of the sensing period and may leave the channel within the same sensing period. Or, it may access the channel although it was absent at the beginning of the sensing period. Thus, it is important to design detectors that can make right decisions in channels containing PU status changes which is also called PU traffic. Intuitively, a performance degradation is observed in almost all spectrum sensing methods when the channel is experiencing PU traffic. To overcome this problem, several studies have been recently proposed towards detection of dynamic PUs.

Studies on PU traffic in the literature can be grouped under the following main topics:

- Studies about the effects of the PU traffic on the detection performance of conventional techniques,

- Studies proposing new sensing techniques (local or cooperative) for channels containing dynamic PUs (or PU traffic).

2.1.1 Effect of PU Traffic on the Performance of Conventional Spectrum Sensing Techniques

In the literature, one of the recently popular research topics is analysis of performance degradation of conventional spectrum sensing methods under PU traffic.

In Wang, Chen, Hines, & Zhao (2009), the effect of PU traffic on detection performance is considered using both local and cooperative sensing techniques. No new method is introduced in this study, but rather spectrum sensing performance of ED is considered for detection of dynamic PUs. PU traffic is modelled by independent and identically distributed (i.i.d.) two-state continuous time Markov process and it is assumed that the PU signal is unknown. Simulation results are given using Neyman-Pearson and Bayesian approaches and are compared against theoretical performance results. Based on these results, detection performance of ED degrades for both local and cooperative sensing schemes when dynamic PUs exist in the channel.

In another work by Chen, Wang, & Zhao (2011), detection performances of four eigenvalue based feature detectors are investigated and it is stated that each one of them shows different characteristics against the PU traffic. As in T. Wang et al. (2009), continuous time Markov process is used to model the PU traffic in this study and it is assumed that the channel is subjected to Rayleigh fading. It is stated that the PU signal waveform is generated using binary phase shift keying (BPSK) modulation scheme. Theoretical derivations are presented for all the considered techniques and, according to simulation results, the maximum eigenvalue detector shows the best detection performance among other eigenvalue based detectors. It is also stated in Chen et al. (2011) that the detection performance depends on the SNR and the length of the observed signal vector.

In some studies, it is assumed that more than one PU status change occurs in the channel. For example, effect of multiple PU status changes on detection performance of ED is discussed in Tang, Chen, Hines, & Alouini (2012) where theoretical derivations for probability of false alarm and probability of detection are verified via simulations. PU traffic is modelled using continuous time Markov process. As expected, PU traffic shows a degrading effect on spectrum sensing performance. The amount of degradation depends on the parameters given as traffic density, traffic model, number of PU status changes, and SNR (Tang et al., 2012).

In a study which compares two different sensing techniques, it is assumed that the channel to be sensed has discontinuous characteristics, i.e. PUs in the channel do not preserve their states during the sensing period (Penna & Garello, 2011). ED and an eigenvalue based detector are considered in that study as the sensing techniques and the theoretical derivations are performed based on a newly introduced parameter named as "signal occupancy rate". The sensing performance of ED and eigenvalue based detectors are considered for the case when discontinuous PUs exist in the channel. As expected, a degradation in detection performance for both detectors is observed according to simulation results.

In Wu, Huang, Wang, & Wong (2013), performance of ED is investigated for the scenario where PU arrives at and then departs from the channel only once during the sensing period. The arrival and departure times of the PU are modelled using exponential distribution and the related theoretical analysis is carried out using Bayesian approach by giving closed-form expressions for probability of false alarm and probability of detection.

It is possible to encounter newly introduced terms in some studies. For example, one of these terms is given as "undetectable primary user transmission (UPT)" introduced by Choi and Yoo (2013). Undetectable PU transmission is defined in Choi & Yoo (2013) as "the PU transmission occupying the channel only between two consecutive sensing epochs and being fully interfered by secondary user transmissions". This is illustrated in Figure 2.2.

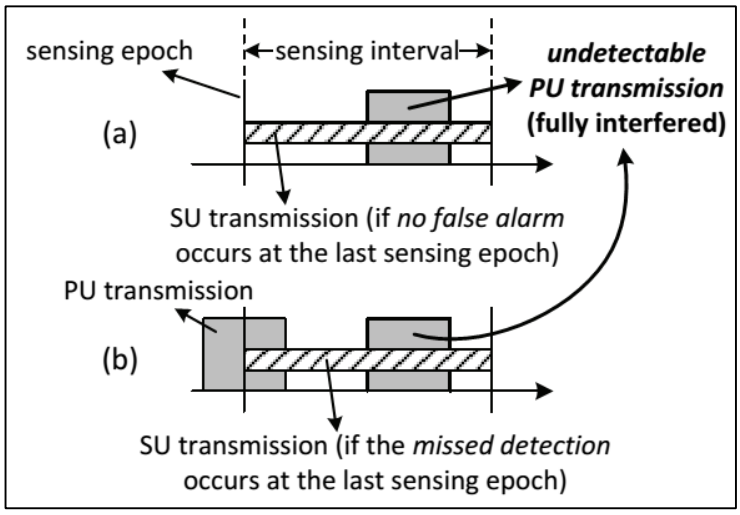

Figure 2.2 Undetectable PU transmission (Choi & Yoo, 2013).

According to Figure 2.2, CR cannot sense the PU transmissions occurring outside the sensing epoch. If the PU's transmission duration is short, this will cause full interference between CR and PU. According to Figure 2.2(a), SU (or CR) has decided in the last sensing epoch that the channel is in idle state and it has started its transmission. However, a PU transmission occurs between consecutive sensing epochs and the PU is subjected to full interference by CR during its transmission. On the other hand, in Figure 2.2(b), interference is caused by missed detection of the PU by the CR in the last sensing epoch. Considering these scenarios, probability of UPT is derived as a function of sensing period in Choi & Yoo (2013) and the theoretical derivations are verified by simulation results. It is also stated that the probability of UPT depends on the duration between consecutive sensing epochs.

2.1.2 New Spectrum Sensing Techniques for Dynamic PUs

Studies on detection of dynamic PUs in the literature can be listed under two groups as follows:

- In the first group, already existing spectrum sensing techniques in the literature are modified to obtain high detection performance under PU traffic.

- In the second group, novel techniques are proposed to overcome the detection problem of dynamic PUs.

Modification of existing techniques for detection of dynamic PUs is one of the most popular topics within the studies on PU traffic in CR literature. In these studies, generally conventional techniques such as ED, cyclostationarity detector, etc. are modified to obtain higher detection performance in channels containing PU traffic.

For efficient spectrum sensing under PU traffic, a modified version of the ED is proposed by Bealieu and Chen (2010). It is assumed in that study that the CR does not have any knowledge about the PU signal and the PU traffic is modelled via Poisson process. The modified detector is obtained by generalized likelihood ratio test (GLRT) whose theoretical derivations are also presented. According to simulation results, it is possible to say that an enhancement in detection performance is achieved compared to conventional ED although this performance increase is very limited.

In Shim, J. Lee, Y. Lee, Y. Lee, & Yoon (2013), cyclostationarity based detector is considered for detection of dynamic PUs. It is assumed that only one status change occurs in the channel during the sensing period and spectral autocoherence function (SAF) is used to derive the test statistic. BPSK modulation scheme is utilized for PU signal and the traffic in the channel is modelled using Poisson process. The detection performance of the proposed technique is compared against ED, and according to simulation results, it provides an increase in performance in terms of probability of detection.

In Zhang, Wang, & Zhang (2011), PU traffic density is estimated using maximum likelihood estimation (MLE) during the sensing period. Then, a decision is taken by CR on whether the traffic density in the channel is high or low. If the traffic is decided as low, then CR begins its transmission. In other words, decision is given indirectly by CR such that the estimated traffic parameters are used in the decision process rather than direct application of a particular test statistic to observed data.

That study aims to answer the question of whether CR should begin its transmission or should continue observing the channel by considering the traffic density in the channel.

To decrease the waiting time for accessing the channel and to increase the transmission duration of CR, use of a switching structure is proposed by Gaaloul, Yang, Radaydeh, & Aloini (2012). Theoretical and simulated performances are obtained separately for accessing single channel and accessing multi-channel schemes. Under single channel accessing scenario, a switching structure is not used since there is only one channel for transmission. For multi-channel accessing scheme, two algorithms named as "Switch-and-Examine Channel (SEC)" and "Switch-and-Stay in Channel (SSC)" are proposed. Two new criteria named as "average service time" and "average waiting time" are introduced for performance evaluation. In the ideal case, average service time is desired to be long and average waiting time to be short. Based on the results of the study, single channel access scheme has longer average service time than multi-channel access scheme under PU traffic. However, it is stated that switching based algorithms show better detection performance when average waiting time is taken into consideration.

The inter-frame sensing scheme in IEEE 802.22 standard is sensitive to PU traffic when a long sensing period is used as stated in Tran & Kong (2013). It is mentioned in Tran & Kong (2013) that there are two factors of PU traffic that affect spectrum sensing performance unfavorably. The first one of these factors is the presence of noise-only samples in the sensing period until dynamic PU arrives at the channel and the second one is existence of signal plus noise samples until the PU departs from the channel. The first factor causes degrading of probability of detection. On the other hand, the second factor makes it difficult to decide whether the channel is in idle state or not. The goal of the study in Tran & Kong (2013) is to reduce the effects of these two factors by estimating the arrival and departure instances of the PU and to improve the sensing performance of ED. After redundant samples are eliminated, energy detection is applied to the remaining samples.

Studies on other topics of PU traffic include the following subjects:

- Optimization of parameters such as sensing duration, sensing frequency, etc. in conventional detectors to achieve better performance results under PU traffic.
- Estimation of traffic density and related parameters to support the detection process.
- Channel status prediction for future sensing periods in the presence of PU traffic.

As an example work on the optimization problem in CR, it is stated in Tang, Chen, Hines, & Alouini (2011) that there is a trade-off between the length of the sensing period and transmission duration. If a long sensing period is used, then detection performance increases; however, system throughput decreases since transmission duration of CR will also decrease. On the other hand, sensing performance will be affected negatively if the length of the sensing period is reduced and transmission duration is increased. This will also cause an increase in missed detection and false alarm probabilities. In Tang et al. (2011), how sensing performance versus system throughput trade-off is affected by the PU traffic is investigated. It is stated that the traffic density and noise power are the main factors affecting the trade-off between the length of the sensing period and transmission duration.

Another study on optimization of sensing and transmission durations is given in Chang & Senadji (2012). The proposed technique is based on a multilayer optimization algorithm. According to simulations, it is observed that the interference and number of missed opportunity constraints are satisfied together.

Prediction of future states of the channels under PU traffic is as important as the optimization problem in CR. It is possible to take more reliable decisions for a particular sensing period by supporting the sensing process with previously obtained prediction results. Furthermore, it can even be considered to make a long-time

planning for spectrum usage based on these prediction results. There are several studies on the prediction issue which is also investigated in this dissertation. Below, major studies on channel status prediction in the literature will be presented.

In Höyhtya, Pollin, & Mammela (2010), traffic patterns of the channels are classified and idle times of these channels are predicted using different prediction techniques for different traffic patterns. A channel selection method is used to obtain the frequency bands with the longest OFF durations for secondary use. Deterministic, Pareto distributed, and exponentially distributed traffic models are used in that study. At the classification stage, whether the traffic is deterministic or stochastic is determined at first. Then, further analyses are carried out to determine the traffic parameters. Since each pattern has its own prediction rules, different OFF durations are obtained for different channels. At the end, the frequency band with the longest OFF duration is chosen for transmission. This process is summarized in Figure 2.3. It is mentioned by Höyhtya et al. (2010) that the number of collisions with a PU can be reduced about 60 % compared to a prediction system that does not perform any classification.

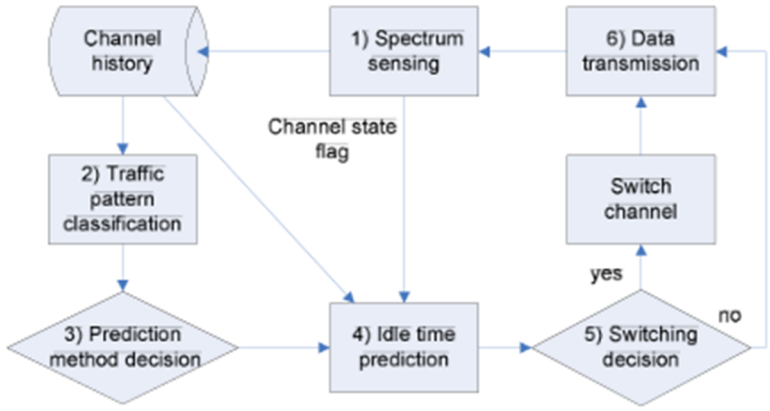

Figure 2.3 System model for predictive transmission (Höyhtya et al., 2010).

Another PU traffic pattern prediction algorithm introduced in Liu, Gabran, & Cabric (2012) utilizes estimated values of the state transition probabilities. In that study, it is assumed that ON/OFF intervals of the PU are distributed exponentially. To make traffic prediction optimal, prediction regions are defined. At the prediction

stage, state transition matrix is estimated first. Then, by comparing these estimated probabilities, a decision is taken for the next period.

In another study, binary time series is used for characterizing the spectrum usage and for spectrum prediction (Yarkan & Arslan, 2007). According to that article, frequency band of interest S with an interval of $[f_{\min}, f_{\max}]$ is determined at first. Then, CR decides its transmission bandwidth, B. As a result, a random binary matrix with size $(S/B)\times B$ is obtained. This process is illustrated in Figure 2.4. Observed frequency bands are labeled by CR as occupied or not by using a threshold. Then, decisions are taken by converting the occupancy status into binary form and CR stores this information in its memory. A regression model is used to obtain the probability of access by analyzing previous observations and the sigmoid function is considered as the transformation function for binary time series to convert the regression result into a probability of success. Based on simulation results, the proposed technique shows high prediction performance, particularly for deterministic schemes.

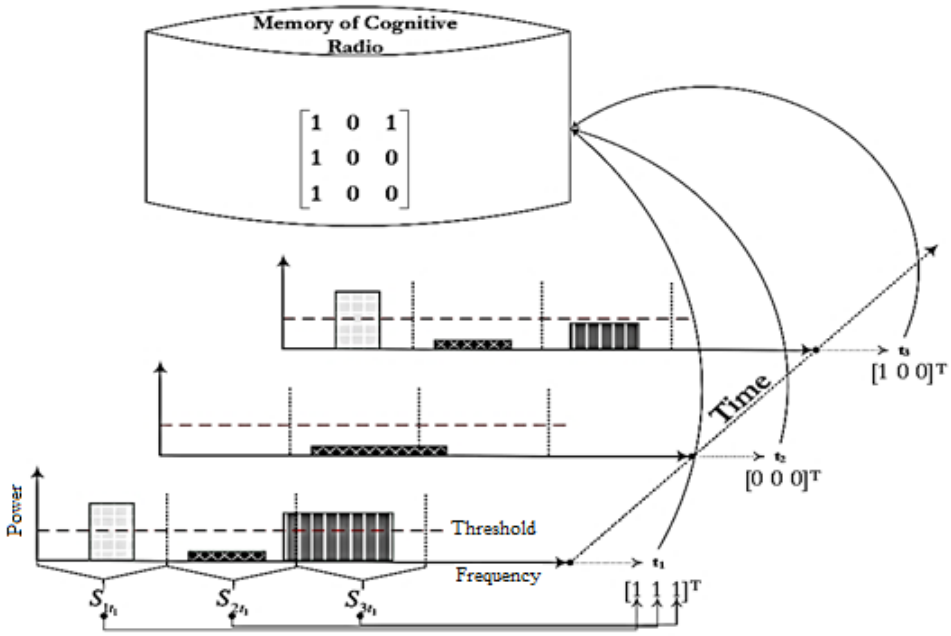

Figure 2.4 Multidimensional structure of spectrum occupation (Yarkan & Arslan, 2007).

Prediction of spectrum holes is achieved by using hidden Markov model in Black, B. Kerans, & A. Kerans (2012). In this study, the reward obtained by the system is aimed to be maximized using the proposed model. For calculation of the transition parameters, Baum-Welch algorithm is used and real world data collected from 450-470 MHz band in Australia is analyzed in the simulations.

Motivated by the assumption that spectrum occupancy is correlated across time, a new spectrum sensing method is proposed in Sadough & Ivrigh (2012). The proposed method can predict the PU activity and it can also maintain the sensing process, even if CR is in operation. Prediction is performed using variable order Markov models. In the sensing stage, blind source separation is used. In that study, multiuser kurtosis maximization algorithm is employed to measure the non-Gaussianity level of the separated signals. According to the simulation results, the proposed technique outperforms conventional spectrum sensing methods.

In a related study by Sung, Kim, & Zander (2010), it is stated that a non-Markovian source traffic model is used since exponential distribution does not properly represent the bursty structure of the wireless source. In that study, a dynamic spectrum access scheme in temporal domain is investigated for a CR which shares a frequency band with a PU during the idle period. The authors state that they propose an optimal strategy to obtain the transmission power of the CR which is based on maximization of spectrum utilization with the constraint of limited interference violations.

Different from the previously discussed studies, prediction is implemented in the presence of sensing error, CR competition, and CR transmission collision in Yao, Ngoga, & Popescu (2012). A novel parameter named “channel usage state (CUS)” is introduced in that study for representing the channel utilization observed at the CR side. The authors use LeZi-update scheme to calculate probability of occurrences under different scenarios. It is shown that CUS prediction outperforms the conventional random channel access in simulations.

Another important topic in the CR literature is to decide which model will be used to represent the PU signal. Gaussian distributed PU signaling scheme is widely used in the literature (Y. Chen et al., 2011; Chiang et al., 2009; Gismalla & Elsusa, 2011, 2012; M. Jin et al., 2012; P. Wang et al., 2010; R. Zhang et al., 2010; Wei et al., 2012; Wei & Tirkkonen, 2012), particularly when the PU signal is assumed to be unknown. On the other hand, there are also studies that use DC signaling (Beaulieu & Chen, 2010; H. Wang et al., 2009; Rostami et al., 2012) or different modulation types such as BPSK and quadrature phase shift keying (QPSK) to model the PU signal (H. Wang et al., 2010; Jin & Xu, 2011; P. Wang et al., 2010; Penna & Garello, 2011; Sharma & Wallace, 2009; Shim et al., 2013; Wang & Zhang, 2009).

If the PU traffic is in question, then it is also required to use a mathematical model to represent the PU status changes in the channel. Studies on PU traffic use various types of distributions for traffic modelling where continuous-time Markov (F. Zhang et al., 2011; Liu et al., 2012; Rao et al., 2013; Tang et al., 2011, 2012; T. Wang et al., 2009; Y. Chen et al., 2011) and Poisson (Beaulieu & Chen, 2010; Shim et al., 2013) processes are the most frequently encountered ones. However, different distributions may also be used to determine average ON and OFF durations of the channel. As an example to this, exponential distribution can be given (Beaulieu & Chen, 2010; Rao et al., 2013; Shim et al., 2013; Tang et al., 2011; T. Wang et al., 2009; Y. Chen et al., 2011; Zhao et al., 2012). In addition, different distributions such as Gamma, Log-normal, Erlang are used in the literature to model the average busy and idle durations of the channel (Tang et al., 2012; Zhao et al., 2012).

2.2 Contributions of the Dissertation

In this dissertation, it is aimed to propose new sensing and prediction schemes for CRs that operate in channels containing PU traffic. To accomplish this task, the following issues were determined as the main topics to be focused in the dissertation:

- To enhance detection performance of conventional spectrum sensing techniques by proposing a new sensing scheme.

- To propose a blind sensing technique which shows better detection performance under PU traffic compared to existing algorithms.

- To predict future states of the channel by investigating new prediction schemes.

Regarding the first topic, a change point estimation based spectrum sensing scheme that can be used together with any type of sensing technique is proposed to achieve high detection performance under PU traffic (Düzenli & Akay, 2013, 2016). In this scheme, the last status change point (LSCP) of the PU in the channel is estimated at first using MLE and dynamic programming (DP). Then, any commonly known test statistic is applied to the remaining samples between LSCP and the end of the observation period (Düzenli & Akay, 2016). To compensate for the error caused by estimation of LSCP and to increase the effect of latter samples in the sensing period, a novel cumulative sum (CuSum) based weighting scheme is also proposed. It is shown that a performance increase in probability of detection is achieved using the proposed LSCP estimation based sensing scheme for all the considered techniques.

As for the second issue, blind spectrum sensing techniques based on GOF testing have been addressed. Detection performances of various GOF tests have been considered for detection of a dynamic PU since this problem has not been addressed in the literature yet. Studies on GOF testing in the CR literature generally use DC signaling scheme and they assume that there is no PU traffic in the channel. GOF testing based methods outperform ED, which is another blind spectrum technique, particularly when the PU signal is assigned as a constant DC level. However, it is stated by N.-Thanh, K.-Xuan, & Koo (2012) that detection performance of GOF tests decreases when other signal types such as sine waveform or Gaussian distributed PU signals are used. Therefore, a novel GOF testing based algorithm is proposed to detect different PU signal waveforms under PU traffic. Considering the obtained simulation results, the proposed algorithm shows better detection performance compared to other blind spectrum sensing techniques.

Prediction of channel status for future periods is the last topic considered in this thesis. Our studies in this subject can be grouped under two titles as follows:

- Channel status prediction when the PU traffic density is constant.
- Channel status prediction when the PU traffic density changes with time.

In both of the problems given above, the previously given decisions can be used to predict the future status of the considered channel. For the constant PU traffic density, Poisson process with a constant rate parameter is used to model the traffic and a new algorithm that estimates four parameters from the previously taken decisions is used for channel status prediction (Düzenli & Akay, 2014). The obtained results are compared against correlation based prediction techniques.

For the case when the PU traffic density changes with time, the rate parameter is assigned as a time-varying stochastic function which corresponds to the so-called Cox process or doubly stochastic Poisson process. We propose a novel prediction algorithm for this traffic model based on transition probabilities among the previously taken decisions (Düzenli & Akay, 2015). As in constant PU traffic density, the results of the simulations are compared against correlation based prediction techniques.

2.3 Outline of the Dissertation

The organization of this dissertation is given as follows:

In Chapter 3, detection of dynamic PUs is considered based on change point estimation. First, a theoretical background for model change detection is presented, and then, CuSum based weighting scheme is introduced. This weighting scheme is applied to sample mean detector and ED along with the LSCP estimation approach. Related theoretical derivations and simulation results are also provided in this chapter.

Chapter 4 mainly focuses on detection of dynamic PUs using blind spectrum sensing techniques particularly based on GOF tests. A novel sensing algorithm based on OS is proposed in that chapter and detection performance of the developed algorithm is compared against various previously proposed GOF tests assuming that different signaling schemes are used for the PU.

In Chapter 5, channel status prediction issue in CR is considered for channels suffering from PU traffic. In the first part of the chapter, PU traffic is modelled using constant valued density parameters. In the second part, it is assumed that traffic density parameters are varying stochastically with time. Two new prediction algorithms are proposed in that chapter and their prediction accuracies are compared against various previously proposed prediction techniques in terms of two performance metrics.

Finally, in Chapter 6, conclusions and suggestions for future works are presented.

CHAPTER THREE
CHANGE POINT ESTIMATION BASED SPECTRUM SENSING FOR DETECTION OF DYNAMIC PRIMARY USERS IN COGNITIVE RADIO

In this chapter, a CuSum based weighting scheme and change point estimation based detector design are considered for detection of dynamic PUs. It is assumed that multiple status changes of the PU may occur in the channel within the sensing period and according to the proposed scheme, the LSCP of the PU is estimated first. Then, a CuSum based weighted detector is applied to the remaining samples between LSCP and the last sample of the sensing period. The benefit of using this weighting scheme is twofold such that the effect of the latter samples in the sensing period are increased on the final decision by multiplying them with higher coefficients and the effect of the error caused by inaccurate estimation of the LSCP can be lessened.

In the first section of the chapter, a brief discussion about the theory of model change detection is presented to constitute a theoretical background for the proposed sensing scheme. This review section discusses DC level change detection problem for the following scenarios:

- All parameters are known
- DC levels before and after change are unknown
- Change time(s) is/are unknown
- All parameters are unknown

In addition to these scenarios, detection of multiple changes - a more challenging case- is also reviewed. DP approach is considered in this first section as well.

In the second section of the chapter, change point estimation based spectrum sensing strategy is introduced. In this section, it is shown that model change detection problem can be associated with spectrum sensing. A CuSum based weighted sample mean detector and its theoretical performance are presented in this

section. By simulating together with different sensing techniques, the advantage of using LSCP approach is demonstrated.

In the last section of this chapter, the proposed CuSum based weighting scheme is applied to ED and related theoretical derivations are presented. Model change detection introduced in Section 3.1 is considered this time for the variance change detection problem and the DP approach is also reformulated. Via simulation results, it is shown that a noticeable performance enhancement can be obtained for ED using the proposed sensing scheme.

3.1 Model Change Detection

In CR, it is important to achieve high PU detection performance to prevent interference. As mentioned in the previous chapters, there are several methods proposed for cases where PU does not change its status during the sensing period. However, this is an unrealistic scenario since PUs may show different behaviours such as they may arrive at or leave the channel. For these situations, robust detectors should be designed to prevent interference of SUs with the PU.

An important step to achieve this aim is obtaining the point where the PU changes its status. If this point can be obtained accurately, then the remaining samples may be used for detection. Also, determination of change points can make estimation of PU traffic density possible.

In the following sections, the theory of model change detection will be reviewed under various scenarios. The techniques presented in this section will be used to propose a new sensing scheme for channels containing PU traffic.

3.1.1 Mathematical Model

Without loss of generality, the techniques to be considered in this section can be introduced simply for the case of one PU status change and can be generalized into

multiple status changes. Accordingly, the following system model will be utilized under various scenarios to discuss the main test statistics used in the theory of model change detection (Kay, 1998)

$$H_0 : x[n] = A_0 + w[n] \qquad ;\ n = 0,1,2,\ldots,N-1$$

$$H_1 : x[n] = \begin{cases} A_0 + w[n] & ;\ n = 0,1,2,\ldots,n_0\text{-}1 \\ A_0 + \Delta A + w[n] & ;\ n = n_0, n_0+1,\ldots,N\text{-}1 \end{cases} \tag{3.1}$$

where $x[n]$ is the observed data samples and $w[n]$ is white Gaussian noise (WGN) with variance σ^2, A_0 is the initial DC level, and ΔA is the amount of jump $(\Delta A > 0)$.

The model given in Equation (3.1) is illustrated in Figure 3.1 where the signal in WGN has a mean value of 1 at first, but at the 50th sample, the mean value changes to 4.

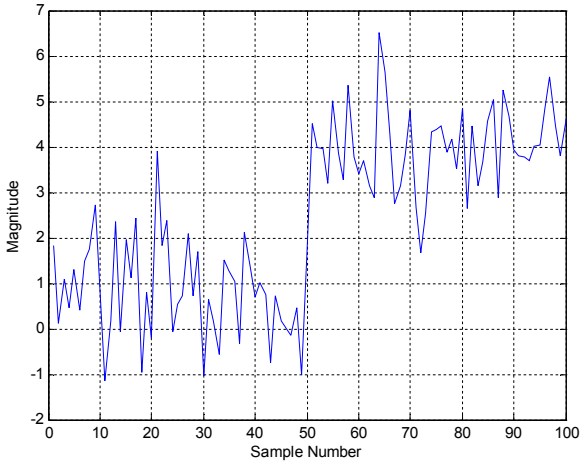

Figure 3.1 Mean change at the 50th sample.

Considering the signal shown in Figure 3.1, the aim in this chapter is to be able to say "PU has changed its state at the 50th sample" and to use the remaining samples for analysis in the proposed sensing scheme.

Scenarios to be analyzed in the following sections are given as follows:

- Known change time, known DC levels,
- Known change time, unknown DC levels,
- Unknown change time, known DC levels,
- Unknown change time, unknown DC levels (all parameters are unknown).

Now, the easiest case where all the parameters are known will be considered.

3.1.2 Known DC Level Jump at Known Time

It is desired to design a detector with high probability of detection and low probability of false alarm. As stated by Kay (1998), Neyman-Pearson (NP) approach is the appropriate framework in deciding which hypothesis is true in Equation (3.1).

At this step, since all the parameters (variance of noise σ^2, initial DC level A_0, and amount of jump $\Delta A > 0$) are known, the solution is relatively easy. Now, let's say that $A_1 = A_0$ and $A_2 = A_0 + \Delta A$. We have the parameter test which is given as

$$\begin{aligned} H_0 &: A = A_1 \quad ; \; n = 0,1,\ldots,N-1 \\ H_1 &: A = \begin{cases} A_1 \; ; \; n = 0,1,2,\ldots,n_0 - 1 \\ A_2 \; ; \; n = n_0, n_0+1,\ldots,N-1 \end{cases} \end{aligned} \tag{3.2}$$

where n_0 is the change point. When all the parameters are known, the test statistic is given as (Kay, 1998)

$$T(\boldsymbol{x}) = \frac{1}{N - n_0} \sum_{n=n_0}^{N-1} \left(x[n] - A_0 \right) > \gamma \tag{3.3}$$

where γ denotes the threshold. According to Equation (3.3), the test statistic $T(\boldsymbol{x})$ computes the average deviation of data from A_0, only over the assumed jump interval since the noise samples are independent so that knowledge of data before the jump is irrelevant.

3.1.3 Unknown DC Levels and Known Jump Time

In the case when n_0 is known but the DC levels before the jump, A_1, and after the jump, A_2, are unknown, the hypothesis testing problem becomes

$$\begin{aligned} H_0 &: A_1 = A_2 \\ H_1 &: A_1 \neq A_2 \end{aligned} \tag{3.4}$$

Since we do not know the DC levels A_1 and A_2, it is possible to use the GLRT to obtain the test statistic as

$$L_G(\boldsymbol{x}) = \frac{p\left(\boldsymbol{x}; A_1 = \hat{A}_1, A_2 = \hat{A}_2\right)}{p\left(\boldsymbol{x}; A_1 = \hat{A}, A_2 = \hat{A}\right)} \tag{3.5}$$

where $\hat{A}$ is the MLE of the DC level under H_0 and $\hat{A}_1$ and $\hat{A}_2$ are the MLEs of the DC level before and after the jump, respectively. The result of the GLRT for Equation (3.5) is given as

$$2\ln L_G(\boldsymbol{x}) = \frac{\left(\hat{A}_1 - \hat{A}_2\right)^2}{\sigma^2\left(\frac{1}{n_0} + \frac{1}{N - n_0}\right)} \tag{3.6}$$

where

$$\hat{A} = \frac{1}{N}\sum_{n=0}^{N-1} x[n], \tag{3.7}$$

$$\hat{A}_1 = \frac{1}{n_0}\sum_{n=0}^{n_0-1} x[n], \tag{3.8}$$

$$\hat{A}_2 = \frac{1}{N-n_0}\sum_{n=n_0}^{N-1} x[n]. \tag{3.9}$$

3.1.4 Known DC Levels and Unknown Jump Time

Another case where unknown parameters exist corresponds to known DC levels and unknown jump time. The GLRT is now given as (Kay, 1998)

$$L_G(\boldsymbol{x}) = \frac{p(\boldsymbol{x}; \hat{n}_0, H_1)}{p(\boldsymbol{x}; H_0)} > \gamma \tag{3.10}$$

where $\hat{n}_0$ is the MLE of the unknown jump time under H_1. Equivalently, we have

$$\ln L_G(\boldsymbol{x}) = \frac{\Delta A}{\sigma^2} \max_{n_0} \left(\sum_{n=n_0}^{N-1} x[n] - A_0 - \frac{\Delta A}{2} \right). \tag{3.11}$$

Hence, we decide H_1 if

$$T(\boldsymbol{x}) = \max_{n_0} \left(\sum_{n=n_0}^{N-1} x[n] - A_0 - \frac{\Delta A}{2} \right) > \gamma \ . \tag{3.12}$$

3.1.5 Unknown DC Levels and Unknown Jump Time

The most extreme case is the one where all the parameters are unknown. For this case, MLEs of DC levels before and after the jump are used. The test statistic is given as (Kay, 1998)

$$T(\boldsymbol{x}) = \max_{n_0} \left(\frac{\left(\hat{A}_1 - \hat{A}_2\right)}{\sigma^2 \left(\frac{1}{n_0} + \frac{1}{N - n_0} \right)} \right) \tag{3.13}$$

where

$$\hat{A}_1 = \frac{1}{n_0} \sum_{n=0}^{n_0 - 1} x[n] \tag{3.14}$$

and

$$\hat{A}_2 = \frac{1}{N - n_0} \sum_{n=n_0}^{N-1} x[n] \tag{3.15}$$

3.1.6 Multiple Change Times

Under high PU traffic, the probability of occurence of multiple status changes increases, particularly when a long sensing period is used (Wang, Chen, Hines, & Zhao, 2009). In this section, multiple status changes with unknown DC levels and unknown change times corresponding to a more challenging problem will be considered. As an example, assume that the observed data contains three status changes and that the location of these changes, $\boldsymbol{n} = \begin{bmatrix} n_0 & n_1 & n_2 \end{bmatrix}^T$, are unknown. Moreover, it is assumed that the DC levels before and after these change points, $\boldsymbol{A} = \begin{bmatrix} A_0 & A_1 & A_2 & A_3 \end{bmatrix}^T$, are also unknown. Then, probability density function (PDF) of the observed data samples is given as (Kay, 1998)

$$p\left(\boldsymbol{x};\boldsymbol{A},\boldsymbol{n}\right)=\frac{1}{\left(2\pi\sigma^{2}\right)^{\frac{N}{2}}}e^{-\frac{1}{2\sigma^{2}}\sum_{n=0}^{n_0-1}\left(x[n]-A_0\right)^2}\cdots e^{-\frac{1}{2\sigma^{2}}\sum_{n=n_{k-1}}^{N-1}\left(x[n]-A_k\right)^2} \tag{3.16}$$

where the number of status changes is $k=3$. It is assumed that the PU uses a DC signal and the channel contains zero-mean WGN with variance σ^2.

The joint MLE of $\boldsymbol{A}=\begin{bmatrix}A_0 & A_1 & A_2 & A_3\end{bmatrix}^T$ and $\boldsymbol{n}=\begin{bmatrix}n_0 & n_1 & n_2\end{bmatrix}^T$ is found by minimizing the cost function $J\left(\boldsymbol{A},\boldsymbol{n}\right)$ which is given as

$$J\left(\boldsymbol{A},\boldsymbol{n}\right)=\sum_{n=0}^{n_0-1}\left(x[n]-A_0\right)^2+\sum_{n=n_0}^{n_1-1}\left(x[n]-A_1\right)^2\cdots+\sum_{n=n_{k-1}}^{N-1}\left(x[n]-A_k\right)^2. \tag{3.17}$$

DP can be used for computing the values of the change times n_0, n_1, and n_2 by minimizing the cost function $J\left(\boldsymbol{A},\boldsymbol{n}\right)$ (Kay, 1998). The A_i values that minimize $J\left(\boldsymbol{A},\boldsymbol{n}\right)$ are actually the MLEs of these parameters which are given as

$$\hat{A}_i=\frac{1}{n_i-n_{i-1}}\sum_{n=n_{i-1}}^{n_i-1}x[n],\qquad i=0,1,\ldots,k \tag{3.18}$$

where $n_{-1}=0$ and $n_k=N$.

Defining the additional term Δ_i as

$$\Delta_i\left[n_{i-1},n_i-1\right]=\sum_{n=n_{i-1}}^{n_i-1}\left(x[n]-\hat{A}_i\right)^2,\qquad i=0,1,\ldots,k \tag{3.19}$$

the function $J\left(\hat{\boldsymbol{A}},\boldsymbol{n}\right)$ can be rewritten as follows

$$J\left(\hat{\boldsymbol{A}},\boldsymbol{n}\right)=\sum_{i=0}^{k}\Delta_i\left[n_{i-1},n_i-1\right]. \tag{3.20}$$

The next step is to minimize the cost function $J\left(\hat{\boldsymbol{A}},\boldsymbol{n}\right)$ over $\boldsymbol{n}$. For this aim, we define a new vector that depends on Δ_i as

$$I_k\left[L\right]=\min_{n_0,n_1,\ldots n_{k-1}}\sum_{i=0}^{k}\Delta_i\left[n_{i-1},n_i-1\right],\quad 0<n_0<n_1<\ldots<n_{k-1}<L+1 \tag{3.21}$$

assigning $L=N-1$ as the length of the data samples which are subjected to minimization.

Based on Equations (3.19) and (3.20), the term $I_k\left[L\right]$ can be rewritten as (Kay, 1998)

$$I_k\left[L\right]=\min_{n_{k-1}}\left[\left(\min_{n_0,n_1,\ldots n_{k-2}}\sum_{i=0}^{k-1}\Delta_i\left[n_{i-1},n_i-1\right]\right)+\Delta_k\left[n_{k-1},n_k-1\right]\right]$$

$$=\min_{n_{k\text{-}1}}\left(I_{k\text{-}1}\left[n_{k\text{-}1}\text{-}1\right]+\Delta_k\left[n_{k\text{-}1},L\right]\right) \tag{3.22}$$

Equation (3.22) states that the minimum error in a channel containing $L+1$ data samples with k status changes is equal to the summation of the errors related to first k intervals and the resulting error in the last interval (Kay, 1998). Actually, a sequential scheme is considered via DP to estimate the change points in the observed data. According to this procedure, DP estimates the status change points sequentially and after obtaining each change point, the size of the analysis interval is updated and reduced.

3.2 Change Point Estimation Based Spectrum Sensing

The DP approach mentioned in the previous section assumes that the number of changes occurring in the channel is known a priori. However, this is not a realistic assumption for CRs. To make this method more appropriate for spectrum sensing and to reduce the computational load of the algorithm, a different approach has been proposed by Düzenli & Akay (2016). According to this strategy, the LSCP of the PU is estimated instead of estimating all change points in the channel. In that case, there is no need to know the number of status changes a priori since always only the last status change point of the PU is desired. In addition, computational cost is also reduced since only one change point is searched for. After the LSCP is estimated, the remaining samples between this point and the last observed sample are used to determine which hypothesis is true. The proposed sensing scheme is schematically illustrated in Figure 3.2. It is clearly seen in Figure 3.2 that the proposed scheme can also be used for channels that contain high PU traffic.

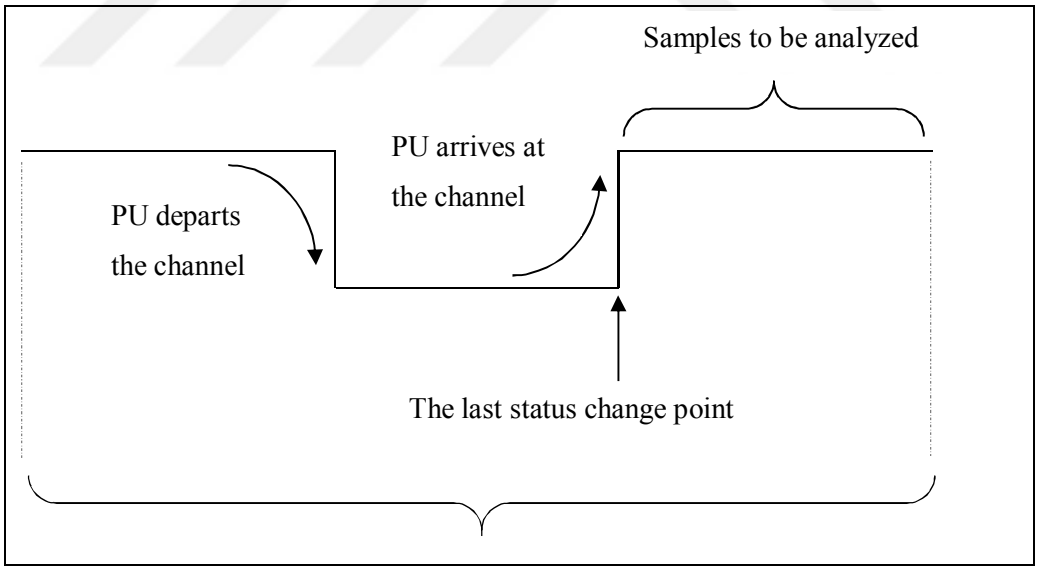

Figure 3.2 Proposed sensing scheme.

The next step after the estimation of the LSCP is to apply a decision function or test statistic to the remaining samples between the LSCP and the last observed data sample. Actually, any type of spectrum sensing technique can be used; however, a CuSum based weighting scheme is embedded to conventional sensing techniques as

a novel approach in this dissertation. The motivation of using such a weighting scheme is based on the following two reasons:

i. The status of the PU in the next sensing period is highly correlated with its last status in the current sensing period (Senadji & Chang, 2013). Therefore, it is intuitive to increase the effect of the latter samples in the sensing period.

ii. The LSCP can be estimated inaccurately for low SNR values. In that case, some undesired observed samples (noise-only samples under H_1 and signal+noise samples under H_0) may adversely affect the detection performance. This problem is illustrated in Figure 3.3.

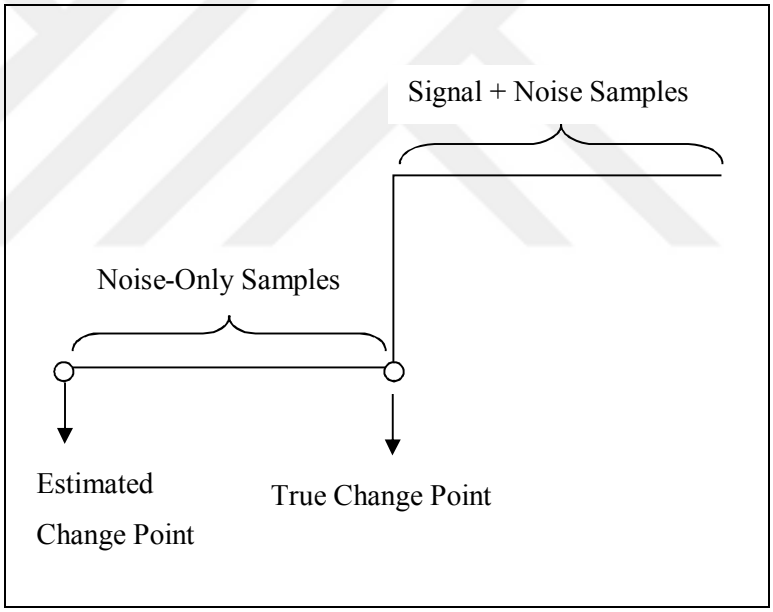

Figure 3.3 Effect of inaccurate change point estimation.

We are motivated by the thinking that more heavily weighting the samples at the end of the sensing period compensates for the performance degradation due to inaccurate estimation of the LSCP of the PU as illustrated in Figure 3.4.

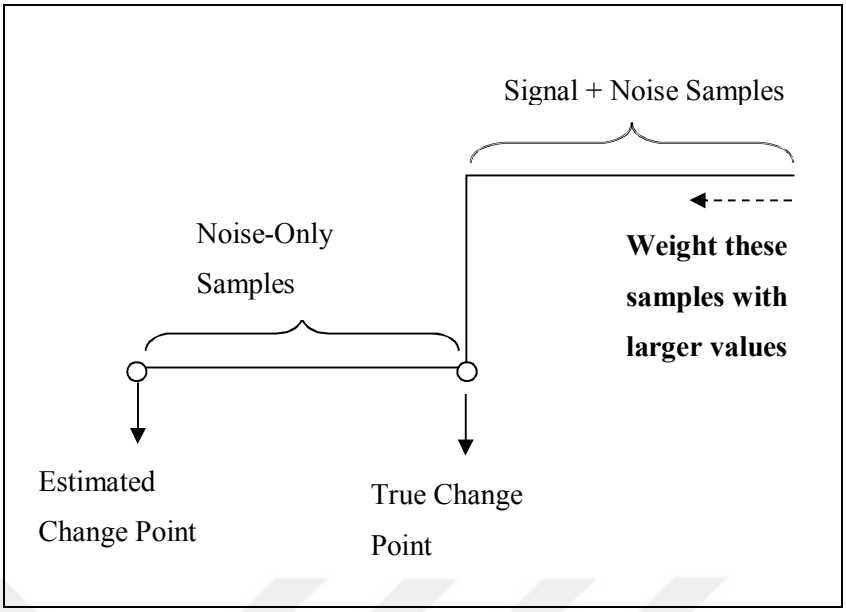

Figure 3.4 Weighting of latter samples in the sensing period more heavily to compensate for the change point estimation error.

3.2.1 CuSum based Weighted Sample Mean Detector

The CuSum based weighting scheme used in our analysis can be given as

$$T(\boldsymbol{x}) = \frac{1}{N}\left(\sum_{n=1}^{N} \sum_{i=1}^{n} T'\left(x\left(N - i + 1 \right) \right) \right) \tag{3.23}$$

where $\boldsymbol{x}$ is the observed signal vector and N is the length of the observed data samples. $T'(\cdot)$ corresponds to an identity operator for sample mean detector here, since the PU signal is assumed to be DC valued and the sample mean detector is the optimal method for detection of DC signals. However, this optimality is valid when there is no PU traffic in the channel. Here, we aim to enhance detection performance under PU traffic by weighting the latter samples in the sensing period more heavily. After this weighting scheme is applied to the sample mean detector, the test statistic given in Equation (3.23) takes the following form

$$T(\boldsymbol{x}) = \frac{1}{N}\left(\sum_{n=1}^{N} \sum_{i=1}^{n} x(N - i + 1) \right). \tag{3.24}$$

Performance of the proposed method has been examined by using Monte Carlo simulations and comparison against previously proposed methods have been carried out via receiver operating characteristics (ROC) curves. In addition, a theoretical performance analysis is also performed. Before discussing the simulation results, the theoretical performance analysis of the proposed test statistic is presented.

At first, the test statistic given in Equation (3.24) can equivalently be rewritten as

$$T(\boldsymbol{x}) = \frac{1}{N} \sum_{n=1}^{N} (N - n + 1) x[N - n + 1]. \tag{3.25}$$

For a theoretical derivation, it is required to obtain PDFs of the test statistic under hypotheses H_0 and H_1. It is clear via central limit theorem (CLT), that the PDFs of the test statistic given in Equation (3.25) under H_0 and H_1 are both Gaussian. Accordingly, mean and variances of these PDFs should be calculated.

Under H_0, $x[n] = w[n]$ for $n = 1, \ldots, N$. Then,

$$\mathrm{E}\left\{ \frac{1}{N} \sum_{n=1}^{N} (N - n + 1) x[N - n + 1] \right\} = \mathrm{E}\left\{ \frac{1}{N} \sum_{n=1}^{N} N w[N - n + 1] \right\} - \mathrm{E}\left\{ \frac{1}{N} \sum_{n=1}^{N} n w[N - n + 1] \right\}$$
$$+ \mathrm{E}\left\{ \frac{1}{N} \sum_{n=1}^{N} w[N - n + 1] \right\} = 0 \tag{3.26}$$

$$\operatorname{var}\left\{\frac{1}{N}\sum_{n=1}^{N}(N-n+1)x[N-n+1]\right\}$$

$$\begin{aligned}
&= \operatorname{var}\left\{\frac{1}{N}\sum_{n=1}^{N}Nw[N-n+1]\right\} + \operatorname{var}\left\{\frac{1}{N}\sum_{n=1}^{N}nw[N-n+1]\right\} + \operatorname{var}\left\{\frac{1}{N}\sum_{n=1}^{N}w[N-n+1]\right\} \\
&\quad -2\operatorname{cov}\left\{\frac{1}{N}\sum_{n=1}^{N}Nw[N-n+1],\frac{1}{N}\sum_{n=1}^{N}nw[N-n+1]\right\} \\
&\quad -2\operatorname{cov}\left\{\frac{1}{N}\sum_{n=1}^{N}nw[N-n+1],\frac{1}{N}\sum_{n=1}^{N}w[N-n+1]\right\} \\
&\quad +2\operatorname{cov}\left\{\frac{1}{N}\sum_{n=1}^{N}Nw[N-n+1],\frac{1}{N}\sum_{n=1}^{N}w[N-n+1]\right\}
\end{aligned}$$

$$= \frac{\sigma^2(N+1)(2N+1)}{6N}. \tag{3.27}$$

A similar derivation can also be performed for hypothesis H_1. However, in this case, $x[n] = s[n] + w[n]$ for $n = 1,\ldots,N$.

The mean of $T(\boldsymbol{x})$ under H_1 is given as

$$\mathrm{E}\left\{\frac{1}{N}\sum_{n=1}^{N}(N-n+1)x[N-n+1]\right\}$$

$$=\mathrm{E}\left\{\frac{1}{N}\sum_{n=1}^{N}N\big(A+w[N-n+1]\big)\right\}-\mathrm{E}\left\{\frac{1}{N}\sum_{n=1}^{N}n\big(A+w[N-n+1]\big)\right\}+\mathrm{E}\left\{\frac{1}{N}\sum_{n=1}^{N}\big(A+w[N-n+1]\big)\right\}$$

$$= NA - \frac{(N+1)A}{2} + A = \frac{(N+1)A}{2} \tag{3.28}$$

and the variance of the test statistic under H_1 is

$$\operatorname{var}\left\{\frac{1}{N}\sum_{n=1}^{N}(N-n+1)x[N-n+1]\right\}$$

$$
\begin{aligned}
&= \operatorname{var}\left\{\frac{1}{N}\sum_{n=1}^{N} N\left(A + w[N-n+1]\right)\right\} \\
&+ \operatorname{var}\left\{\frac{1}{N}\sum_{n=1}^{N} n\left(A + w[N-n+1]\right)\right\} + \operatorname{var}\left\{\frac{1}{N}\sum_{n=1}^{N}\left(A + w[N-n+1]\right)\right\} \\
&-2\operatorname{cov}\left\{\frac{1}{N}\sum_{n=1}^{N} N\left(A + w[N-n+1]\right), \frac{1}{N}\sum_{n=1}^{N} n\left(A + w[N-n+1]\right)\right\} \\
&-2\operatorname{cov}\left\{\frac{1}{N}\sum_{n=1}^{N} n\left(A + w[N-n+1]\right), \frac{1}{N}\sum_{n=1}^{N}\left(A + w[N-n+1]\right)\right\} \\
&+2\operatorname{cov}\left\{\frac{1}{N}\sum_{n=1}^{N} N\left(A + w[N-n+1]\right), \frac{1}{N}\sum_{n=1}^{N}\left(A + w[N-n+1]\right)\right\}
\end{aligned}
\tag{3.29}
$$

According to Equation (3.29), the same variance value as for hypothesis H_0 is obtained. Thus, the PDF of the test statistic is given as

$$
T(\boldsymbol{x}) = \frac{1}{N}\sum_{n=1}^{N}(N-n+1)x[N-n+1] \sim \begin{cases} \mathcal{N}\left(0, \dfrac{\sigma^2(N+1)(2N+1)}{6N}\right) & \text{under} \quad H_0 \\ \mathcal{N}\left(\dfrac{(N+1)A}{2}, \dfrac{\sigma^2(N+1)(2N+1)}{6N}\right) & \text{under} \quad H_1 \end{cases}
\tag{3.30}
$$

According to Equation (3.30), probability of detection, P_D, can be written as

$$
P_D = \Pr\left[T(x) > \gamma; H_1\right] = Q\left(Q^{-1}(P_{FA}) - \frac{\dfrac{(N+1)A}{2}}{\sqrt{\dfrac{\sigma^2(N+1)(2N+1)}{6N}}}\right)
\tag{3.31}
$$

where P_{FA} is the probability of false alarm, $P_{FA} = \Pr\left[T(x) > \gamma; H_0\right]$, and Q and Q^{-1} denote the right tail probability and inverse right tail probability functions of the standard Gaussian distribution, respectively.

A comparison between theoretical performance and simulation results are shown in Figures 3.5 through 3.7 in dB scale. As can be seen from the figures, theoretical derivation of P_D versus P_{FA} provides an exact representation for the performance of the proposed test statistic. Also, the results are consistent even SNR level and observation size of data change.

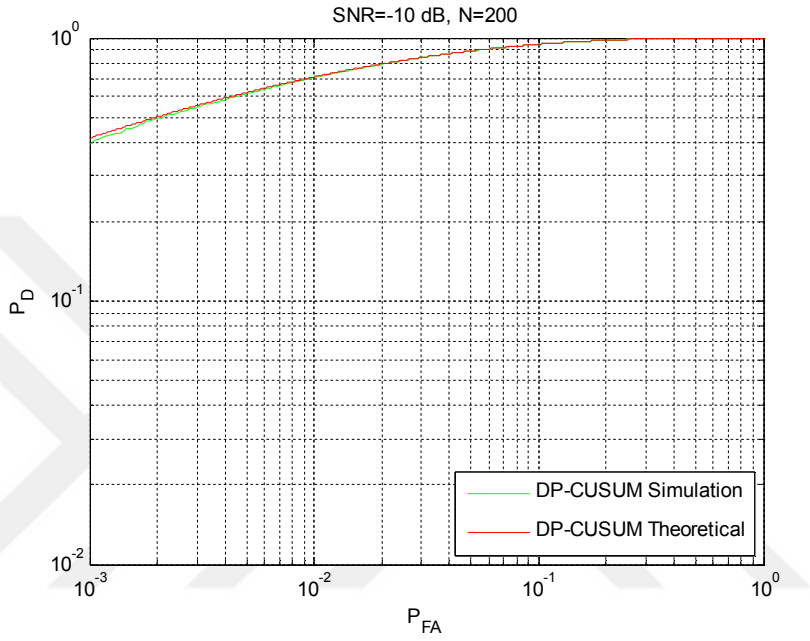

Figure 3.5 Theoretical and experimental performance comparison for the proposed method for $N = 200$ and $\mathrm{SNR} = -10$ dB.

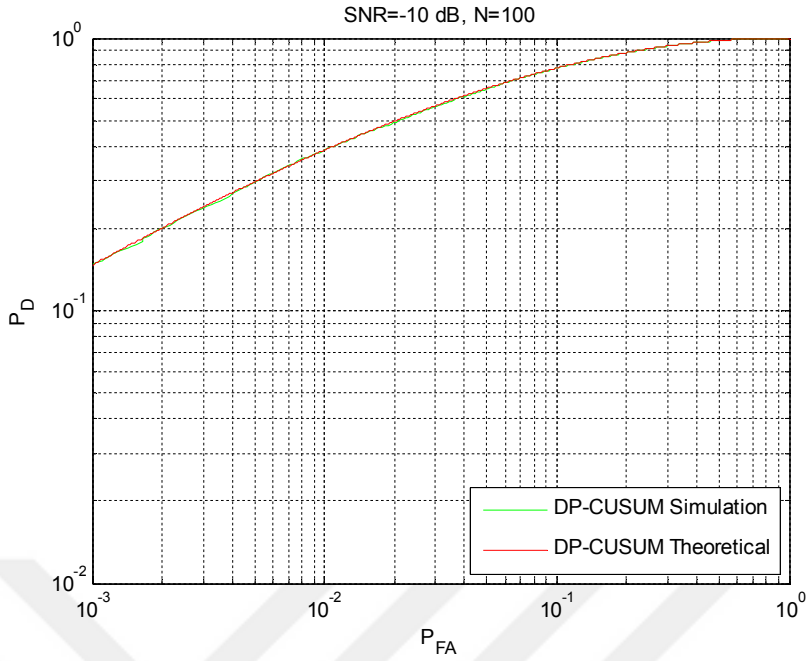

Figure 3.6 Theoretical and experimental performance comparison for the proposed method for $N = 100$ and $\mathrm{SNR} = -10$ dB.

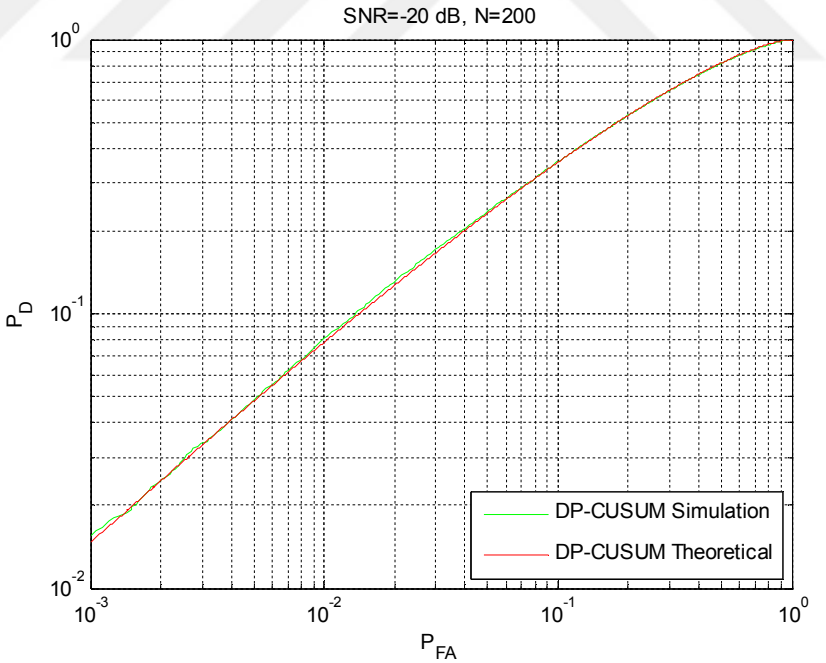

Figure 3.7 Theoretical and experimental performance comparison for the proposed method for $N = 100$ and $\mathrm{SNR} = -20$ dB.

In modelling the PU traffic, we consider the cases of strictly one status change and at most two status changes of the PU during the sensing period. The signal model used for the case of strictly one status change is given as

$$H_0 : x[n] = \begin{cases} s[n] + w[n] & ; n = 1, \ldots, i_1 \\ w[n] & ; n = i_1 + 1, \ldots, N \end{cases}$$
$$H_1 : x[n] = \begin{cases} w[n] & ; n = 1, \ldots, j_1 \\ s[n] + w[n] & ; n = j_1 + 1, \ldots, N \end{cases} \quad (3.32)$$

where $s[n]$ is the DC valued PU signal, $w[n]$ is zero-mean WGN with variance σ_w^2, and i_1 and j_1 are the indices of the status change points under H_0 and H_1, respectively.

For the case of two status changes, the signal model is given as

$$H_0 : x[n] = \begin{cases} w[n] & ; n = 1, \ldots, i_1 \\ s[n] + w[n] & ; n = i_1 + 1, \ldots, i_2 \\ w[n] & ; n = i_2 + 1, \ldots, N \end{cases}$$
$$H_1 : x[n] = \begin{cases} s[n] + w[n] & ; n = 1, \ldots, j_1 \\ w[n] & ; n = j_1 + 1, \ldots, j_2 \\ s[n] + w[n] & ; n = j_2 + 1, \ldots, N \end{cases} \quad (3.33)$$

where i_1 and j_1 denote the indices of the first status change and i_2 and j_2 denote the indices of the second status change under H_0 and H_1, respectively. It is assumed that cases of one and two changes have equal probability of occurence.

When the LSCP estimation strategy is applied to CuSum based weighted sample mean detector and Equations (3.32) and (3.33) are used as the PU signal models, the distributions of the proposed test statistic are given under H_0 and H_1 as follows

$$T(\boldsymbol{x}) \sim \begin{cases} \mathcal{N}\left(0, \dfrac{\sigma^2\left(N - i_{lscp} + 1\right)\left(2\left(N - i_{lscp}\right)+1\right)}{6\left(N - i_{lscp}\right)}\right) & \text{under} \quad H_0^{reduced} \\ \mathcal{N}\left(\dfrac{\left(N - j_{lscp} + 1\right)A}{2}, \dfrac{\sigma^2\left(N - j_{lscp} + 1\right)\left(2\left(N - j_{lscp}\right)+1\right)}{6\left(N - j_{lscp}\right)}\right) & \text{under} \quad H_1^{reduced} \end{cases} \tag{3.34}$$

where A is the amplitude of the DC valued PU signal and i_{lscp} and j_{lscp} are the LSCPs under hypotheses H_0 and H_1, respectively. Now, the parameter N in Equation (3.30) corresponds to $N - i_{lscp}$ under $H_0^{reduced}$ and $N - j_{lscp}$ under $H_1^{reduced}$ in Equation (3.34). $H_0^{reduced}$ and $H_1^{reduced}$ contain the reduced number of samples after the LSCP. These new hypotheses can be defined as

$$\begin{aligned} H_0^{reduced} &: x[n] = w[n]; \qquad n = i_{lscp} + 1, \ldots, N \\ H_1^{reduced} &: x[n] = s[n] + w[n]; \qquad n = j_{lscp} + 1, \ldots, N \end{aligned} \tag{3.35}$$

According to Equation (3.34), the related threshold, γ, and P_D can be found as

$$\gamma = Q^{-1}\left(P_{FA}\right)\sqrt{\frac{\sigma^2\left(N - i_{lscp} + 1\right)\left[2\left(N - i_{lscp}\right)+1\right]}{6\left(N - i_{lscp}\right)}} \tag{3.36}$$

and

$$P_D = \Pr\left[T(\boldsymbol{x}) > \gamma; H_1\right] \tag{3.37}$$

$$= Q\left(\sqrt{\frac{\left(N - i_{lscp} + 1\right)\left[2\left(N - i_{lscp}\right)+1\right]\left(N - j_{lscp}\right)}{\left(N - j_{lscp} + 1\right)\left[2\left(N - j_{lscp}\right)+1\right]\left(N - i_{lscp}\right)}}Q^{-1}\left(P_{FA}\right) - \frac{\left(N - j_{lscp} + 1\right)A}{2\sqrt{\dfrac{\sigma^2\left(N - j_{lscp} + 1\right)\left[2\left(N - j_{lscp}\right)+1\right]}{6\left(N - j_{lscp}\right)}}}\right)$$

Theoretical P_D given in Equation (3.37) is compared against the simulation results in Figures 3.8 and 3.9 assuming that strictly one and strictly two status changes occur in the channel. In both figures, the amplitude of the DC valued PU signal is given as $A=1$. The variance of the WGN is assigned based on the given SNR values. In both figures, solid lines represent the simulation curves and the dashed lines represent the theoretical curves.

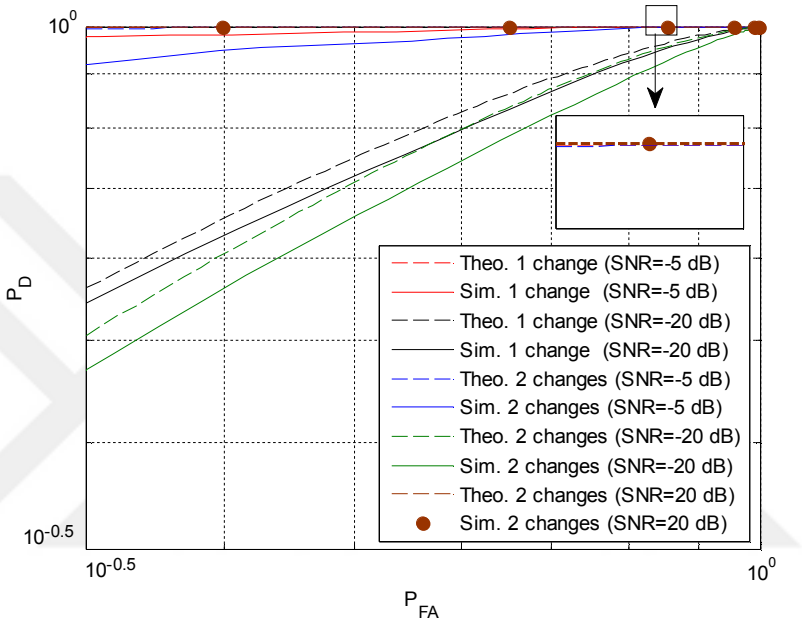

Figure 3.8 Theoretical vs. simulation results for $N=100$ and under different SNR levels, and different number of PU status changes.

In Figure 3.8, it is assumed that the length of the observation vector is given as $N=100$. For the case of strictly one status change, the PU status change points under H_0 and H_1 are taken as 30 and 40, respectively. For the case of two status changes, the first and second change points of the PU are given as 20 and 50 under H_0, and 30 and 60 under H_1, respectively. For different SNR levels, P_D versus P_{FA} curves are shown. According to results in Figure 3.8, it is possible to say that the amount of discrepancy between theoretical and simulation curves grows with an increase in the number of PU status changes in the channel. Also, the estimation of the LSCP becomes more difficult and this possibly causes an increase in the mismatch between the theoretical and simulation results. When SNR is very high (20

dB) and there are two status changes in the channel, the theoretical and simulation curves exactly overlap as seen in Figure 3.8.

In Figure 3.9, the results are presented assuming $N=10$ and $N=20$ to see how the observation length affects the detection performance. For strictly one status change and for $N=10$, the indices of the status changes i_1 and j_1 are assigned as 6 and 7 under H_0 and H_1, respectively. For $N=20$, these parameters are chosen as $i_1=9$ and $j_1=10$. A performance degradation is expected when the number of observed samples are reduced as seen in Figure 3.9. However, the discrepancy between the theoretical and simulation curves are smaller compared to the case of $N=100$ since the percentage error of the LSCPE algorithm decreases together with a decrease in the length of the observed data.

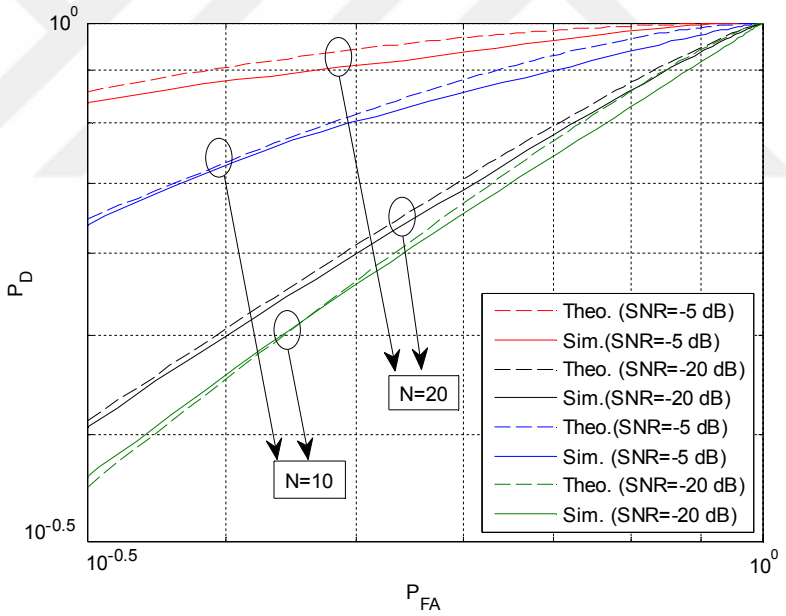

Figure 3.9 Theoretical vs. simulation results for $N=10$ and $N=20$ under different SNR levels, and different number of PU status changes.

In the next simulations, the effect of the proposed LSCP estimation strategy to the previously proposed techniques is considered. Accordingly, LSCP estimation is applied to our proposed method, cyclostationarity detector introduced in Y. Lee, S. Lee, Yoo, Liu, & Yoon (2014), improved ED proposed by Beaulieu & Chen (2010)

and conventional ED, respectively. In our figures, these methods are abbreviated as follows: “CuSum” for our proposed method, “Cyclo. detector” for the method introduced in Lee et al. (2014), “Improved ED” for the improved ED proposed by Beaulieu & Chen (2010) and “ED” for conventional ED. An additional technique denoted by “ToAD” referring to “Time of Arrival and Departure” is used for comparison in one PU status change since, in Tran & Kong (2013), it is stated that this method is valid only for one status change of the PU. Moreover, a change point estimation is also carried out in Tran & Kong (2013). Therefore, the LSCP estimation algorithm is not applied to this method. For other techniques, abbreviations take “LSCPE” prefix when the LSCP estimation algorithm is used before the calculation of the test statistics. Also, solid and dashed lines are reserved to represent the cases when the LSCP estimation algorithm is utilized and not utilized, respectively.

Poisson process is used to determine the indices of the change points. For the case of strictly one PU status change, the arrival and departure rates of the Poisson process are taken as equal to 1. However, these parameters are chosen differently in the case of at most two status changes to make undesired signal samples more influential on detection performance (Düzenli & Akay, 2016). According to this scenario, under hypothesis H_0, arrival rate λ_a and departure rate λ_d are taken as equal to 3 and 1, respectively. Inversely, these parameters are assigned as $\lambda_a = 1$ and $\lambda_d = 3$ under H_1.

In Figures 3.10 and 3.11, P_D vs. P_{FA} results are presented for strictly one PU status change and at most two PU status changes, respectively. In both figures, the observed data length N is taken as 200 and SNR= −5 dB. For simulations, 100 P_{FA} values are obtained at first by dividing the interval $[0,1]$ into 100 points and then the threshold values are obtained for each technique individually. At the end, the results of the considered test statistics are compared with these threshold values under both H_0 and H_1, and a decision is taken about whether the the channel is idle or busy.

In Figure 3.10, where it is assumed that strictly one PU status change occurs in the channel, it can be seen that the proposed LSCP estimation algorithm provides noticeable performance enhancement in terms of P_D for all the considered techniques. Even if LSCP algorithm is not used, CuSum based weighted sample mean detector outperforms other methods. Another change point estimation based detector, ToAD performs poorer than cyclostationarity detector and our proposed method, but it has higher P_D values than improved and conventional EDs. It is worth to note that the improved and conventional EDs show similar performance in simulations, although it is stated in Beaulieu & Chen (2010) that improved ED outperforms conventional ED in terms P_D.

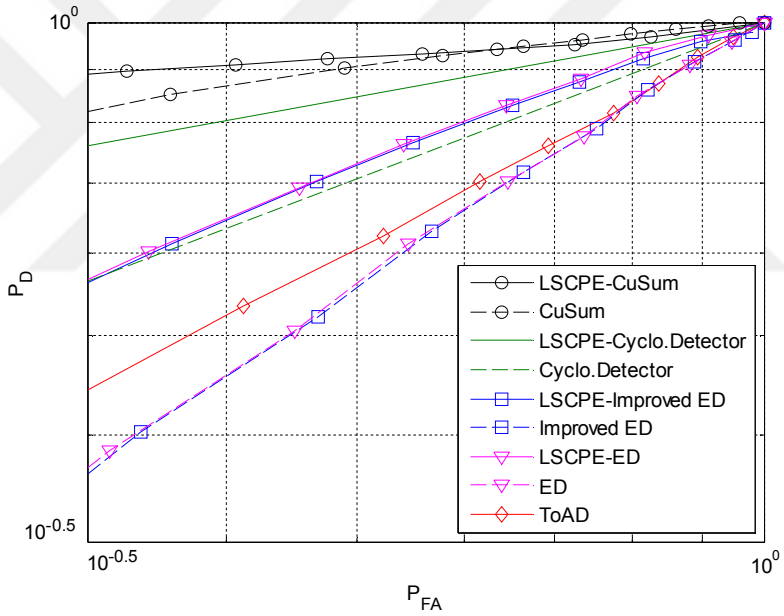

Figure 3.10 P_D vs. P_{FA} for strictly one PU status change with and without LSCP estimation algorithm.

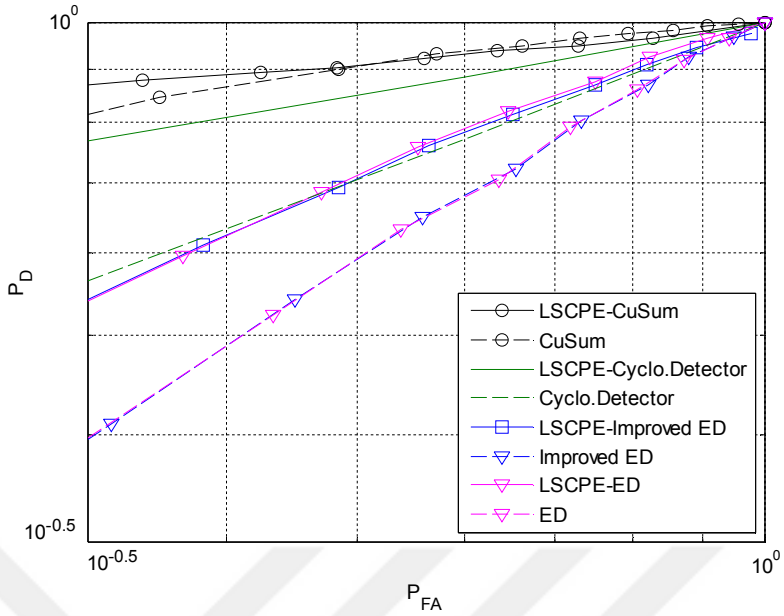

Figure 3.11 P_D vs. P_{FA} for at most two PU status changes with and without LSCP estimation algorithm.

In Figure 3.11, it is assumed that at most two PU status changes occur in the channel during the sensing period. Again, as in Figure 3.10, an enhancement in detection performance is achieved for all the considered techniques using LSCP estimation algorithm. Furthermore, the proposed CuSum weighted sample mean detector has the highest P_D values even when the LSCP estimation algorithm is not utilized. Improved and conventional EDs show similar performance again and the LSCP estimation algorithm provides the same amount of increase in detection performance for both techniques. Elimination of the undesirable samples in the observed data can be given as the main reason of the provided performance enhancement by our LSCP estimation algorithm.

3.2.2 CuSum based Weighted Energy Detector (CuS-WED)

Up to now, theoretical calculations and simulations are carried out assuming that the PU signal is DC valued, and accordingly, the LSCP estimation algorithm is embedded into CuSum weighted sample mean detector. As stated before, CuSum weighting scheme is applicable to other conventional detectors as well. In this

section, CuSum weighting scheme and LSCP estimation strategy are adapted to ED to detect dynamic PUs with unknown signals. ED is the optimal method for detection of unknown PU signals. However, this optimality disappears with the assumption of the PU traffic in the channel. It is aimed in the following analysis to achieve a performance enhancement for ED by showing that the proposed sensing scheme also works even when the PU signal is assumed to be unknown.

It is possible to use the same traffic models in Equations (3.32) and (3.33) here, for the cases of one and two PU status changes, respectively. However, the PU signal is assumed to be random having zero-mean Gaussian distribution such that $s[n] \sim \mathcal{N}\left(0, \sigma_s^2\right)$ where $s[n]$ represents the PU signal. Use of Gaussian distribution for modelling the PU signal is reasonable since the signal arriving at the CR receiver might actually correspond to a sum of multiple non-line-of-sight propagation signals (N.-Thanh et al., 2012).

CuS-WED can be defined by modifying the test statistic in Equation (3.24) as

$$T\left(\boldsymbol{x}\right) = \frac{1}{N}\left(\sum_{n=1}^{N}\sum_{i=1}^{n} x^2[N-i+1]\right) \tag{3.38}$$

by assigning $T'(.)$ in Equation (3.23) as a squaring operator now. The test statistic in Equation (3.38) can be rewritten also in the following equivalent form as

$$T\left(\boldsymbol{x}\right) = \frac{1}{N}\sum_{n=1}^{N}\left(N-n+1\right)x^2\left[N-n+1\right]. \tag{3.39}$$

As in the CuSum based weighted sample mean detector, it is sufficient to obtain the mean and variance of $T\left(\boldsymbol{x}\right)$ under hypotheses H_0 and H_1 invoking the CLT. Under H_0, $x[n] = w[n]$ for $n = 1, \ldots, N$. Then, mean and variance of $T\left(\boldsymbol{x}\right)$ under H_0 can be found, respectively, as

$$\mathrm{E}\left\{\frac{1}{N}\sum_{n=1}^{N}(N-n+1)x^2\left[N-n+1\right]\right\}=\frac{(N+1)}{2}\sigma_w^2 \tag{3.40}$$

and

$$\mathrm{var}\left\{\frac{1}{N}\sum_{n=1}^{N}(N-n+1)x^2\left[N-n+1\right]\right\}=\frac{(N+1)(2N+1)}{3N}\sigma_w^4. \tag{3.41}$$

Under H_1, $x[n]=s[n]+w[n]$ for $n=1,\ldots,N$. Therefore, mean of $T(\boldsymbol{x})$ under H_1 is

$$\mathrm{E}\left\{\frac{1}{N}\sum_{n=1}^{N}(N-n+1)x^2\left[N-n+1\right]\right\}=\frac{N+1}{2}\left(\sigma_s^2+\sigma_w^2\right) \tag{3.42}$$

and the variance of $T(\boldsymbol{x})$ under H_1 can be found as

$$\mathrm{var}\left\{\frac{1}{N}\sum_{n=1}^{N}(N-n+1)x^2\left[N-n+1\right]\right\}=\frac{(N+1)(2N+1)}{3N}\left(\sigma_s^2+\sigma_w^2\right)^2. \tag{3.43}$$

Now, PDF of $T(\boldsymbol{x})$ can be written using the mean and variance terms obtained in Equations (3.40) through (3.43) as

$$T(\boldsymbol{x})=\frac{1}{N}\sum_{n=1}^{N}(N-n+1)x^2\left[N-n+1\right]\sim\begin{cases}\mathcal{N}\left(\dfrac{(N+1)}{2}\sigma_w^2,\dfrac{(N+1)(2N+1)}{3N}\sigma_w^4\right) & ;H_0\\ \mathcal{N}\left(\dfrac{N+1}{2}\left(\sigma_s^2+\sigma_w^2\right),\dfrac{(N+1)(2N+1)}{3N}\left(\sigma_s^2+\sigma_w^2\right)^2\right) & ;H_1\end{cases} \tag{3.44}$$

According to Equation (3.44), the threshold value γ and P_D can be calculated as

$$\gamma = \left(Q^{-1}\left(P_{FA}\right)\sqrt{\frac{(N+1)(2N+1)}{3N}\sigma_w^4} \right) + \frac{(N+1)}{2}\sigma_w^2 \tag{3.45}$$

and

$$P_D = \Pr\left[T(\boldsymbol{x}) > \gamma; H_1\right] = Q\left(\frac{\gamma - \frac{(N+1)}{2}\left(\sigma_s^2 + \sigma_w^2\right)}{\sqrt{\frac{(N+1)(2N+1)}{3N}\left(\sigma_s^2 + \sigma_w^2\right)^2}} \right) \tag{3.46}$$

$$= Q\left(\frac{\left[\left(Q^{-1}\left(P_{FA}\right)\sqrt{\frac{(N+1)(2N+1)}{3N}\sigma_w^4} \right) + \frac{(N+1)}{2}\sigma_w^2 \right] - \frac{(N+1)}{2}\left(\sigma_s^2 + \sigma_w^2\right)}{\sqrt{\frac{(N+1)(2N+1)}{3N}\left(\sigma_s^2 + \sigma_w^2\right)^2}} \right)$$

The derivation of the PDFs of the CuS-WED test statistic under H_0 and H_1 is given in the Appendix of the dissertation. Similar results to Equations (3.40) through (3.46) can also be found in Xie & Hu (2014) where the power of the weights is also used in calculation of the test statistic.

Using Equation (3.46), theoretical versus simulation results are plotted in Figure 3.12. The number of observed samples is taken as $N = 100$ and the results are given for the SNR values of -5 and -15 dB. According to Figure 3.12, it possible to say that the theoretical performance curves closely match with the simulated curves independent of the SNR level. However, detection performance decreases for low SNR values as can be seen from the figure.

The next step after theoretical analysis of CuS-WED is to embed the LSCP estimation algorithm into this decision statistic. Here, PU is assumed to be Gaussian distributed as $s[n] \sim \mathcal{N}\left(0, \sigma_s^2\right)$ which is different from the DC valued signalling scheme used in Section 3.2.1. According to the traffic models in Equations (3.32) and (3.33), when the PU is in the channel, observed data $x[n]$ is Gaussian with

$x[n] \sim \mathcal{N}\left(0, \sigma_s^2 + \sigma_w^2\right)$ where σ_s^2 and σ_w^2 are the variances of the PU signal and noise, respectively. In the absence of the PU, the model for $x[n]$ is given as $x[n] \sim \mathcal{N}\left(0, \sigma_w^2\right)$. According to this scheme, it is clear that the variance is the only changing parameter in the observed data depending on whether the PU is in the channel or not. Therefore, the LSCP estimation algorithm is reduced to estimation of the last variance change point, and the DP approach introduced in Section 3.1.6 is modified to estimate the variance change points, now.

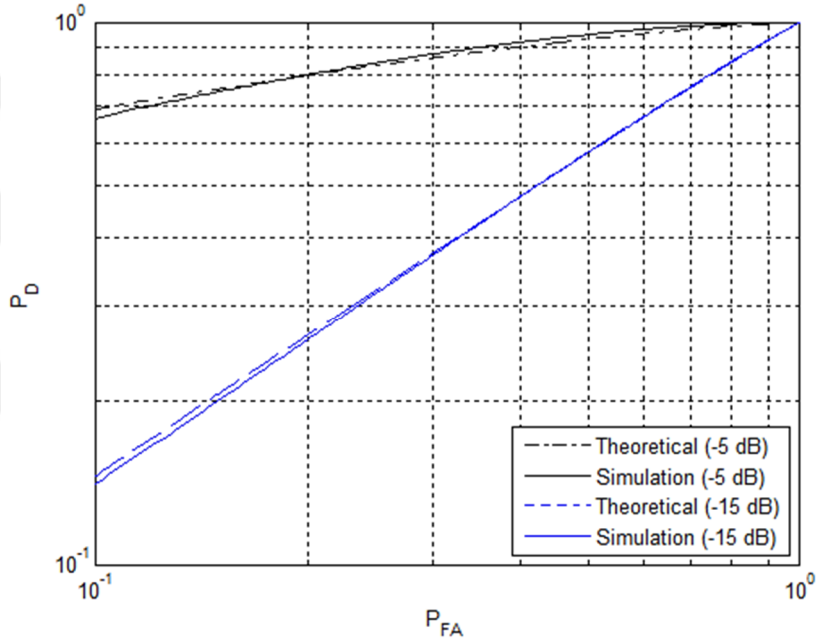

Figure 3.12 Theoretical vs. simulation results for CuS-WED for SNR values of −5 and −15 dB, $N = 100$.

It is required to obtain log-likelihood function of the observed data to obtain the MLEs of the variance change points. Assuming that k variance changes occur in the channel, the related log-likelihod function can be written as

$$\ln p\left(\boldsymbol{x}; \boldsymbol{\sigma}^2, \boldsymbol{n}\right) = \ln\left(\frac{1}{\left(2\pi\sigma_0^2\right)^{\frac{n_0}{2}}}\right) - \frac{1}{2\sigma_0^2}\sum_{n=0}^{n_0\text{-}1} x^2[n] + \cdots + \ln\left(\frac{1}{\left(2\pi\sigma_k^2\right)^{\frac{n_k - n_{k\text{-}1}}{2}}}\right) - \frac{1}{2\sigma_k^2}\sum_{n=n_{k\text{-}1}}^{n_k\text{-}1} x^2[n] \quad (3.47)$$

where $\boldsymbol{x}$ is the observed data vector, $\boldsymbol{\sigma^2}$ is the vector of unknown variance values and $\boldsymbol{n}$ contains the variance change points in $\boldsymbol{x}$. Joint maximization of Equation (3.47) with respect to $\boldsymbol{\sigma^2}$ and $\boldsymbol{n}$ gives the MLE of these unknown parameter vectors. The MLE of the DC level vector $\boldsymbol{A}$ was carried out by taking derivative of Equation (3.17) with respect to $\boldsymbol{A}$ and equating it to zero**.** Here, this procedure is modified to find the MLE of the variance vector $\boldsymbol{\sigma^2}$. First, differentiation of Equation (3.47) is carried out with respect to $\boldsymbol{\sigma^2}$. Then, it is equated to zero as

$$\frac{\partial \ln p\left(\boldsymbol{x};\boldsymbol{\sigma^2},\boldsymbol{n}\right)}{\partial \boldsymbol{\sigma^2}} = 0 . \tag{3.48}$$

Solving Equation (3.48), MLE of the variance values $\sigma_0^2,\sigma_1^2,\ldots,\sigma_k^2$ can be found as

$$\hat{\sigma}_i^2 = \frac{1}{n_i - n_{i-1}} \sum_{n=n_{i-1}}^{n_i-1} x^2[n] \tag{3.49}$$

where $i = 0,1,\ldots,k$, $n_{-1} = 0$, and $n_k = N$. Now, it is possible to rewrite Equation (3.47) using these estimated variance values as

$$\ln p\left(\boldsymbol{x};\hat{\boldsymbol{\sigma}}^2,\boldsymbol{n}\right) = \ln\left(\frac{1}{\left(2\pi\hat{\sigma}_0^2\right)^{\frac{n_0}{2}}}\right) - \frac{1}{2\hat{\sigma}_0^2}\sum_{n=0}^{n_0-1} x^2[n] + \ldots + \ln\left(\frac{1}{\left(2\pi\hat{\sigma}_k^2\right)^{\frac{n_k-n_{k-1}}{2}}}\right) - \frac{1}{2\hat{\sigma}_k^2}\sum_{n=n_{k-1}}^{n_k-1} x^2[n]. \tag{3.50}$$

At this step, a definition similar to Equation (3.19) can be made with some modifications as

$$\Delta_i\left[n_{i-1}, n_i - 1\right] = \ln\left(\frac{1}{\left(2\pi\hat{\sigma}_i^2\right)^{\frac{n_i-n_{i-1}}{2}}}\right) - \frac{1}{2\hat{\sigma}_i^2}\sum_{n=n_{i-1}}^{n_i-1} x^2[n], \qquad i = 0,1,\ldots,k. \tag{3.51}$$

Using Equation (3.51), log-likelihood function to be maximized can be written as

$$\ln p\left(\boldsymbol{x};\hat{\boldsymbol{\sigma}}^2,\boldsymbol{n}\right)=\sum_{i=0}^{k}\Delta_i\left[n_{i\text{-}1},n_i\text{-}1\right] \tag{3.52}$$

which only depends on the vector of unkown change points $\boldsymbol{n}$.

The next step is to maximize the log-likelihood function $\ln p\left(\boldsymbol{x};\hat{\boldsymbol{\sigma}}^2,\boldsymbol{n}\right)$ with respect to $\boldsymbol{n}$. For this maximization, a new vector which is analogous to the vector $I_k\left[L\right]$ introduced in Equation (3.21) can be defined as

$$I_k\left[L\right]=\max_{n_0,n_1,\ldots n_{k-1}}\sum_{i=0}^{k}\Delta_i\left[n_{i-1},n_i-1\right],\qquad 0<n_0<n_1<\ldots<n_{k-1}<L+1 \tag{3.53}$$

The rest of the algorithm can be carried out as discussed in Kay (1998). Although DP requires a priori knowledge of the number of the status changes in the channel, only the estimation of the LSCP is needed here again.

After the LSCP estimation step is completed, CuS-WED can be applied to the remaining samples between LSCP and the end of the sensing period. For performance comparison, weighted ED proposed in Xie & Hu (2014) and conventional ED are also simulated. For the case of one status change in the channel, ToAD is also used in simulations. These techniques are indicated in Figures 3.13 and 3.14 as "Weighted ED" for weighted ED in Xie & Hu (2014), "Conventional ED" for conventional ED, "ToAD" for the method introduced in Tran & Kong (2013) and "Proposed" for the proposed sensing scheme in this dissertation. In both figures, the observed data length N is taken as equal to 200. In simulations, the PU signal is modelled as $\mathcal{N}\left(0,1\right)$ and the power of the noise is determined based on the SNR level of -5 dB. For the proposed sensing scheme, estimation of the LSCP is carried out first, and then, CuS-WED is applied to the remaining samples. For each considered technique, the threshold values are obtained using given P_{FA} values. The

threshold values of the proposed sensing scheme are calculated according to the following equation

$$\gamma = Q^{-1}\left(P_{FA}\right)\sqrt{\frac{\left(N - i_{lscp} + 1\right)\left[2\left(N - i_{lscp}\right) + 1\right]}{3\left(N - i_{lscp}\right)}\sigma_w^4 + \frac{\left(N - i_{lscp} + 1\right)}{2}\sigma_w^2} \tag{3.54}$$

where i_{lscp} denotes the last status change point under hypothesis H_0. As in Section 3.2.1, the simulation results are considered for strictly one and at most two PU status changes.

In Figure 3.13, it is assumed that strictly one PU status change is generated under both H_0 and H_1 according to Poisson process with parameters $\lambda_a = \lambda_d = 1$. According to the results given in Figure 3.13, the proposed sensing scheme outperforms other techniques. In addition, it can be inferred from the figure that weighting of the latter samples provides higher P_D values. As expected, conventional ED shows the worst detection performance among the considered techniques.

In Figure 3.14, it is assumed that at most two PU status changes occur in the channel during the sensing period. As in Section 3.2.1, the probabilities of occurrence of either one or two PU status changes are equal to 0.5. The traffic parameters are given as $\lambda_a = 3$ and $\lambda_d = 1$ under H_0 and $\lambda_a = 1$ and $\lambda_d = 3$ under H_1. As in Figure 3.13, again the proposed sensing scheme has the highest P_D values among the considered techniques particularly at low P_{FA} values which are more desirable in real life scenarios. The weighted ED again shows close performance to our proposed method.

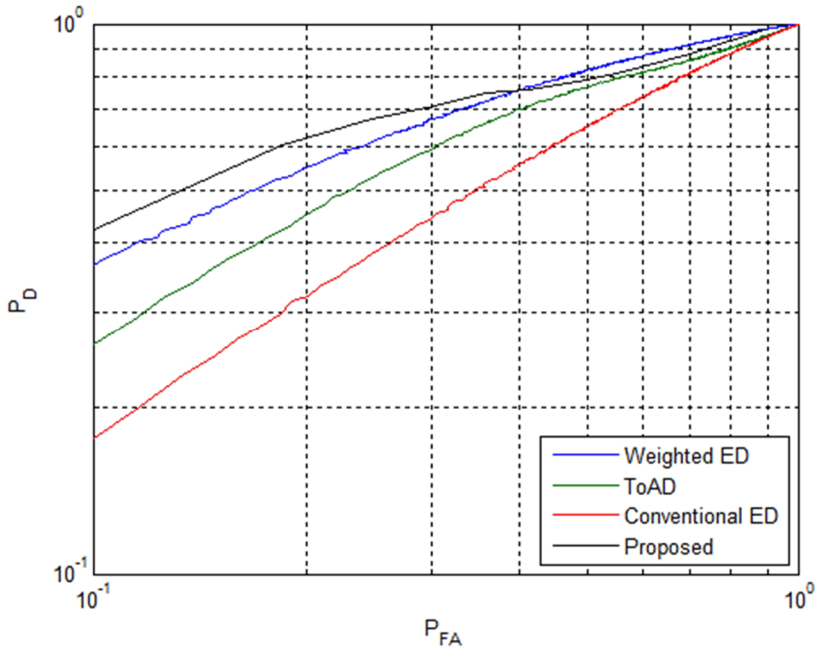

Figure 3.13 P_D vs. P_{FA} for strictly one PU status change with $N = 200$ and SNR= –5 dB.

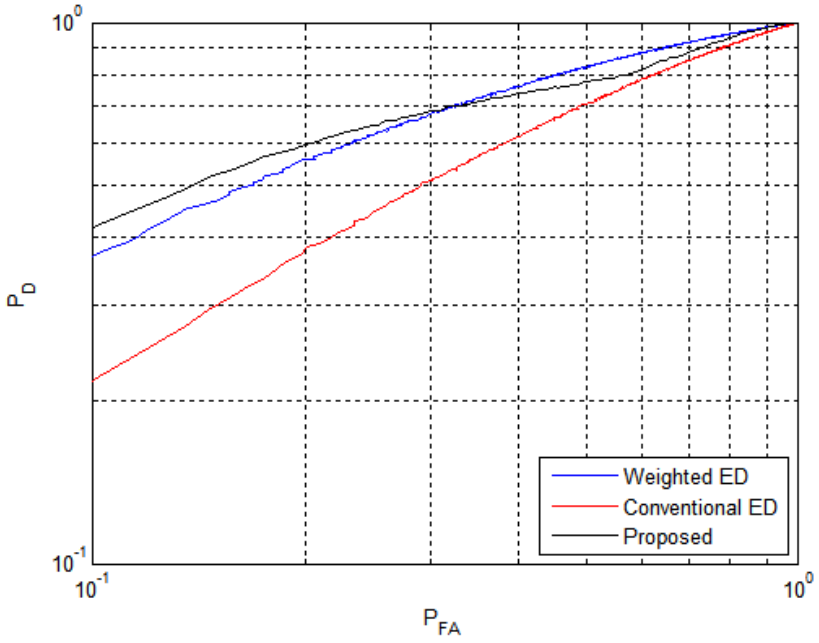

Figure 3.14 P_D vs. P_{FA} for at most two PU status changes with $N = 200$ and SNR= –5 dB.

CHAPTER FOUR
DETECTION OF DYNAMIC PRIMARY USERS USING GOODNESS OF FIT (GOF) TESTS

In this chapter of the dissertation, spectrum sensing techniques based on GOF testing are addressed. Detection performances of various GOF tests are determined based on simulation results. In addition, performance analyses have been carried out for detection of dynamic PUs. Considering GOF tests for detection of dynamic PUs is critical since this problem has not been addressed in the literature yet.

In the first section, the problem definition for GOF testing is presented. Various GOF test statistics are introduced in this section.

In the second section of the chapter, it is shown that GOF test statistics exhibit better detection performance than ED when the PU signal is constant (DC signal). The effect of using different PU signal types on detection performance is also discussed in that section.

Finally, in the third section, GOF based spectrum sensing is applied for detection of dynamic PUs. A new OS based sensing algorithm is introduced and the related simulation results are presented in this section. It is shown that our proposed method outperforms other GOF tests and ED in terms of P_D.

4.1 Introduction

Spectrum sensing techniques previously proposed in the literature can be grouped under two categories (Teguig, Le Nir, & Scheers, 2015):

Coherent sensing methods: Cyclostationary detector, matched filter, waveform based sensing, etc.
Blind sensing methods: Energy detection, GOF testing, order statistics, etc.

For coherent sensing methods, it is assumed that there is knowledge of some parameters of the PU signal (Axell et al., 2012; Yücek & Arslan, 2009). For example, cyclostationarity detectors need knowledge of the cyclic frequency of the PU. In the matched filter technique, the type of the PU signal should be exactly known by CR which is actually not very realistic in real life. In waveform based sensing, it is assumed that the PU signal can be classified into one of the waveform classes in the CR data set. Besides all these, there are also various blind spectrum sensing techniques proposed in the literature (Arshad & Moessner, 2013; H. Yang et al., 2009; Lei et al., 2011; Rostami et al. 2012; Teguig et al., 2014; Urkowitz, 1967). As the most popular one, ED does not need any knowledge of the PU signal type (Urkowitz, 1967).

As one of the blind spectrum sensing techniques, the GOF testing and related test statistics are introduced in the following sections.

4.2 GOF Testing

In GOF testing, the main purpose is to determine if the observed data comes from a particular distribution or not. This can be represented mathematically as (Stephens, 1974; Zhang, 2002)

$$\begin{aligned} &\text{Null hypothesis:} && F_N(x) = F_0(x) \\ &\text{Alternative hypothesis:} && F_N(x) \neq F_0(x). \end{aligned} \tag{4.1}$$

Here, $F_0(x)$ is a known cumulative distribution function (CDF) under the null hypothesis which is evaluated for the data samples under test, $\boldsymbol{x}$, and $F_N(x)$ is the empirical CDF of $\boldsymbol{x}$ which is calculated as (Rostami et al., 2012)

$$F_N(x) = \frac{\{i : x_i \leq x, 1 \leq i \leq N\}}{N} \tag{4.2}$$

Here, N is the total number of samples together with data ordering $x_{(1)} \le x_{(2)} \le \ldots \le x_{(N)}$.

This modeling scheme can be adapted to spectrum sensing problem in CR. The binary hypothesis testing problem for spectrum sensing is given as follows (Yücek & Arslan, 2009)

$$\begin{aligned} H_0 &: x[n] = w[n], \qquad n = 1, 2, \ldots, N \\ H_1 &: x[n] = s[n] + w[n], \qquad n = 1, 2, \ldots, N \end{aligned} \tag{4.3}$$

where $x[n]$ contains noise-only samples under H_0 and signal+noise samples under H_1. For GOF testing, Equation (4.3) can be modified as (Rostami et al., 2012; Teguig et al., 2014, 2015)

$$\begin{aligned} H_0 &: F_N(x) = F_0(x), \\ H_1 &: F_N(x) \neq F_0(x). \end{aligned} \tag{4.4}$$

In this model, $F_N(x)$ is the empirical CDF of the observed data $\boldsymbol{x}$ and $F_0(x)$ is the known CDF of noise distribution under H_0.

The crucial point for the model in Equation (4.4) is how to measure the distance between $F_N(x)$ and $F_0(x)$. There are various tests in the literature to measure this distance. The common steps for all these tests can be summarized as follows (Arshad & Moessner, 2013):

Step #1: Received data samples are sorted in ascending order.

Step #2: A threshold is calculated for a given probability of false alarm, P_{FA}.

Step #3: The test statistic for a given test is calculated.

Step #4: Result of Step #3 is compared against the threshold calculated in Step #2 and the decision is made based on the result of this comparison.

Among these four steps, Step #3 is the most important one since it determines the performance of overall process. There are several test statistics proposed in the literature for GOF testing and each one of them has different properties. Now, in this section of the report, most widely used GOF test statistics will be introduced.

The main GOF tests considered in this chapter are listed below:

- Anderson – Darling (AD) test (Arshad & Moessner, 2013; H. Yang, et al., 2009; Lei et al., 2011; Rostami et al., 2012),
- Kolmogorov – Smirnov (KS) test (Arshad & Moessner, 2013; Lei et al., 2011; Stephens, 1974; Zhang, 2002),
- Cramer – von Misses (CM) test (Lei et al., 2011; Stephens, 1974),
- Log Likelihood Ratio (LLR) based tests (Teguig et al., 2015; Zhang, 2002),
- Order statistics (OS) (Glen et al., 2001; Rostami et al., 2012).

4.2.1 Anderson-Darling (AD) Test

In the AD test, it is aimed to measure the distance between the observed data and the known noise distribution. If the result of this measurement is smaller than a certain threshold, then H_0 is decided as the valid hypothesis.

The AD decision statistic is given as (Arshad & Moessner, 2013)

$$T_{AD} = N \int_{-\infty}^{\infty} \left[F_N(x) - F_0(x) \right]^2 \psi\left(F_0(x)\right) dF_0(x) \tag{4.5}$$

where $\psi(\cdot)$ is a weight function with $\psi(u) = \left[u(1-u)\right]^{-1}$ defined over $0 \le u \le 1$. It is possible to simplify the AD test statistic in Equation (4.5) by performing the integral. Then, T_{AD} can be obtained as (Arshad & Moessner, 2013)

$$T_{AD} = -\frac{N^2 + \sum_{i=1}^{N} (2i-1)\left(\ln z_i + \ln(1 - z_{N+1-i})\right)}{N} \tag{4.6}$$

where $z_i = F_0(x_i)$.

The asymptotic distribution of T_{AD} under H_0 is given by (Arshad & Moessner, 2013)

$$F\left(T_{AD} \mid H_0; x\right) = \frac{\sqrt{2\pi}}{x} \sum_{j=0}^{+\infty} a_j (4j+1) e^{\left(-\frac{(4j+1)^2 \pi^2}{8x}\right)} \int_0^{\infty} \left(\frac{x}{8\left(w^2+1\right)} - \frac{(4j+1)^2 \pi^2 w^2}{8x} \right) dw \tag{4.7}$$

where $a_j = (-1)^j \Gamma\left(j + \frac{1}{2}\right) / \Gamma\left(\left(\frac{1}{2}\right) j!\right)$ with $\Gamma(\cdot)$ denoting the Gamma function (Arshad & Moessner, 2013). Using Equation (4.7), the threshold for AD test, γ_{AD}, can be calculated for a given P_{FA} using the following equation

$$P_{FA} = 1 - F\left(T_{AD} \mid H_0; \gamma_{AD}\right). \tag{4.8}$$

In the end, T_{AD} is compared against the threshold which is found using Equation (4.8) and if $T_{AD} > \gamma_{AD}$, hypothesis H_0 is rejected and the PU is considered to exist in the channel. Otherwise, H_0 is accepted.

Obtaining γ_{AD} using Equation (4.8) may be difficult since $F\left(T_{AD} \mid H_0; x\right)$ in Equation (4.7) is mathematically intractable. For this reason, threshold values obtained by simulations or special tables are widely used in the literature (Stephens, 1974).

AD testing procedure can be summarized in four steps:

1. Sort the observed signal samples $\boldsymbol{x} = \left[x_1, x_2, \ldots, x_N\right]$ in ascending order as $x_{(1)} \leq x_{(2)} \leq \ldots \leq x_{(N)}$ and let $\tilde{\boldsymbol{x}} = \left[x_{(1)}, x_{(2)}, \ldots, x_{(N)}\right]$.

2. Transform the elements of $\tilde{\boldsymbol{x}}$ using the known noise CDF, $F_0\left(x\right)$. Thus, $z_i = F_0\left(x_i\right)$.

3. Calculate the test statistic T_{AD} as

$$T_{AD} = -\frac{N^2 + \sum_{i=1}^{N} (2i-1)\left(\ln z_i + \ln(1 - z_{N+1-i})\right)}{N}. \tag{4.9}$$

4. If $T_{AD} > \gamma_{AD}$ decide H_1 is true, else decide H_0.

4.2.2 Kolmogorov – Smirnov (KS) Test

As in the AD test, the KS test aims to obtain how far the empirical CDF of the received signal is from the known CDF of the noise. It is also possible to interpret the KS test as "graphically the maximum vertical distance between the two distributions, $F_N\left(x\right)$ and $F_0\left(x\right)$" as in Arshad & Moessner (2013). Accordingly, the KS decision statistic is defined as (Lei et al., 2011)

$$T_{KS} = \max\left|F_N\left(x\right) - F_0\left(x\right)\right| \tag{4.10}$$

where $F_N(x)$ is the empirical CDF as defined in Equation (4.2). According to Equation (4.10), the test statistic T_{KS} converges to zero under hypothesis H_0.

As a distribution-free test statistic, T_{KS} has a distribution function that is independent of the distribution of noise under H_0. Similar to AD testing, there are also studies providing tables for obtaining the threshold values for KS testing (Stephens, 1974). Alternatively, these threshold values can be obtained using Monte Carlo simulations.

4.2.3 Cramer - von Misses (CM) Test

In the CM test, the distance between $F_N(x)$ and $F_0(x)$ is defined as (Lei et al., 2011; Stephens, 1974)

$$T_{CM} = N\int_{-\infty}^{+\infty}\left[F_N(x)-F_0(x)\right]^2 dF_0(x). \tag{4.11}$$

The CM test statistic can be obtained by breaking the integral in Equation (4.11) into n parts. Then, the resulting test statistic is given as

$$T_{CM} = \sum_{i=1}^{N}\left[z_i - \frac{(2i-1)}{2N}\right]^2 + \left(\frac{1}{12N}\right) \tag{4.12}$$

where $z_i = F_0(x_i)$.

4.2.4 Log Likelihood Ratio (LLR) GOF Tests

In GOF testing, it is possible to derive the test statistics by two basic equations which are given as (Zhang, 2002)

$$Z = \int_{-\infty}^{+\infty} Z_t dw(t) \tag{4.13}$$

$$Z_{\max} = \sup_{t\in(-\infty,\infty)} \{Z_t w(t)\} \tag{4.14}$$

where $w(t)$ is some weight function.

It is clear that performance of a test statistic generated using Equations (4.13) and (4.14) depends on Z_t and $w(t)$ which are used for calculating Z and $Z_{\max}$. For Z_t, two functions are used in the literature. They are given as Pearson statistic and the log-likelihood ratio (LLR) which are given, respectively, as (Zhang, 2002)

$$X_t^2 = \frac{N\{F_N(t) - F_0(t)\}^2}{F_0(t)\{1-F_0(t)\}} \tag{4.15}$$

and

$$G_t^2 = 2N\left[F_N(t)\log\left\{\frac{F_N(t)}{F_0(t)}\right\} + \{1-F_N(t)\}\log\left\{\frac{1-F_N(t)}{1-F_0(t)}\right\}\right]. \tag{4.16}$$

It is possible to derive the three traditional GOF test statistics introduced above (AD, KS, and CM) using Equations (4.13) through (4.16). Using different weight functions and choosing X_t^2 as Z_t, the traditional GOF tests are derived as in Table 4.1. It is also stated in (Zhang, 2002) that sometimes it is required to modify the empricial CDF $F_N(x)$ at its discontinuity points x_i $(i=1,2,\ldots,N)$ by introducing $F_N(x_i) = \frac{(i-c)}{(N+1-2c)}$ where c is a constant between 0 and 1. The value of c is taken to be 0.5 by Zhang (2002), and then, the empirical CDF is defined as

$F_N(x_i) = \frac{(i-0.5)}{N}$ rather than as $F_N(x_i) = \frac{i}{N}$ for calculations of the test statistics in Equations (4.19) through (4.21).

According to Table 4.1, it is possible to obtain various GOF test statistics by using different weight functions and statistics. For example, if $w(t)$ and Z_t are taken as

$$w(t) = F_0(t) \tag{4.17}$$

and

$$Z_t = X_t^2 = \frac{N\{F_N(t) - F_0(t)\}^2}{F_0(t)\{1 - F_0(t)\}} \tag{4.18}$$

then, the AD test statistic is obtained by computing the result of the integral in Equation (4.13).

Table 4.1 Derivation of traditional GOF tests using Equations (4.13) through (4.16).

Weight Function $w(t)$	Statistic Z or $Z_{\max}$	Name of obtained GOF Test
$w(t) = N^{-1} F_0(t)\{1 - F_0(t)\}$	$Z_{\max} = \sup_{t \in (-\infty, \infty)} \{Z_t w(t)\}$ where $Z_t = X_t^2 = \frac{N\{F_N(t) - F_0(t)\}^2}{F_0(t)\{1 - F_0(t)\}}$	Kolmogorov – Smirnov
$w(t) = F_0(t)$	$Z = \int_{-\infty}^{+\infty} Z_t dw(t)$ where $Z_t = X_t^2 = \frac{N\{F_N(t) - F_0(t)\}^2}{F_0(t)\{1 - F_0(t)\}}$	Anderson – Darling
$dw(t) = F_0(t)\{1 - F_0(t)\} dF_0(t)$	$Z = \int_{-\infty}^{+\infty} Z_t dw(t)$ where $Z_t = X_t^2 = \frac{N\{F_N(t) - F_0(t)\}^2}{F_0(t)\{1 - F_0(t)\}}$	Cramer – von Misses

Employing this approach, it is also possible to generate new powerful and distribution symmetric tests by choosing $w(t)$ and Z_t as in Table 4.2 (Zhang, 2002).

Table 4.2 Derivation of new GOF tests using Equations (4.13) through (4.16).

Weight Function $w(t)$	Statistic Z or $Z_{\max}$	Name of obtained GOF Test
$w(t)=1$	$Z_{\max}=\sup_{t\in(-\infty,\infty)}\{Z_t w(t)\}$ where $Z_t=G_t^2=2N\left[F_N(t)\log\left\{\frac{F_N(t)}{F_0(t)}\right\}+\{1-F_N(t)\}\log\left\{\frac{1-F_N(t)}{1-F_0(t)}\right\}\right]$	ZK
$dw(t)=F_N(t)^{-1}\{1-F_N(t)\}^{-1}dF_N(t)$	$Z=\int_{-\infty}^{+\infty}Z_t dw(t)$ where $Z_t=G_t^2=2N\left[F_N(t)\log\left\{\frac{F_N(t)}{F_0(t)}\right\}+\{1-F_N(t)\}\log\left\{\frac{1-F_N(t)}{1-F_0(t)}\right\}\right]$	ZA
$dw(t)=F_0(t)^{-1}\{1-F_0(t)\}^{-1}dF_0(t)$	$Z=\int_{-\infty}^{+\infty}Z_t dw(t)$ where $Z_t=G_t^2=2N\left[F_N(t)\log\left\{\frac{F_N(t)}{F_0(t)}\right\}+\{1-F_N(t)\}\log\left\{\frac{1-F_N(t)}{1-F_0(t)}\right\}\right]$	ZC

In Table 4.2, the resultant test statistics ZK, ZA, and ZC are given as (Zhang, 2002)

$$ZK=\max_{1\le i\le N}\left(\left(i-\frac{1}{2}\right)\log\left\{\frac{i-\frac{1}{2}}{NF_0\left(X_{(i)}\right)}\right\}+\left(N-i+\frac{1}{2}\right)\log\left[\frac{N-i+\frac{1}{2}}{N\left\{1-F_0\left(X_{(i)}\right)\right\}}\right]\right) \quad (4.19)$$

$$ZA = -\sum_{i=1}^{N}\left[\frac{\log\left\{F_0\left(X_{(i)}\right)\right\}}{N-i+\frac{1}{2}} + \frac{\log\left\{1-F_0\left(X_{(i)}\right)\right\}}{i-\frac{1}{2}}\right] \tag{4.20}$$

$$ZC = \sum_{i=1}^{N}\left[\log\left(\frac{F_0^{-1}\left(X_{(i)}\right)-1}{\frac{\left(N-\frac{1}{2}\right)}{\left(i-\frac{3}{4}\right)}-1}\right)\right]^2. \tag{4.21}$$

Since the test statistics ZK, ZA, and ZC use the likelihood ratio, they are alternatively named as LLR based GOF tests. According to Zhang (2002), the LLR based GOF tests are more successful compared to traditional GOF tests (AD, KS, and CM).

4.2.5 OS based GOF Testing

OS based GOF testing is one of the GOF testing methods that uses the quantiles of the observed data to measure the degree of fit of a distribution to data. In this technique, decision is taken by using the ρ-vector of the data (Rostami et al., 2012). ρ-vector is considered in several studies on OS based GOF tests (Glen, Leemis, & Barr, 2001). Thus, calculation of ρ-vector is very crucial in OS based spectrum sensing. Computation of the ρ-vector can be carried out using the following steps (Rostami et al., 2012):

Step #1- Transformation: Elements of the received signal vector, $\boldsymbol{x}$, are transformed via the known noise CDF, $F_0(x)$ as

$$z_i = F_0(x_i), \quad i = 1, 2, \ldots, N \tag{4.22}$$

Then, a new vector $\boldsymbol{z} = \left[z_1, z_2, \ldots, z_N\right]^T$ is defined.

Step #2 - Sorting: Elements of $\boldsymbol{z}$ are arranged in ascending order of magnitude as $z_{(1)} \le z_{(2)} \le \ldots \le z_{(N)}$. The sorted vector $\tilde{\boldsymbol{z}} = \left[z_{(1)}, z_{(2)}, \ldots, z_{(N)}\right]^T$ is formed.

Step #3 - Beta Transformation: By transforming the elements of $\tilde{\boldsymbol{z}}$ using Beta CDF, elements of ρ-vector are obtained as $\rho_i = F_\beta\left(z_{(i)}; i, N-i+1\right)$. Thus, ρ-vector is formed as $\boldsymbol{\rho} = \left[\rho_1, \rho_2, \ldots, \rho_N\right]^T$. Here, $F_\beta\left(y; \alpha, \beta\right)$ denotes the Beta CDF with shape parameters α and β.

After this step has been completed, various test statistics based on ρ-vector can be defined. For example, some candidate test statistics are given below (Glen et al., 2001)

$$T_{OS}^1 = \sum_{i=1}^{N} \left|\rho_i - 0.5\right|, \quad T_{OS}^2 = \sum_{i=1}^{N} \left(\rho_i - 0.5\right)^2, \text{ etc.} \tag{4.23}$$

Also in Rostami et al. (2012), the authors state that based on simulations, they could obtain the maximum probability of detection using the following test statistic

$$T_{OS}^3 = \sum_{i=1}^{N} \left| \rho_{(i)} - \frac{i}{\left(N+1\right)^2} \right| \tag{4.24}$$

where $\rho_{(i)}$ is the i^{th} element of the sorted ρ-vector (in ascending order).

In the end, a decision is taken by comparing the test statistic with a pre-determined threshold, γ_{OS}, as in other GOF test statistics. This can be expressed as

$H_0 : T_{OS} \leq \gamma_{OS}$, channel is idle,

$H_1 : T_{OS} > \gamma_{OS}$, channel is busy.

Up to now, the following GOF tests have been introduced:

- AD Test
- KS Test
- CM Test
- LLR based tests (ZK, ZA, ZC)
- OS based test.

In the next section, simulation results based on these tests are presented. In addition, a new GOF test which is also based on OS is proposed for detection of dynamic PUs with different signalling schemes.

4.3 Simulation Studies

In this section, simulation results for perfomance analysis of GOF tests will be presented. Besides, a new OS based test statistic is presented. Before discussing the results, the mathematical model used in the simulations is introduced.

The studies on GOF based spectrum sensing generally use the following system model

$$\begin{aligned} H_0 &: x[n] = w[n], \qquad n = 1, 2, \ldots, N \\ H_1 &: x[n] = s[n] + w[n], \qquad n = 1, 2, \ldots, N \end{aligned} \tag{4.25}$$

where $s[n]$ is the PU signal, $w[n]$ is white Gaussian noise with $\mathcal{N}(0,1)$ and N is the total number of observed samples. In Lei et al. (2011), Rostami et al. (2012) and H. Wang et al. (2009), the PU signal $s[n]$ is assumed to be equal to 1, i.e. a DC

signal with unit amplitude. According to this signal model (where the PU signal is a constant DC value), GOF tests can outperform ED (H. Wang et al., 2009; Lei et al., 2011; Rostami et al., 2012). In Figure 4.1, detection performances of GOF tests and ED are shown using ROC curves. The considered techniques are labelled in figures as "OS" for order statistics based algorithm given in Rostami et al. (2012), "ED" for energy detector, "ZK", ZC", and "ZA" for the LLR based GOF tests, "AD" for Anderson-Darling test, "KS" for Kolmogorov-Smirnov test and "CM" for Cramer-von Misses test. In Figure 4.1, it is assumed that the PU signal $s[n]=1$, SNR=–5 dB, and $N=50$. Data under hypotheses H_0 and H_1 have been generated for 10^5 times, and for each iteration, the considered methods are calculated for both hypotheses. At the end of the iterations, ROC curves have been plotted using those obtained values.

When we look at Figure 4.1, it is clear that GOF tests show better detection performance than ED in terms of P_D vs. P_{FA}.

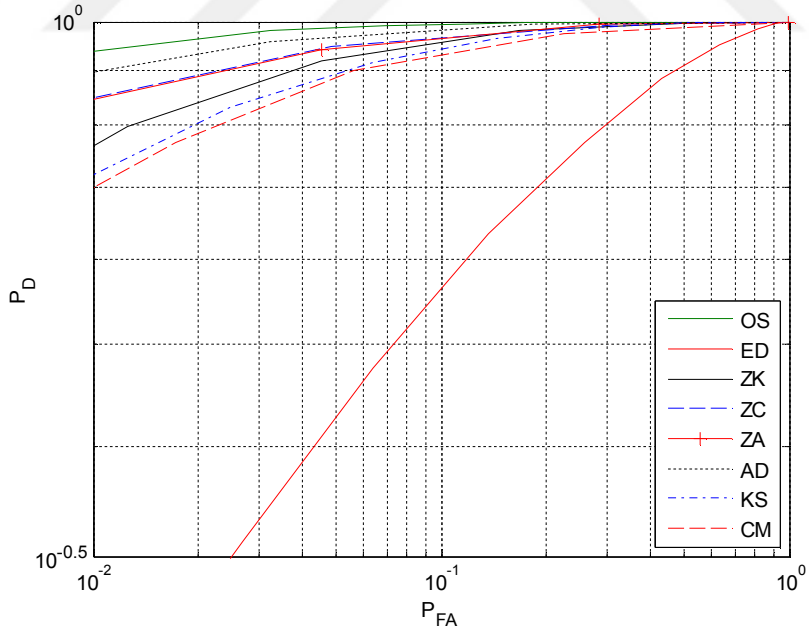

Figure 4.1 P_D vs. P_{FA} for a DC PU signal. SNR= –5 dB and $N=50$.

Even though all of the GOF tests outperform ED in Figure 4.1, it is stated in N.-Thanh et al. (2012) that these results are valid only when the PU signal is assumed to be constant (or DC signal). In the same study, it is claimed that DC signals are used very rarely in communication systems and more realistic signal types should be used for simulations. Therefore, the following signal models are used in N.-Thanh et al. (2012) to obtain more realistic performance results:

1) PU signal includes only one single carrier frequency f_c as in the following sine waveform

$$m(t) = A\sin\left(2\pi f_c t + \varphi\right) \tag{4.26}$$

where A is the amplitude of the signal and φ is the arbitrary initial phase. The discrete version of $m(t)$ is given as

$$m_i = A\sin\left(\frac{2\pi}{K} i + \varphi\right),\ i = 1, 2, \ldots, N \tag{4.27}$$

where $K = f_s / f_c$ is the ratio between the sampling frequency and the carrier frequency. In simulations, K is assumed to be 6 similar to N.-Thanh et al. (2012).

2) The second signal model used in the simulations is based on Gaussian distribution. This model can also be considered as a realistic signal model since the signal arriving at the CR receiver might actually correspond to a sum of multiple non-line-of-sight propagation signals as stated in N.-Thanh et al. (2012). According to this scheme, a random PU signal is generated using the distribution $\mathcal{N}\left(0, \sigma_s^2\right)$ where σ_s^2 is the variance of the PU signal.

In Figure 4.2, results for PU $\sim \mathcal{N}\left(0, \sigma_s^2\right)$ are shown. It is clear from Figure 4.2 that GOF tests show considerably worse probability of detection performances compared

to ED. However, all these tests were more successful than ED in Figure 4.1 where a DC signalling scheme was used. Therefore, application of GOF testing to spectrum sensing in CR requires further investigation.

It is intuitive that increasing the number of observed samples provides an enhancement in probability of detection performance. This can also be seen from Figure 4.3 where $N = 100$. Compared to Figure 4.2, an enhancement in detection performance is observed for most of the considered methods.

It is clear from Figures 4.2 and 4.3 that increasing the number of observed samples (or length of the sensing period) also increases the detection performance for all the considered techniques. However, use of longer sensing periods will increase the possibility of PU status changes in the channel. This will affect the detection performance negatively. Therefore, PU traffic in the channel should also be taken into consideration.

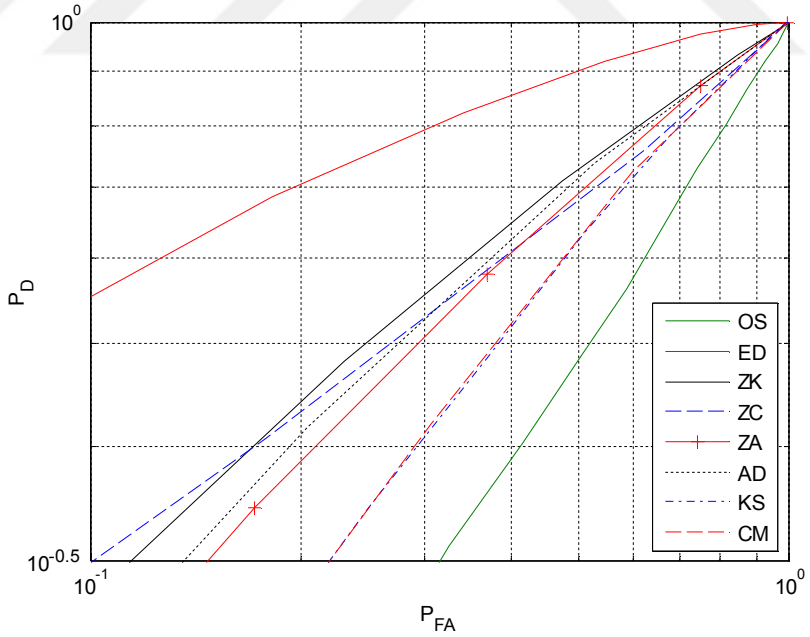

Figure 4.2 P_D vs. P_{FA} for $s[n] \sim \mathcal{N}\left(0, \sigma_s^2\right)$. SNR= –5 dB and $N = 50$.

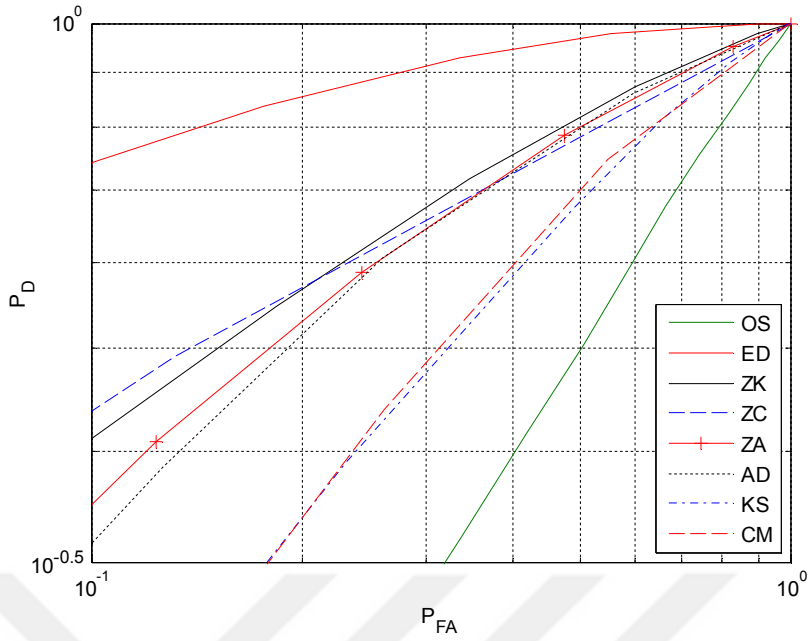

Figure 4.3 P_D vs. P_{FA} for $s[n] \sim \mathcal{N}\left(0, \sigma_s^2\right)$. SNR= –5 dB and $N = 100$.

For a channel containing one PU status change, the mathematical model can be redefined as follows;

$$\begin{aligned} H_{01} &: x[n] = w[n], && n = 1, 2, \ldots, N \\ H_{02} &: x[n] = m[n] + w[n], && n = 1, 2, \ldots, i_1 \\ & x[n] = w[n], && n = i_1 + 1, i_1 + 2, \ldots, N \end{aligned} \tag{4.28}$$

$$\begin{aligned} H_{11} &: x[n] = m[n] + w[n], && n = 1, 2, \ldots, N \\ H_{12} &: x[n] = w[n], && n = 1, 2, \ldots, j_1 \\ & x[n] = m[n] + w[n], && n = j_1 + 1, j_1 + 2, \ldots, N \end{aligned}$$

where H_{01} and H_{02} are the sub-hypotheses of H_0 and similarly, H_{11} and H_{12} are the sub-hypotheses of H_1. i_1 and j_1 are the departure and arrival points for the PU under H_{02} and H_{12}, respectively. We assume that the sub-hypotheses H_{01} and H_{02}

have equal probabilities of occurrence under hypothesis H_0. Similarly, H_{11} and H_{12} have equal probabilities of occurrence under H_1, as well.

Simulation results obtained by assuming that there is only one PU status change in the channel are shown in Figure 4.4. Poisson distribution has been used to assign the change point during simulations since this distribution is widely used for traffic modelling in the literature (Beaulieu & Chen, 2010; Shim et al., 2013). The arrival rate and departure rate have been selected as $\lambda_a = \lambda_d = 1$ for the simulations. The performance degradation for all the methods is apparent in Figure 4.4.

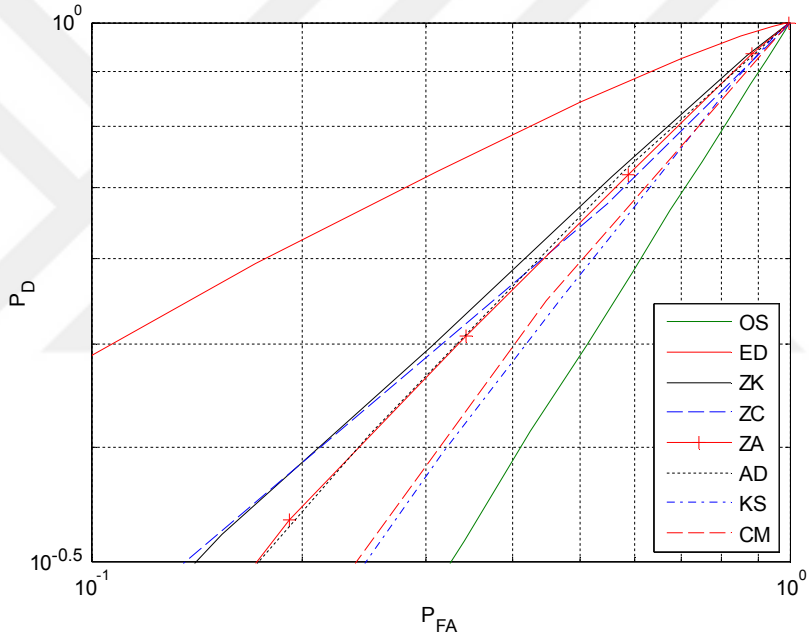

Figure 4.4 P_D vs. P_{FA} for $\lambda_a = \lambda_d = 1$, $s[n] \sim \mathcal{N}\left(0, \sigma_s^2\right)$, SNR= –5 dB, and $N = 100$.

Up to now, it has been shown that a certain degree of performance degradation occurs for GOF tests when a different signalling scheme is used rather than the DC signal. Also, this degradation becomes much worse with PU traffic in the channel caused by longer sensing periods.

At this point, we propose an OS based GOF test which shows better performance under PU traffic. The proposed test statistic differs from the conventional OS since it

weights latter samples in the sensing period with higher values. The test statistic used in our algorithm has been obtained by maximizing the probability of detection via modifying the test statistic in Equation (4.24) as

$$T_N = \sum_{i=1}^{N} \left| \rho_{(\mathrm{i})}^{\frac{i}{(N+1)}} - \frac{i}{(N+1)^2} \right| \tag{4.29}$$

The proposed algorithm has the following steps:

Step #1. Take the weighted sum of axis-reversed and squared observed samples and perform a normalization by dividing the result to the square of the length of the sensing period

$$y_i = \frac{1}{N^2} \sum_{n=1}^{i} (N-n+1)\, x^2 [N-n+1] \tag{4.30}$$

and form $\boldsymbol{y} = [y_1, y_2, \ldots, y_N]^T$.

Step #2. Calculate the values of Chi-square CDF with one degree of freedom evaluated at the elements of $\boldsymbol{y}$ obtained in Step #1

$$z_i = F_{\chi_1^2}(y_i), \quad i = 1, 2, \ldots, N. \tag{4.31}$$

Here, $F_{\chi_1^2}(\cdot)$ corresponds to Chi–square CDF with one degree of freedom (Johnson, Kotz, & Balakrishnan, 1994). Then, define $\boldsymbol{z} = [z_1, z_2, \ldots, z_N]^T$.

Step #3. Arrange the elements of $\boldsymbol{z}$ in ascending order of magnitude as $z_{(1)} \le z_{(2)} \le \ldots \le z_{(N)}$ and form the sorted vector $\tilde{\boldsymbol{z}} = \left[z_{(1)}, z_{(2)}, \ldots, z_{(N)} \right]^T$.

Step #4. Transform the elements of $\tilde{z}$ using Beta CDF, to obtain ρ-vector as $\rho_i = F_\beta\left(z_{(i)}; i, N-i+1\right)$ and $\boldsymbol{\rho} = \left[\rho_1, \rho_2, \ldots, \rho_N\right]^T$. Here, $F_\beta\left(y; \alpha, \beta\right)$ denotes Beta CDF with shape parameters α and β.

Step #5. Sort the elements of $\boldsymbol{\rho}$ in ascending order of magnitude as $\rho_{(1)} \leq \rho_{(2)} \leq \ldots \leq \rho_{(N)}$.

Step #6. Calculate the test statistic in Equation (4.29) using sorted $\boldsymbol{\rho}$ values.

Step #7. Take a decision by comparing the result of the test statistic with a pre-determined threshold, γ_{T_N}, as in other GOF test statistics

$$\begin{aligned} H_0 &: T_{proposed} \leq \gamma_{T_N}, \quad \text{channel is idle} \\ H_1 &: T_{proposed} > \gamma_{T_N}, \quad \text{channel is busy.} \end{aligned} \tag{4.32}$$

Simulation results of the proposed algorithm are shown in Figures 4.5 and 4.6 where the proposed algorithm is labelled as "T_N". It is assumed that PU randomly arrives at or departs from the channel during the sensing period according to Poisson process with unity arrival and departure rates $\lambda_a = \lambda_d = 1$.

In Figure 4.5, the simulation results are shown when the PU signal is Gaussian distributed, PU $\sim \mathcal{N}\left(0, \sigma_s^2\right)$ where the variance is taken as $\sigma_s^2 = 0.3162$ to obtain an SNR value of -5 dB. According to Figure 4.5, it is clear that the proposed algorithm shows the best performance in terms of P_D. It also achieves a better detection performance than ED.

In Figure 4.6, the PU signal is obtained using the definition given in Equation (4.27) with $K = 6$, $\varphi = \frac{\pi}{4}$, and $A = 0.7953$ corresponding to an SNR level of -5

dB. According to Figure 4.6, a performance degradation is observed compared to Figure 4.5 particularly for OS based sensing. For other techniques, similar results as with the Gaussian PU signal (Figure 4.5) are obtained.

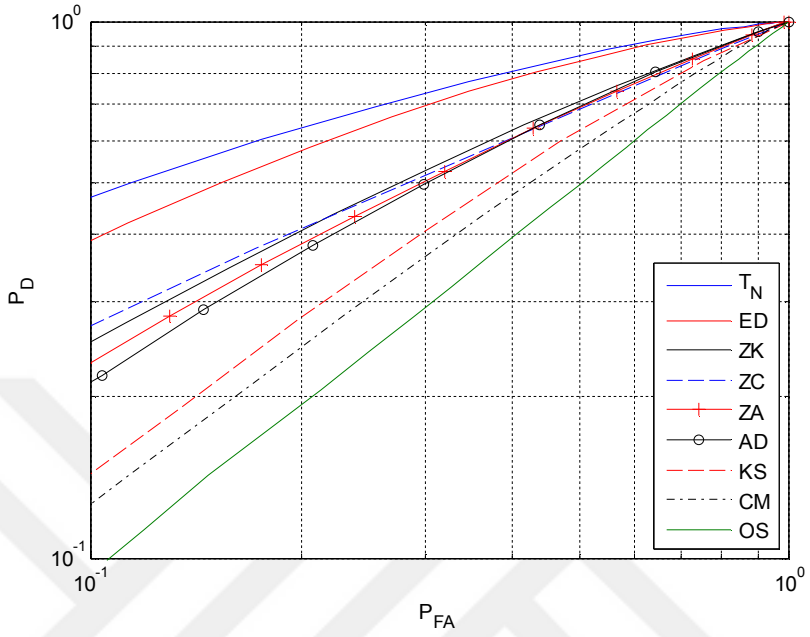

Figure 4.5 P_D vs. P_{FA} for $\lambda_a = \lambda_d = 1$, SNR= –5 dB, $N = 100$, and $s[n] \sim \mathcal{N}(0, 0.3162)$.

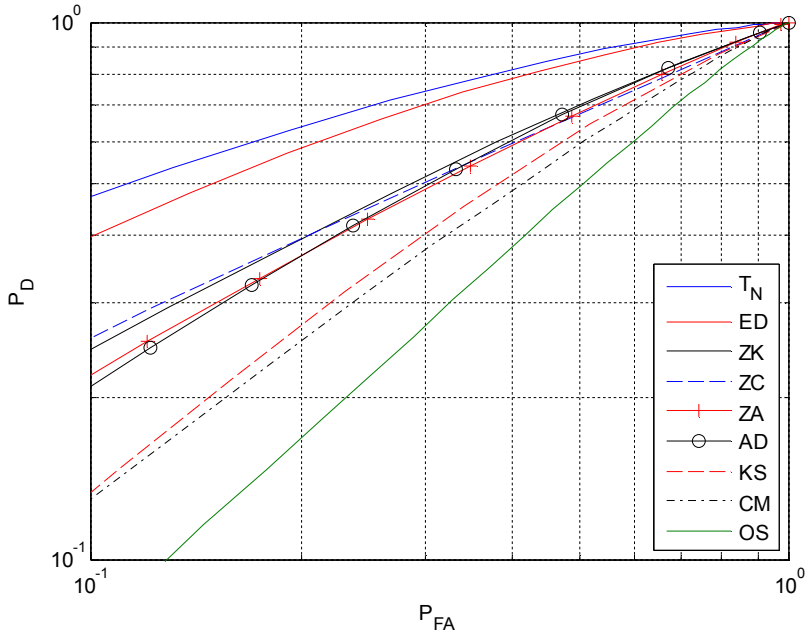

Figure 4.6 P_D vs. P_{FA} for $\lambda_a = \lambda_d = 1$, SNR= –5 dB, $N = 100$, and $s[n] = 0.7953 \sin\left(\frac{\pi}{3}n + \frac{\pi}{4}\right)$.

As a more general case, complex valued PU signals are also considered during the simulations. According to this scheme, as the first signal model, the sinusoidal carrier introduced in Equation (4.26) is converted into a complex exponential as

$$m(t) = Ae^{j(2\pi f_c t+\varphi)} \tag{4.33}$$

where A is the magnitude of the complex exponential signal and φ is the arbitrary initial phase as in Equation (4.26). The discrete version of $m(t)$ in Equation (4.33) is given as

$$m_i = Ae^{j\left(\frac{2\pi}{k}i+\varphi\right)} \tag{4.34}$$

where $K = f_s / f_c$ is the ratio between the sampling frequency and the carrier frequency.

In the second signal model, a zero-mean circularly symmetric complex Gaussian (CSCG) model with $s[n] \sim \mathcal{CN}\left(0, \sigma_s^2\right)$ is used as the PU signal. This signal model is often used in the literature to represent unknown PU signals (Kortun et al., 2010; Kundargi & Tewfik, 2010; Lim et al., 2009; Ma et al., 2008; Moragues et al. 2009).

For both complex exponential and CSCG distributed PU signal models, noise is assumed to be zero mean CSCG with $w[n] \sim \mathcal{CN}(0,1)$. The magnitude of the complex exponential, A, and the variance of the CSCG PU signal, σ_s^2, are obtained based on the given SNR values. It is assumed that one PU status change may occur with a probability of 0.5 based on the model given in Equation (4.28). For all the considered techniques, the magnitude of the complex valued PU signal is used in calculation of test statistics.

In Figures 4.7 and 4.8, the length of the observation vector is taken as $N=100$ and SNR is assumed to be equal to -5 dB as in Figures 4.5 and 4.6. In addition, data under hypotheses H_0 and H_1 are generated according to Equation (4.28) for 10^5 times. For each iteration, the methods considered in this report have been calculated for both hypotheses. ROC curves have been plotted according to the obtained values at the end of the iterations.

In Figure 4.7, it is assumed that the PU signal is a complex exponential defined according to Equation (4.34) with $K=6$, $\varphi=\frac{\pi}{4}$, and $A=0.5623$ as corresponding to the SNR level of -5 dB. At first glance, it is seen from Figure 4.7 that the detection performance of OS based technique achieves higher P_D performance compared to Figure 4.5 and CM test has the lowest P_D values. A degradation is also observed for P_D performance of LLR test statistic ZK, although this is not the case for other LLR based test statistics ZA and ZC. Indeed, an enhancement is seen for all the other methods except ZK and CM in Figure 4.7. As a final comment, our proposed sensing algorithm outperforms other techniques in terms of detection performance as in Figure 4.5.

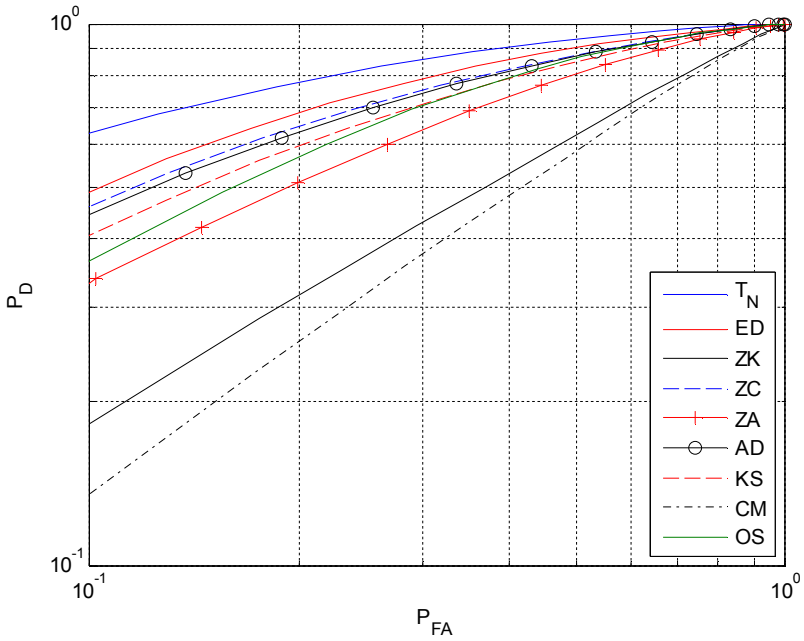

Figure 4.7 P_D vs. P_{FA} for $\lambda_a=\lambda_d=1$, SNR= -5 dB, $N=100$, and $s[n]=0.5623e^{j\left(\frac{\pi}{3}n+\frac{\pi}{4}\right)}$.

In Figure 4.8, it is assumed that the PU signal is CSCG given as $s[n] \sim \mathcal{CN}\left(0, \sigma_s^2\right)$ where the variance is taken as $\sigma_s^2 = 0.3162$ to obtain an SNR value of -5 dB. According to Figure 4.8, CM test still has the lowest detection performance in terms of P_D and ZK has the lowest P_D values again among the other LLR based tests. As in complex exponential PU signal, our proposed algorithm shows the highest detection performance followed by ED.

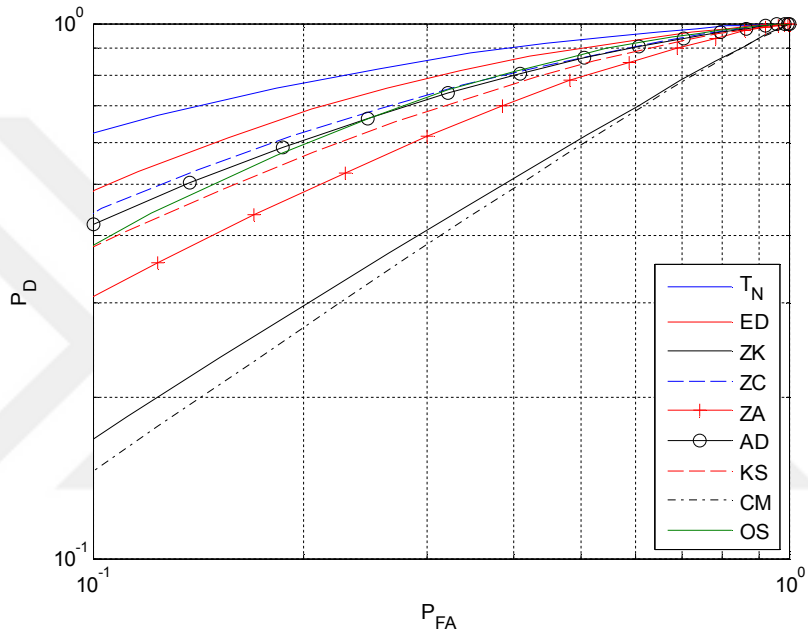

Figure 4.8 P_D vs. P_{FA} for $\lambda_a = \lambda_d = 1$, SNR= -5 dB, $N = 100$, and $s[n] \sim \mathcal{CN}\left(0, 0.3162\right)$.

Considering both Figures 4.7 and 4.8, it is possible to say that while the proposed algorithm has the highest detection performance among the considered techniques, it is also the most robust sensing method since its performance is independent of the PU signal being real or complex valued.

Performance of the considered techniques are also evaluated using P_D versus SNR plots as shown in Figures 4.9 and 4.10 where complex valued PU signals are used during the simulations. In both figures, P_{FA} is assumed to be equal to 0.1 and the threshold value for each method is obtained via simulations using this P_{FA} value.

It is assumed that one PU arrives at the channel under H_1 according to Poisson distribution with $\lambda_a = 1$ during the sensing period. Noise is given as $\mathcal{CN}(0,1)$ and the magnitude or variance of the complex PU signal is assigned based on the given SNR value.

In Figure 4.9, the simulation results are given for the case where the PU signal is assumed to be a complex exponential as $s[n] = Ae^{j\left(\frac{\pi}{3}n+\frac{\pi}{4}\right)}$ for $n = 1, 2, \ldots, N$. It can be seen that our proposed algorithm has the highest P_D values even at low SNR levels. Another interesting observation is that the CM test shows higher detection performance than ZA and ZK tests particularly when SNR is less than -5 dB, even though the CM test displayed the lowest P_D values in Figures 4.7 and 4.8. Therefore, it is possible to say that the CM test is more robust to noise than the ZA and ZK tests.

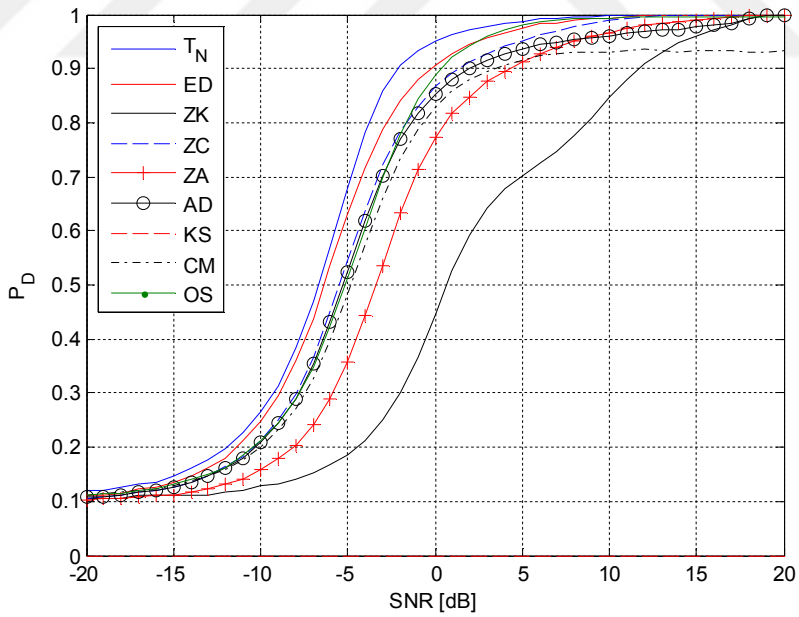

Figure 4.9 P_D vs. SNR for $\lambda_a = 1$, $P_{FA} = 0.1$, $N = 100$, and $s[n] = Ae^{j\left(\frac{\pi}{3}n+\frac{\pi}{4}\right)}$.

In Figure 4.10, the simulation results are shown for the case when the PU signal is assumed to be Gaussian distributed, $s[n] \sim \mathcal{CN}\left(0, \sigma_s^2\right)$. The variance of the PU

signal, σ_s^2, is determined using the given SNR values in the simulations. It is seen that our proposed algorithm outperforms other techniques again in terms of P_D. ED and OS based sensing algorithms follow it. As in Figure 4.9, the CM test shows better detection performance than ZK and ZA particularly at low SNR values. Also, it is worth to note that almost all the techniques suffer from a slight performance degradation.

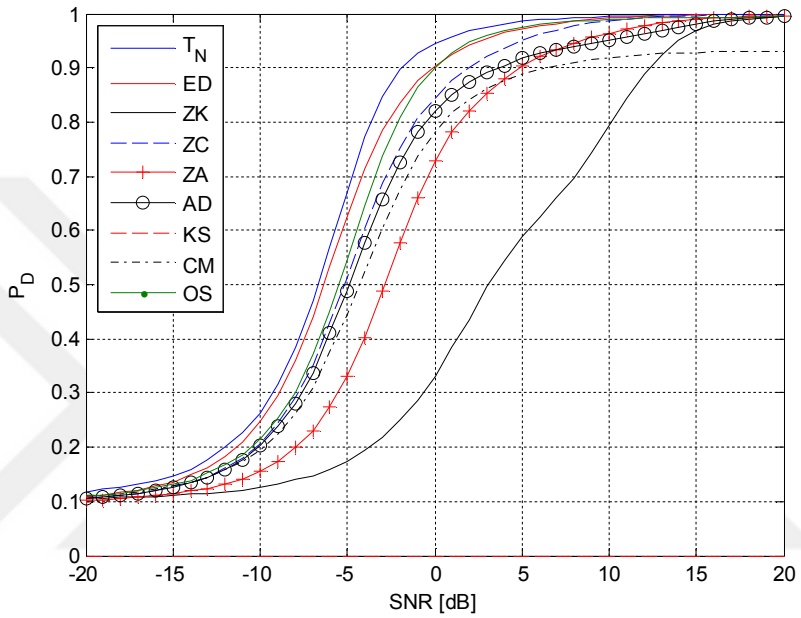

Figure 4.10 P_D vs. SNR for $\lambda_a = 1$, $P_{FA} = 0.1$, $N = 100$, and $s[n] \sim \mathcal{CN}\left(0, \sigma_s^2\right)$.

CHAPTER FIVE
PREDICTION OF CHANNEL STATUS IN COGNITIVE RADIO

In this chapter of the dissertation, issue of channel status prediction in CRs is investigated. Simulations are performed using correlation based prediction techniques introduced by Uyanik, Canberk, & Oktuğ (2012) and the prediction scheme given in Liu et al. (2012). Two novel prediction algorithms are proposed. Based on simulation results, we can state that the proposed methods display high prediction performance in terms of two performance metrics which are System Utility (SYSU) and Primary User Disturbance Ratio (PUDR) (Uyanik et al., 2012).

In general, most of the previously proposed spectrum sensing techniques in CR perform analyses to obtain current status of the channel. However, the channel status may show variability in the future sensing periods causing interference between the primary and secondary users. Furthermore, not knowing the trend of the channel may prevent the SU from accessing the spectrum holes, and therefore may cause losing of spectral opportunities. Hence, it is critical to predict future status of the channel for protecting the PU from interferences and for more efficient use of the spectral vacancies by SU. To solve the prediction problem in CR, various algorithms are proposed in this chapter.

There are two sections in this chapter which discuss prediction issue assuming that the PU traffic density is homogeneous (PU traffic density does not depend on time) and non-homogeneous (PU traffic density changes with time). For both cases, Poisson distribution is used to model the PU traffic by utilizing constant and variable rates to determine the arrival and departure times of the PU. For the case of non-homogeneous PU traffic, the arrival and departure rates are assumed to be obtained based on a stochastic distribution.

In Section 5.1, correlation based prediction techniques introduced by Uyanik et al. (2012) are discussed first. Then, assuming that the PU traffic density is constant and does not change with time, a prediction algorithm based on the previously given

decisions in the channel is proposed. At the end of the section, simulation results are presented in terms of SYSU and PUDR.

In Section 5.2, PU traffic density is assumed to be non-homogeneous as a more realistic scenario such that the arrival and departure rates change stochastically with time. In this scenario, a prediction algorithm based on transition probabilities between the states of the channel is proposed. At the end of the section, performance of the proposed prediction algorithm is compared against correlation based techniques and the method proposed in Liu et al. (2012) since it is a similar prediction technique.

5.1 Prediction of Channel Status for Homogeneous PU Traffic Density

In this section, constant arrival and departure rates are used to model the PU traffic in the channel. Before beginning to discuss the considered prediction methods, the parameters used in these techniques will be introduced. All the methods given in this section use the following two vectors which are named in Uyanik et al. (2012) as "history" and "prediction" windows. History window, W_H, contains the previously given binary decisions as 0 or 1 corresponding to "idle" or "busy" states in the past sensing periods, respectively, and the prediction window, W_P, contains the prediction results for the future sensing periods. The size of the prediction window is equal to 1 when the prediction is carried out for only the next sensing period. However, this size can be increased when it is desired to predict the further future states of the channel. In correlation based techniques, an additional parameter named as "Pearson correlation coefficient" is used (Uyanik et al., 2012). It is calculated as

$$P(\boldsymbol{x},\boldsymbol{r}) = \frac{1}{N-1}\sum_{i=1}^{N}\left(\frac{x(i)-E[\boldsymbol{x}]}{\sigma_x}\right)\times\left(\frac{r(i)-E[\boldsymbol{r}]}{\sigma_r}\right) \tag{5.1}$$

where $\boldsymbol{x}$ represents the sample index vector, $\boldsymbol{r}$ is the modeled PU activity sample vector, $E[\cdot]$ is the expectation operator, and σ denotes standart deviation. In

correlation based techniques, the result of Equation (5.1) is compared against some correlation threshold value, δ_C, and then, each algorithm performs prediction using different approaches based on the result of this comparison (Uyanik et al., 2012). The correlation based prediction methods will be discussed briefly in the following sections.

5.1.1 Correlation based Prediction Scheme

According to the correlation based prediction scheme, Pearson correlation coefficient is compared against a previously determined threshold, δ_C. If it is greater than the threshold, then the prediction window is filled with the last decision of the history window. If the correlation coefficient is smaller than δ_C, meaning that the decisions in the history window are uncorrelated with each other, then the majority of the decisions in the history window is obtained and assigned to cells in the prediction window. This procedure is summarized below in Figure 5.1 (Uyanik et al., 2012).

Require: W_H and δ_C.
$Majority\_Result \leftarrow Majority(W_H)$
if $|corr\_Coef(X, W_H)| > \delta_C$ **then**
$W_P \leftarrow [H_{|W_H|} \cdots H_{|W_H|}]$
else
$W_P \leftarrow [Majority\_Result \cdots Majority\_Result]$
end if
return Prediction vector W_P

Figure 5.1 Correlation based prediction algorithm.

5.1.2 Correlation and Linear Regression based Prediction

Correlation and linear regression based prediction technique is actually quite similar to correlation based prediction algorithm in Figure 5.1. Again, the Pearson correlation coefficient is calculated and compared against δ_C. If it is smaller than δ_C, then the majority of the decisions in the prediction window is considered as the prediction result. A difference occurs when the correlation coefficient is greater than δ_C. In this case, a linear regression analysis is carried out rather than directly assigning the last decision as in correlation based prediction algorithm.

In linear regression analysis step, it is aimed to locate a straight line on the history window by computing linear regression coefficients. This is illustrated in Figure 5.2.

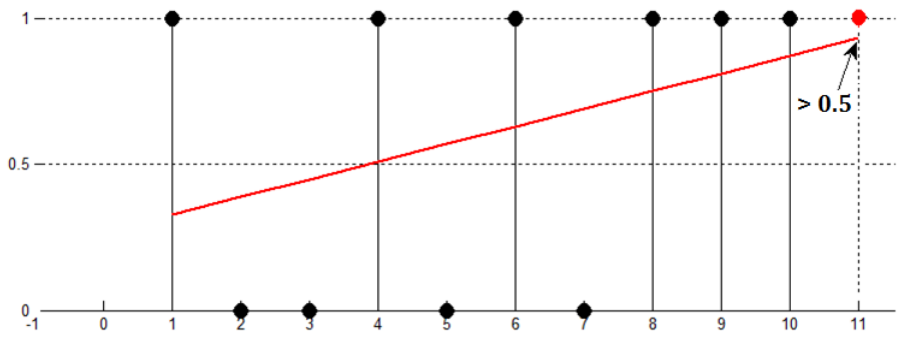

Figure 5.2 Schematic illustration of linear regression based prediction.

In Figure 5.2, the previously given decisions in the history window are shown. According to this figure, it is assumed that there are ten previously given decisions in the history window and it is aimed to predict the status of the channel in the next sensing period (the value at the 11^{th} index). The red line shows the values of linear regression coefficients. The coefficient at the 11^{th} index is greater than 0.5. Then, the prediction window is filled with 1 meaning that the channel will be in busy status. If it is smaller than 0.5, then the prediction result becomes zero meaning that the channel is idle. This procedure is summarized in Figure 5.3 (Uyanik et al., 2012).

Require: W_H and δ_C.

$Majority\_Result \leftarrow Majority(W_H)$

if $|corr\_Coef(X, W_H)| > \delta_C$ **then**

$W_P \leftarrow$ Binary decisions obtained by linear regression

(Obtain binary values by comparing linear regression coefficients with 0.5)

else

$W_P \leftarrow [Majority\_Result \cdots Majority\_Result]$

end if

return Prediction vector W_P

Figure 5.3 Correlation and linear regression based prediction algorithm.

5.1.3 Autocorrelation based Prediction Scheme

In this technique, autocorrelation coefficients of the decisions in the history window are calculated at different lag points. If there is a periodicity in the decisions, this will appear at the lag point where the second largest autocorrelation coefficient is located. In this way, a nearly periodic pattern in the history window is obtained and the prediction is carried out by considering the elements of this periodic pattern vector. An illustration which makes understanding the autocorrelation based prediction scheme easier is shown in Figure 5.4.

In Figure 5.4, a similar history window as in Figure 5.2 is used for illustration purposes. According to the obtained autocorreleation coefficients in Figure 5.4, the second largest peak is at the lag value of 2. This means that a nearly periodic pattern (with a period of two samples) is present in the history window and the prediction of next sensing period can be performed by copying this pattern as the prediction period as shown in Figure 5.4. The pseudo-code of the algorithm is given in Figure 5.5 (Uyanik et al., 2012).

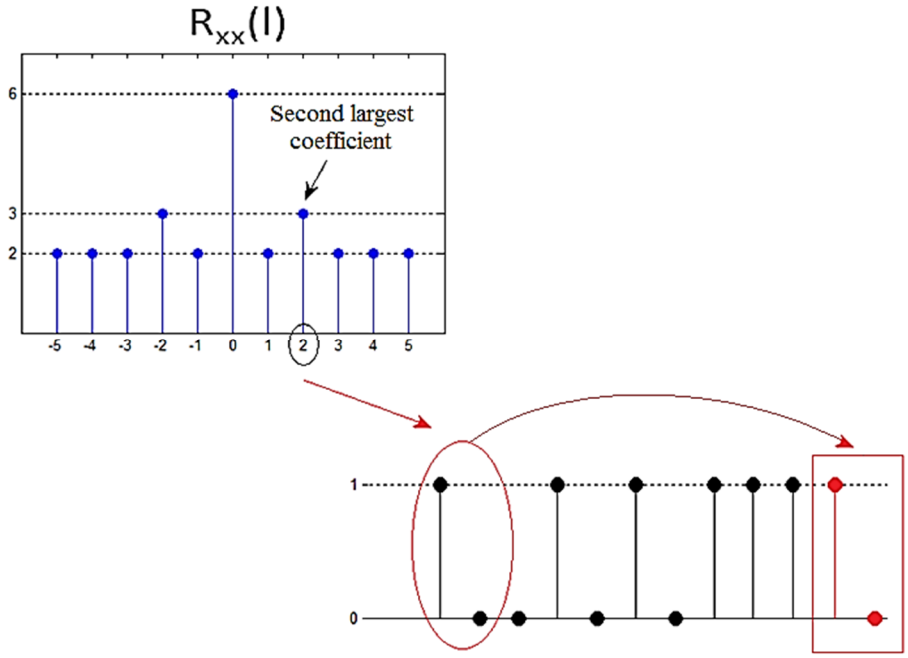

Figure 5.4 Autocorrelation based prediction.

Require: W_H and δ_C.

$Majority\_Result \leftarrow Majority(W_H)$

Obtain autocorr. coefficients of W_H up to lag $|W_H|/2$

$max\_Coeff \leftarrow \max(coefficients)$

if $|corr\_Coef(X, W_H)| > \delta_C$ **then**

$periodicity \leftarrow$ lag number of max_Coeff

$W_P \leftarrow$ Points Determined via Periodicity Analysis

else

$W_P \leftarrow [Majority\_Result \cdots Majority\_Result]$

end if

return Prediction vector W_P

Figure 5.5 Autocorrelation based prediction algorithm.

5.1.4 Proposed Prediction Scheme

In our proposed prediction scheme, history and prediction windows are utilized as well. Some additional parameters, which are based on empirical rates of arrivals and departures, are also used. These parameters can be listed as follows (Düzenli & Akay, 2014; Kababulut et al., 2015):

- *Rate_of_arrivals*: Ratio of number of 0-1 transitions in the history window to history window length.

- *Rate_of_departures*: Ratio of number of 1-0 transitions in the history window to history window length.

- *Last_active_index*: Index of the last sample of history window where decision of 1 is located.

- *Last_idle_index*: Index of the last sample of history window where decision of 0 is located.

These four parameters are illustrated in Figure 5.6. According to this figure, a departure in the channel corresponds to a 1-0 transition in the history window and inversely, an arrival is shown by a 0-1 transition. Rates of arrivals and departures can be found by counting the 1-0 and 0-1 transitions in the history window, respectively, and then dividing the total number of these transitions to the history window length. As shown in Figure 5.6, the *last_active_index* and *last_idle_index* are the indices of the last "1" and last "0" decisions in the history window, respectively.

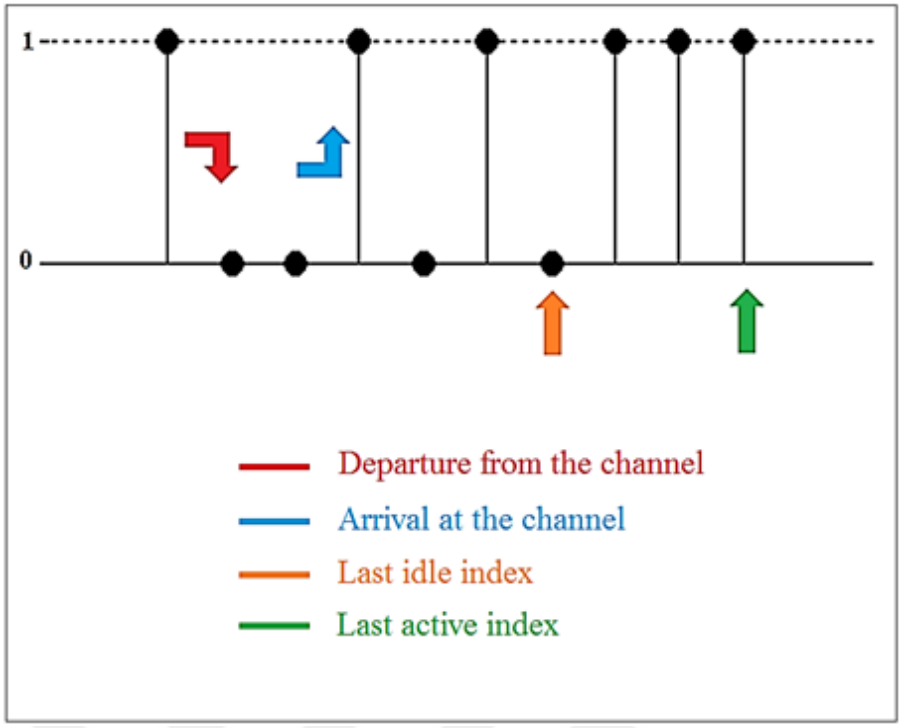

Figure 5.6 Illustration of four parameters used in our proposed algorithm.

As stated in Kay (1998), the reciprocal of the arrival and departure rates represent the average busy and idle durations, respectively. Using this knowledge, it can be said that the channel will tend to be busy if the length of the samples between *last_idle_index* and the next sensing period is smaller than the mean busy duration of the PU. Similarly, if the length of the samples between *last_active_index* and the next sensing period is smaller than the mean idle duration of the PU, then the decision for the next period will tend to be idle again. Before these comparisons, it must be checked whether *last_active_index* is greater than *last_idle_index* or not. This scheme is summarized in Figure 5.7 below.

Require: W_H , $rate\_of\_arrivals$, $rate\_of\_departures$, $last\_active\_index$ and $last\_idle\_index$.

if $last\_active\_index > last\_idle\_index$ **then**

$W_P \leftarrow \left(|W_H| - last\_idle\_index < rate\_of\_arrivals^{-1}\right)$

else

$W_P \leftarrow \left(|W_H| - last\_active\_index > rate\_of\_departures^{-1}\right)$

end if

return Prediction vector W_P

Figure 5.7 Proposed algorithm.

5.1.5 Simulation Results

At the simulation stage, two new performance metrics introduced in Uyanik et al. (2012) are used.

These metrics are given as:

System Utility (SYSU): This metric shows the ratio between the succesfully used slots (PU prediction is correct on null hypothesis) and the number of overall spectrum hole slots as shown in Equation (5.2). SYSU represents how the SU successfully used the channel without a collision with the PU

$$SYSU = \frac{Number\ of\ Succesfully\ Used\ Slots}{Number\ of\ Spectrum\ Hole\ Slots}. \tag{5.2}$$

Primary User Disturbance Ratio (PUDR): Definition of PU Disturbance Ratio is given as

$$PUDR = \frac{Number\ of\ Collision\ Slots}{Number\ of\ Active\ PU\ Slots}. \tag{5.3}$$

According to Equation (5.3), PUDR shows the rate of collisions between SU and PU. In the ideal case, it is desired that SYSU and PUDR equal to 1 and 0, respectively.

In this section, it is assumed that the channel is used by the PU with a homogeneous Poisson traffic density. Average ON and OFF durations are taken to be equal to each other during the simulations. The related arrival and departure rates are assigned as $\lambda_a = \lambda_d = 0.2$ to get a high PU traffic density. In addition to this assumption, it is accepted that the decisions in the history window are correct corresponding to perfect spectrum sensing. In the simulations, AND and OR logics are also used for comparison in addition to correlation based techniques introduced in the previous sections. Although "majority" of the decisions is used in correlation based methods, it is also considered as an individual prediction technique during the simulations. Thus, the considered techniques are labelled in the figures as "AND", "OR", "MAJORITY", "CORRELATION", "LINEAR REGRESSION", "AUTO-CORRELATION", and "PROPOSED" for "and" logic, "or" logic, majority based prediction, correlation based prediction, correlation and linear regression based prediction, autocorrelation based prediction, and for our proposed algorithm, respectively.

For generating previously given decisions in the history window, homogeneous Poisson process is used. According to this process, exponentially distributed inter arrival times are generated first using the probability integral transformation. PDF of inter arrival times is given as

$$P_{T_k}(t_k) = \begin{cases} \lambda e^{-\lambda t_k} & ; t_k \geq 0 \\ 0 & ; otherwise \end{cases} \tag{5.4}$$

We can find the CDF by integrating the PDF of inter arrival times. After this integration, the following CDF is obtained

$$F_{T_k}(t_k) = 1 - e^{-\lambda t_k} . \tag{5.5}$$

Using the probability integral transformation, it is possible to generate any random variable with an arbitrary PDF via

$$Y = F_x^{-1}(u) \tag{5.6}$$

where u is a standard uniform random variable, $u \sim U(0,1)$, and $F_x^{-1}(\cdot)$ is the inverse of a previously known CDF. Using this technique, we can generate exponentially distributed inter arrival times.

First, $F_{T_k}^{-1}(t_k)$ is obtained from Equation (5.5) as

$$F_{T_k}^{-1}(t_k) = -\frac{1}{\lambda}\ln(1-t_k). \tag{5.7}$$

Then, it is possible to obtain the i^{th} arrival time as

$$t_i = t_{i-1} - \frac{1}{\lambda}\ln(1-u) \tag{5.8}$$

where $u \sim U(0,1)$. This procedure is illustrated in Figure 5.8.

Simulations have been carried out for 3 varying parameters which are given as

- History Window Length $|W_H|$, (Figure 5.9);
- Prediction Window Length $|W_P|$, (Figure 5.10);
- PU Traffic ON and OFF Durations ($1/\lambda$), (Figure 5.11).

In simulations, 150 runs have been carried out for each parameter value set. Each run has a length of 1000 simulation time units $(simTimeUnit)$ as stated in Uyanik et al. (2012).

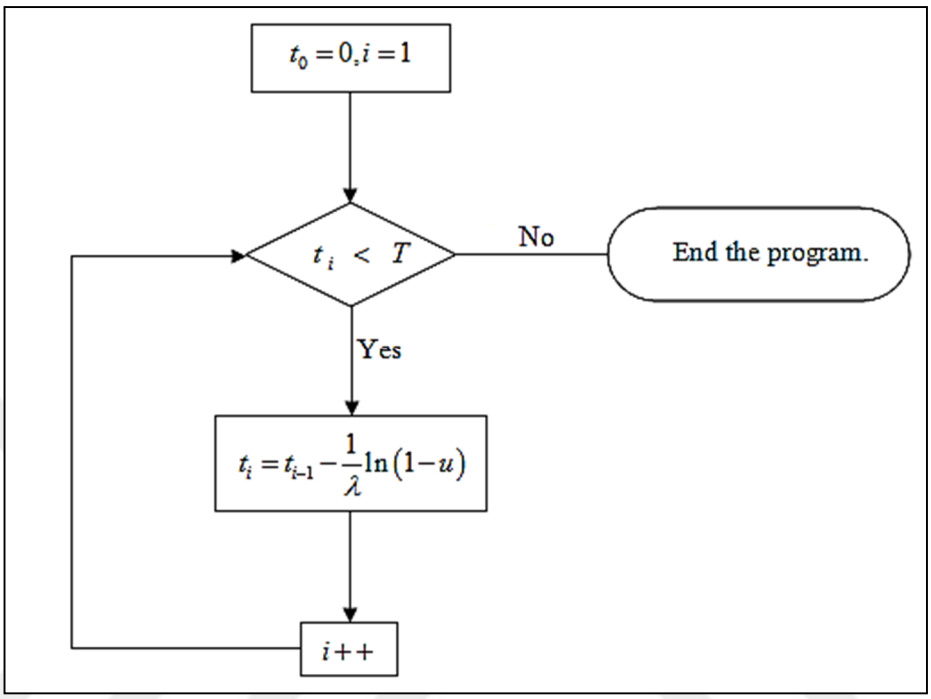

Figure 5.8 Flowchart of generating arrival times of Poisson process.

In Figure 5.9, it is shown how SYSU and PUDR react to different lengths of history window. The PU traffic rates are taken to be as $\lambda_{ON} = \lambda_{OFF} = 0.2$ $\left(simTimeUnit^{-1}\right)$, $|W_P| = 1$, and $\delta_C = 0.3$. The length of the history window varies as 5, 10, 20, and 30.

As expected, AND logic exhibits the highest performance in terms of SYSU since any existence of a "0" in the history window results in a "0" for the next decision period. However, it has also the highest PUDR among other methods.

OR logic shows the lowest collision rate in terms of PUDR in contrast to AND logic. This is expected since any presence of "1" in the history window will cause

SU to decide not to use the channel. This is the reason for the lowest SYSU performance of OR logic.

As far as the other methods are considered, it can be seen that a more balanced behaviour is present compared to AND and OR logic. Our proposed method is not affected from a change in the history window length since it assumes that the mean busy and idle durations are stationary for overall simulation process. Also, it outperforms other techniques (except AND and OR) in terms of SYSU and PUDR.

According to Figure 5.10, performance degradation is observed for all the considered techniques in terms of both SYSU and PUDR particularly for longer prediction window lengths. This performance decrease is reasonable since the accuracy of the prediction decreases when further predictions are carried out. AND and OR logic maintain their extreme behaviours compared to other methods. Our proposed method is noticeable here again among the other methods in terms of both performance parameters.

Finally, in Figure 5.11, the parameter λ has been changed and varied as $1/5$, $1/10, 1/20$, and $1/30$. Other parameters are given as, $|W_H|=10$, $|W_P|=1$, and $\delta_C=0.3$. By decreasing the value of λ, the mean durations of ON and OFF periods are increased referring to a lower PU traffic. It is intuitive that a performance enhancement (increase in SYSU and decrease in PUDR) is observed for all the methods. This is apparent in Figure 5.11. Under this scenario as well, our proposed algorithm exhibits a better performance compared to other techniques.

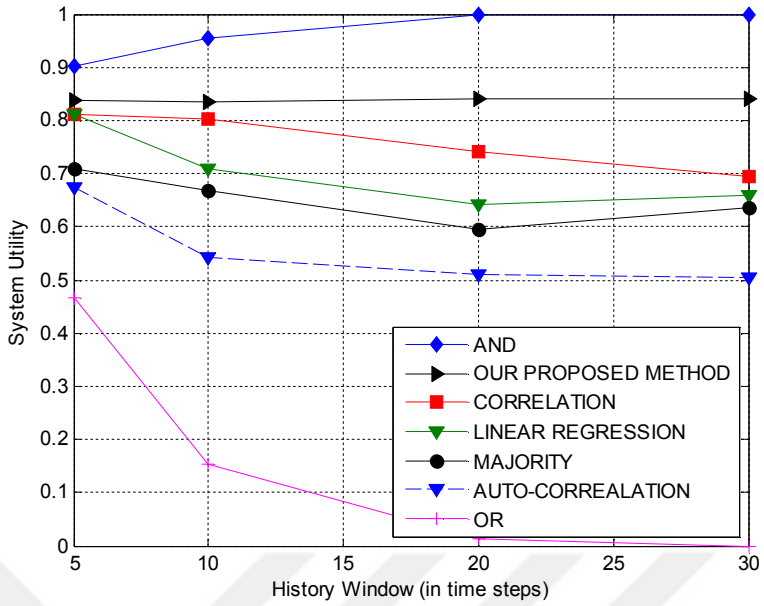

(a)

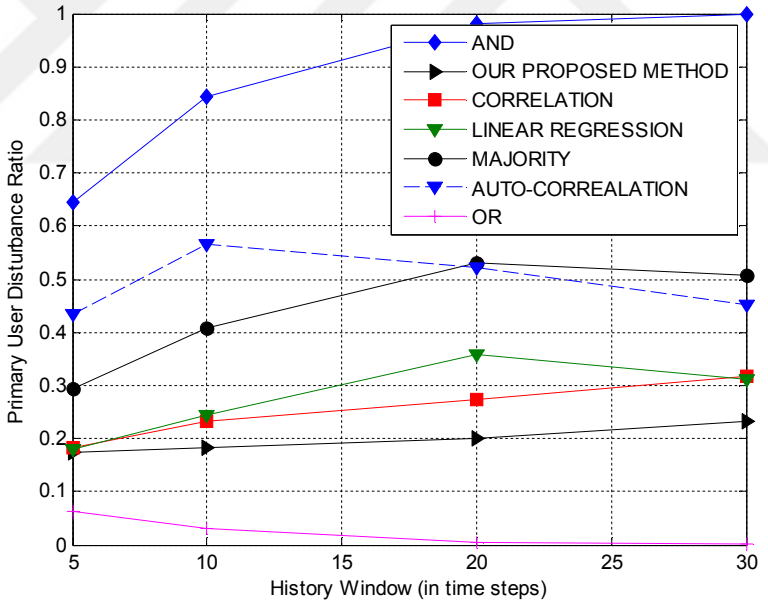

(b)

Figure 5.9 Performances of algorithms with varying history window sizes $|W_H|$. (a) System utility, (b) Primary user disturbance ratio.

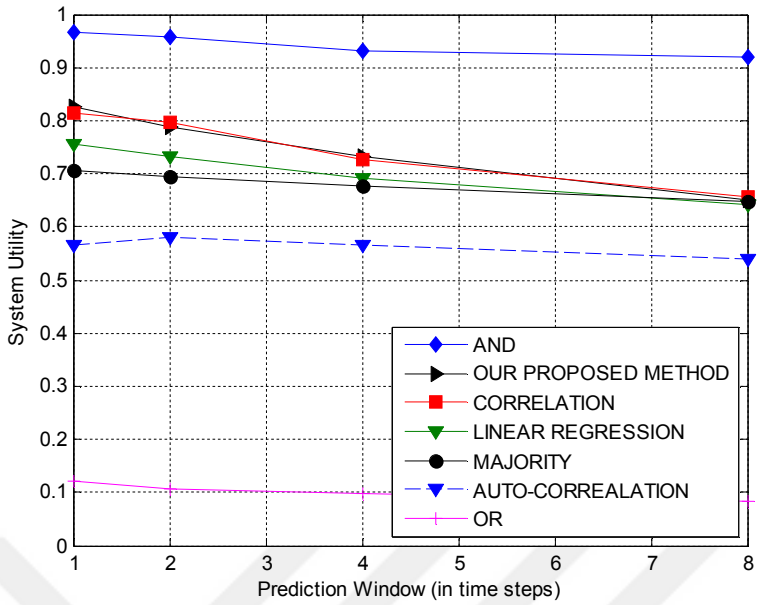

(a)

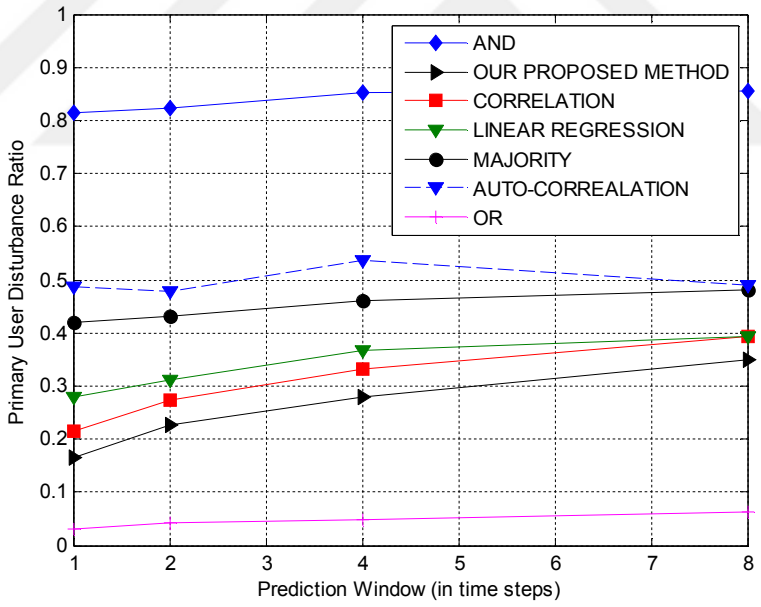

(b)

Figure 5.10 Performances of algorithms with varying prediction window sizes $|W_P|$. (a) System utility, (b) Primary user disturbance ratio.

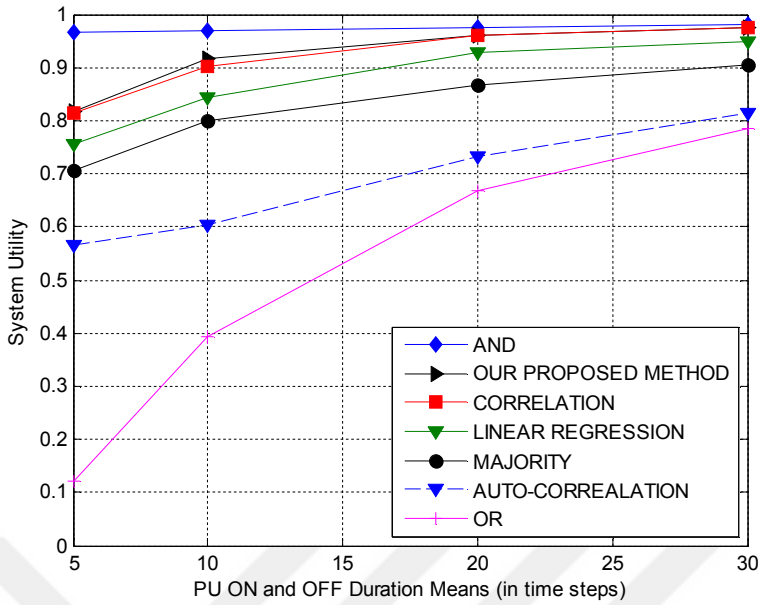

(a)

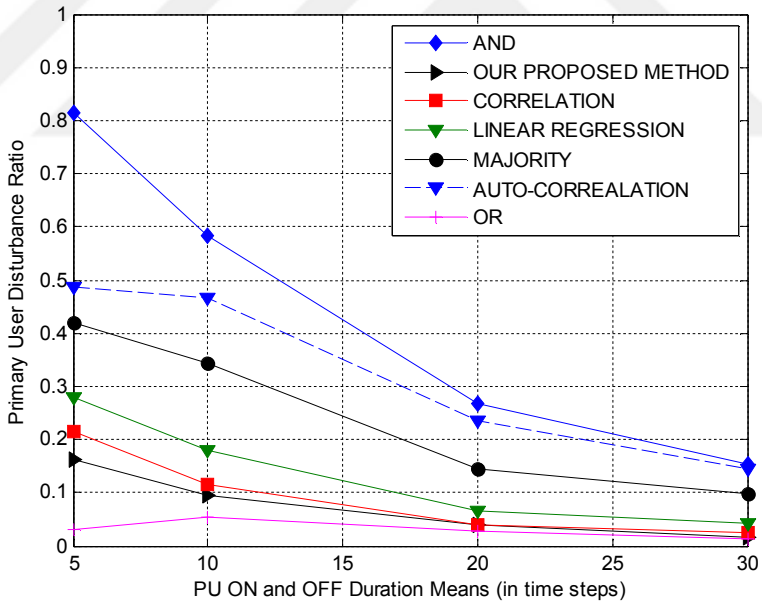

(b)

Figure 5.11 Performances of algorithms with varying means of primary user traffic. (a) System utility, (b) Primary user disturbance ratio.

5.2 Prediction of Channel Status for Nonhomogeneous PU Traffic Density

In the previous section, PU traffic density in the channel was assumed to be constant and did not change with time. In this section, it is assumed that the traffic density changes in a stochastic manner with time, corresponding to a more realistic scenario. To obtain a stochastically varying traffic density, the arrival and departure rate parameters of Poisson process are changed randomly during the generation of data. Markov Modulated Poisson Process (MMPP), which is actually a kind of doubly stochastic Poisson process (DSPP), is used for generating nonhomogenous PU traffic data.

In this section, firstly generation of the random data using non-homonegous Poisson processes is discussed in a general manner. Then, MMPP is presented to show how the previously given decisions are generated in simulations. Next, the proposed algorithm is introduced based on the parameters of MMPP. Finally, the related simulation results are discussed at the end of the section.

5.2.1 Nonhomogenous Poisson Processes (NHPPs)

NHPP is an extension of homogenous Poisson process (HPP). Its rate is represented by a deterministic rate function $\lambda(t)$. When this rate function takes a constant value α, then NHHP reduces to the homogenous Poisson process with rate $\lambda = \alpha$.

There are several methods in the literature to generate random numbers from a NHPP (Pasupathy, 2011). In general, the expectation function, $\Lambda(t)$, is used in almost all the methods. $\Lambda(t)$ can be found by integrating the rate function $\lambda(t)$ from 0 to t; that is, $\Lambda(t) = \int_0^t \lambda(y)\,dy$.

An inversion based approach can be used to generate inter arrival times for a NHPP. The critical point in this approach is to define the inverse of the CDF of inter arrival times which depends on the expectation function $\Lambda(t)$.

Derivation of the CDF can be performed as follows (Pasupathy, 2011);

$$F_{t_i}(x) = \Pr\left\{X_i \le x \middle| T_j = t_j, j = 1,2,3,\ldots,i\right\}$$

$$= \Pr\left\{N_{t_i+x} - N_t \ge 1 \middle| T_j = t_j, j = 1,2,3,\ldots,i\right\}$$

$$= \Pr\left\{N_{t_i+x} - N_t \ge 1\right\}$$

$$= 1 - \Pr\left\{N_{t_i+x} - N_t = 0\right\}$$

$$= 1 - \exp\left(-\Lambda(t_i + x) + \Lambda(t_i)\right). \tag{5.9}$$

The important question regarding Equation (5.9) is: "Is it possible to obtain $F_{t_i}^{-1}(x)$?". If the answer is yes, a similar algorithm is carried out as in the HPP. This algorithm is given in Figure 5.12 below (Pasupathy, 2011).

(0)Initialize t=0.

(1) Generate $x \sim F_t$ given by Eq. (5.9).

(2) Set $t \leftarrow t + x$.

(3) Deliver t.

(4) Go to Step (1).

Figure 5.12 Inversion algorithm for generating a NHPP.

An example NHPP generated by the inversion algorithm is shown in Figure 5.13 where we take $\lambda(t) = 2t$. As can be seen from Figure 5.13, the frequency of arrivals

is low at the beginning; however, it increases linearly as time passes in accordance with the rate function $\lambda(t)$.

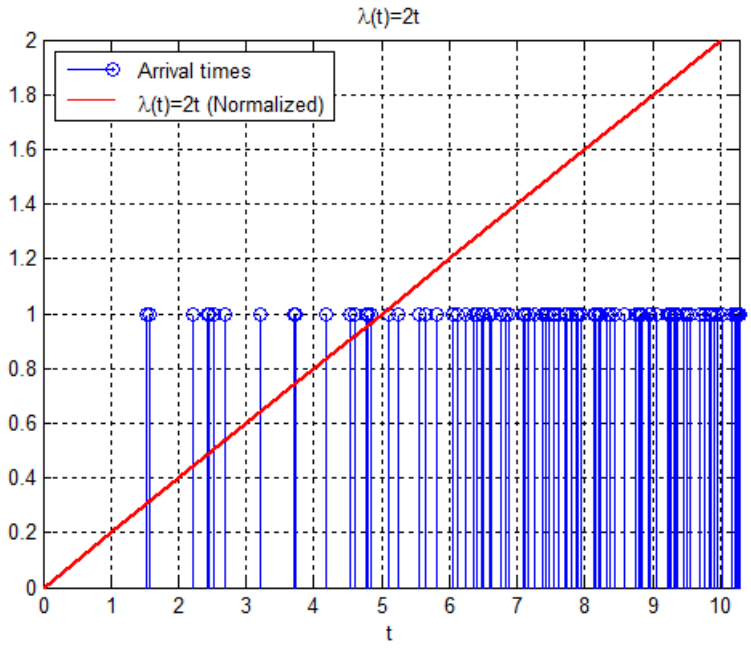

Figure 5.13 Example NHPP with the rate function $\lambda(t) = 2t$.

Although the inversion algorithm in Figure 5.12 seems straightforward, sometimes it may not be possible to obtain $F_{t_i}^{-1}(x)$ (for example, $\Lambda(t)$ may be a quadratic function of t). For these cases, a thinning algorithm was proposed by Lewis and Shedler (1979) which is given in Figure 5.14 below.

(0) Initialize t=0.

(1) Generate $u_1 \sim U(0,1)$.

(2) Set $t \leftarrow t - \frac{1}{\lambda_u} \ln u_1$.

(3) Generate $u_2 \sim U(0,1)$ independent of u_1.

(4) If $u_2 \le \frac{\lambda(t)}{\lambda_u}$ then deliver t.

(5) Go to Step (1).

Figure 5.14 Thinning algorithm for generating a NHPP.

In Figure 5.15 and Figure 5.16, two examples for generating NHPP using thinning algorithm are shown. In Figure 5.15, $\lambda(t)$ is given as $\lambda(t)=6-5\sin\left(\frac{4\pi t}{T}\right)$ (normalized to make its amplitude equal to 1). As can be seen from Figure 5.15, the frequency of arrivals depends on $\lambda(t)$. When the amplitude of the sinusoidal rate function increases, the number of arrivals also increases.

In Figure 5.16, the rate function is given as $\lambda(t)=10e^{-0.1t}$ (normalized to make its amplitude equal to 1). Observing Figure 5.16, the number of arrivals is high since the rate function $\lambda(t)$ takes larger values at the beginning. The value of $\lambda(t)$ decreases with time and the inter arrival times increase as opposed to Figure 5.15. It is noteworthy that generation of these processes would be much more complicated using the inversion algorithm since computation of the inverse of the CDF would become tedious or maybe impossible.

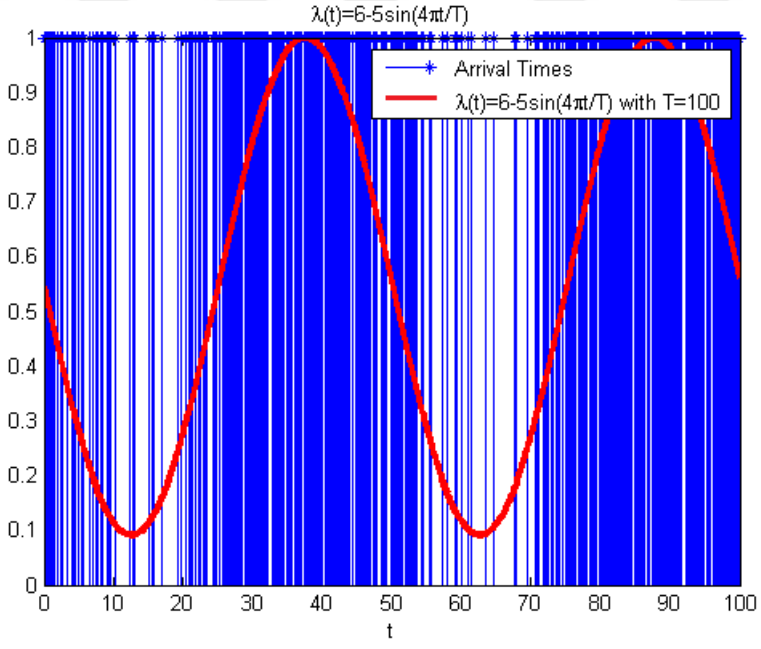

Figure 5.15 Using sinusoidal rate function for generating a NHPP.

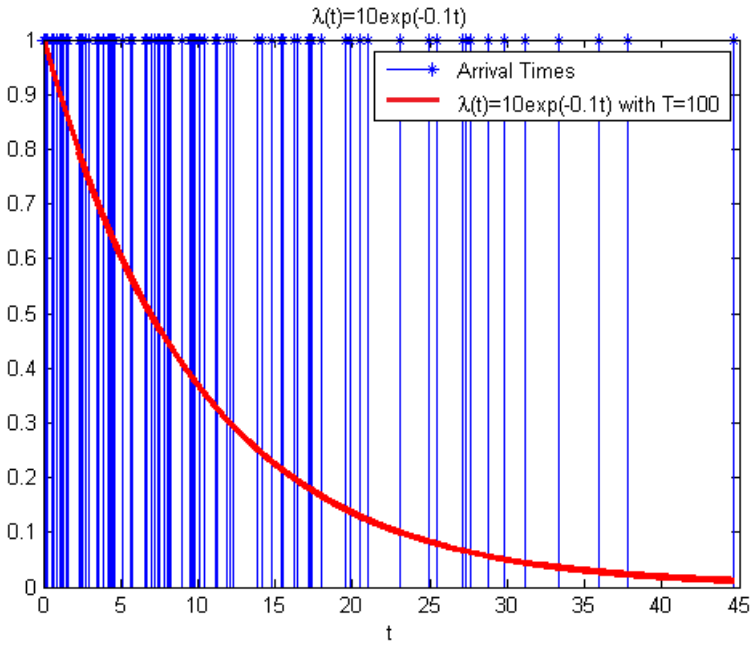

Figure 5.16 Using exponential rate function for generating a NHPP.

5.2.2 Doubly Stochastic Poisson Processes (DSPPs)

Doubly stochastic Poisson processes (DSPPs) correspond to generalized forms of NHPPs where the rate function $\lambda(t)$ is not only time-varying but also a stochastic process. These processes are alternatively called Cox processes (Basu & Dassios, 1999).

Generation of a Cox process can be carried out by generating a realization of a non-negative stochastic process and then using it as the rate function of a NHPP. It may be challenging to find the inverse of the CDF of the resulting expectation function $\Lambda(t)$. Hence, at the NHPP generation step, it is more appropriate to use the thinning algorithm mentioned in the previous section. The related algorithm for generating a Cox process is given in Figure 5.17 below (Burnecki & Weron, 2005).

(0) Generate a realization $\lambda(t)$ of the intensity process $\Lambda(t)$ for a sufficiently large time period; set $\lambda_u = \max(\lambda(t))$.

(1) Initialize t=0.

(2) Generate $u_1 \sim U(0,1)$.

(3) Set $t \leftarrow t - \frac{1}{\lambda_u} \ln u_1$.

(4) Generate $u_2 \sim U(0,1)$ independent of u_1.

(5) If $u_2 \leq \frac{\lambda(t)}{\lambda_u}$ then deliver t.

(6) Go to Step (1).

Figure 5.17 Generation of a DSPP using the thinning algorithm.

5.2.3 Markov Modulated Poisson Process (MMPP)

Markov modulated Poisson process (MMPP) is a DSPP whose rate varies according to an n-state Markov chain. It is a highly preferred tool particularly for modeling the network and Internet traffic since it is possible to model bursty traffic channels with these processes. Hence, in our simulations, we have also preferred this process to generate inter arrival times.

Number of states in the modulating Markov process determines which class the MMPP belongs to; for instance, an MMPP modulated with a two-state Markov process is termed MMPP(2). It can be seen easily that when the values in the states of the modulating Markov process are equal, then the resulting MMPP(2) becomes a HPP (Basu & Dassios, 1999).

An example of a two-state Markov process is shown in Figure 5.18.

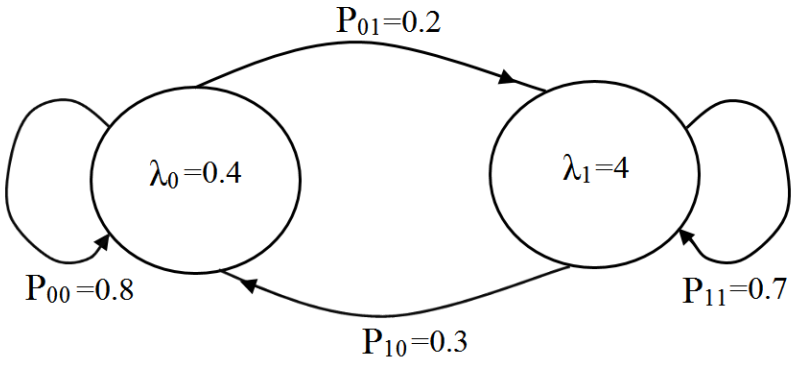

Figure 5.18 A two-state Markov process; MMPP (2).

The related initial probabilities for the above Markov process are equal such that

$$P_0(\lambda = 0.4) = P_0(\lambda = 4) = 0.5 \tag{5.10}$$

where P_0 is the initial probability. The transition matrix, $\boldsymbol{P}$, is given as

$$\boldsymbol{P} = \begin{bmatrix} P_{00} & P_{01} \\ P_{10} & P_{11} \end{bmatrix} = \begin{bmatrix} 0.8 & 0.2 \\ 0.3 & 0.7 \end{bmatrix}. \tag{5.11}$$

In Figure 5.18, there are two states with the values of 0.4 and 4 which are also the arrival rates for MMPP(2) to be generated. According to the given initial probabilities and the transition matrix, it is expected that transitions between 0.4 and 4 will occur. This is shown in Figure 5.19.

After arrival rates are determined, they are used to generate the arrival times in the NHPP. Following this step, the procedure is the same as with the generation of a NHPP. In this section, MMPP(2) process is generated using the thinning algorithm given in Figure 5.14.

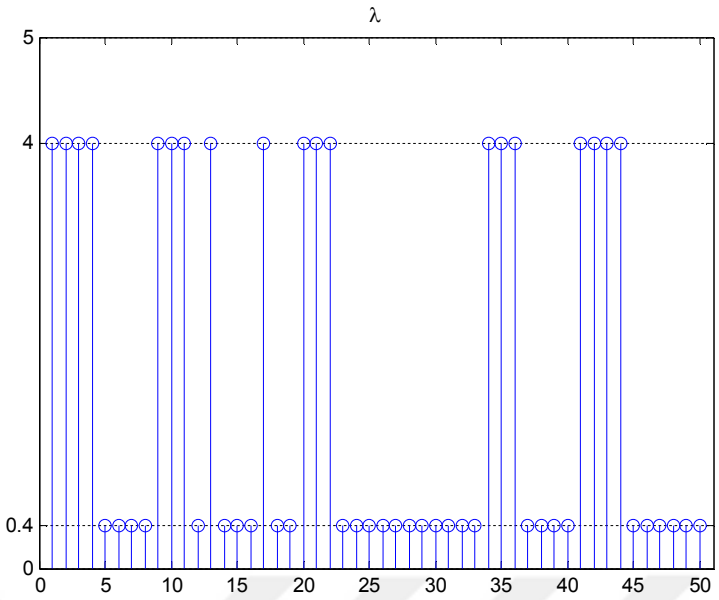

Figure 5.19 Generated arrival rates.

5.2.4 Proposed Algorithm

The empirical probabilites obtained using the previously taken decisions in the history window are mainly used in our proposed algorithm. Accordingly, transition probabilities among the states, P_{00}, P_{01}, P_{10}, and P_{11}, are obtained using the decisions in the history window and the prediction is carried out based on comparison of these probability values.

The estimated transition probabilites can be obtained using the following equations;

$$\hat{P}_{00} = P\left(H_{|W_H+1|}=0, H_{|W_H|}=0\right) = P\left(H_{|W_H+1|}=0 \mid H_{|W_H|}=0\right).P\left(H_{|W_H|}=0\right) \quad (5.12)$$

$$\hat{P}_{01} = P\left(H_{|W_H+1|}=1, H_{|W_H|}=0\right) = P\left(H_{|W_H+1|}=1 \mid H_{|W_H|}=0\right).P\left(H_{|W_H|}=0\right) \quad (5.13)$$

$$\hat{P}_{10} = P\left(H_{|W_H+1|}=0, H_{|W_H|}=1\right) = P\left(H_{|W_H+1|}=0 \mid H_{|W_H|}=1\right).P\left(H_{|W_H|}=1\right) \quad (5.14)$$

$$\hat{P}_{11} = P\left(H_{|W_H+1|}=1, H_{|W_H|}=1\right) = P\left(H_{|W_H+1|}=1 \mid H_{|W_H|}=1\right).P\left(H_{|W_H|}=1\right) \quad (5.15)$$

where H, $|W_H|$, $H_{|W_H|}$, and $H_{|W_H|+1}$ represent the history window, length of the history window, the last decision in the history window, and the slot to be predicted, respectively.

In addition to those parameters, the multiplicative probability terms in Equations (5.12) through (5.15) are calculated as follows;

$$P\left(H_{|W_H|}=0\right)=\frac{N_0}{|W_H|} \tag{5.16}$$

$$P\left(H_{|W_H|}=1\right)=\frac{N_1}{|W_H|} \tag{5.17}$$

$$P\left(H_{|W_H+1|}=0 \mid H_{|W_H|}=0\right)=\frac{N_{00}}{|W_H|} \tag{5.18}$$

$$P\left(H_{|W_H+1|}=1 \mid H_{|W_H|}=0\right)=\frac{N_{01}}{|W_H|} \tag{5.19}$$

$$P\left(H_{|W_H+1|}=0 \mid H_{|W_H|}=1\right)=\frac{N_{10}}{|W_H|} \tag{5.20}$$

$$P\left(H_{|W_H+1|}=1 \mid H_{|W_H|}=1\right)=\frac{N_{11}}{|W_H|}. \tag{5.21}$$

In Equations (5.16) through (5.21), N_0 is the number of idle (or 0) decisions and, N_1 is the number of busy (or 1) decisions in the history window. N_{00}, N_{01}, N_{10}, and N_{11} correspond to numbers of 0-0, 0-1, 1-0, and 1-1 transitions in the history window, respectively.

After all these probabilites are calculated, the prediction of channel status can be made by comparing them with each other as in the algorithm given in Figure 5.20.

Require: $\hat{P}_{00}$, $\hat{P}_{01}$, $\hat{P}_{10}$ and $\hat{P}_{11}$

if $H_{|W_H|} == 0$ **then**

  if $\hat{P}_{01} > \hat{P}_{00}$ **then**

    $W_P \leftarrow 1$

  else

    $W_P \leftarrow 0$

  end if

else

  if $\hat{P}_{11} > \hat{P}_{10}$ **then**

    $W_P \leftarrow 1$

  else

    $W_P \leftarrow 0$

  end if

end if

return Prediction vector W_P

Figure 5.20 Proposed algorithm.

According to Figure 5.20, the last decision in the history window is checked first. If it is 0, then $\hat{P}_{01}$ and $\hat{P}_{00}$ are compared to predict the next status of the channel. If the last decision in the history window equals to 1, then $\hat{P}_{10}$ and $\hat{P}_{11}$ are compared.

5.2.5 Simulation Results

In the simulations, PU traffic is modelled by a two-state MMPP and the same parameters given in Equations (5.10) and (5.11) are used for data generation. It is assumed that 1000 binary decision samples are available and each trial is run for 150 times during simulations. The mean of 150 trials is used to obtain the final results. The correlation based techniques introduced in Section 5.1 are also used in this section and prediction performance is evaluted in terms of SYSU and PUDR again.

In addition to the techniques mentioned in Section 5.1, the algorithm proposed in Liu et al. (2012) is also considered in this section, since it has some similarities with our proposed algorithm. A semi-Markov process is used in Liu et al. (2012) to model the PU traffic. Transition probabilities are derived based on this model.

In Figures 5.21(a) and 5.21(b), the SYSU and PUDR performances of the considered methods are shown for varying history window lengths, $|W_H|$. According to those figures, again as in Figure 5.9, AND logic has the best SYSU and the worst PUDR performances. Conversely, OR logic is the method with the lowest SYSU and the lowest PUDR.

It can be observed from Figure 5.21(a) that the performance of the algorithm proposed in Liu et al. (2012) increases with the length of the history window. However, there is not a remarkable change for other methods. It is possible to say that our proposed algorithm achieves higher prediction performance in terms of SYSU criterion for all the considered history window lengths.

In Figure 5.21(b), the prediction performance results are presented in terms of PUDR criterion. According to this figure, PUDR decreases with an increase in the history window length for the proposed method, causing an increase in its prediction performance. On the other hand, prediction performance decreases for correlation based techniques for longer history window lengths since the correlation among the decisions reduces when the history window length is increased. The algorithm introduced in Liu et al. (2012) achieves the lowest PUDR. However, its performance decreases with the increase of the history window length as in correlation based prediction methods. Our proposed algorithm has high PUDR values for smaller history window lengths. However, it has the lowest PUDR values together with Liu et al. (2012), except for OR logic, particularly for $|W_H| \geq 15$.

In Figure 5.22, prediction performance of the considered techniques are evaulated for varying prediction window lengths, $|W_P|$.

In Figure 5.22(a), performances of the considered techniques are shown for varying prediction window lengths in terms of SYSU. The technique introduced in Liu et al. (2012) has the lowest SYSU values (except OR logic) and our proposed prediction algorithm shows the highest SU performance (except AND logic) for almost all the considered prediction window lengths.

In terms of PUDR in Figure 5.22(b), the technique introduced in Liu et al. (2012) shows the best performance after OR logic and our proposed algorithm shows an average performance. Looking at Figure 5.22(b), one can conclude that it is required to develop algorithms that exhibit better prediction performance in terms PUDR for varying prediction window lengths and when the PU traffic density in the channel changes stochastically with time.

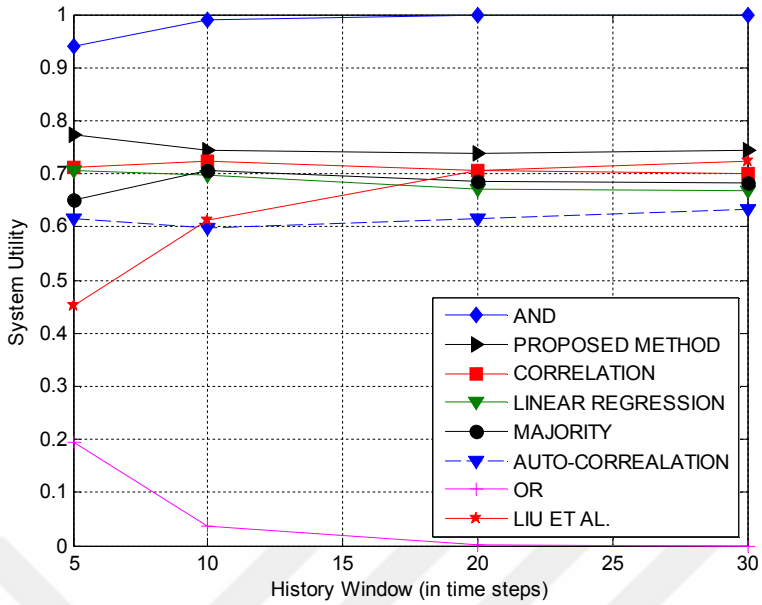

(a)

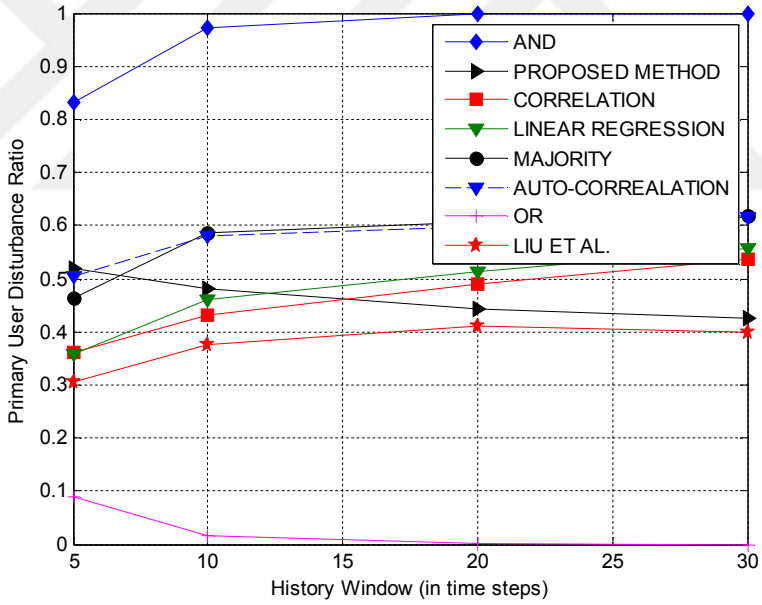

(b)

Figure 5.21 Performances of algorithms with varying history window sizes $|W_H|$. (a) System utility, (b) Primary user disturbance ratio.

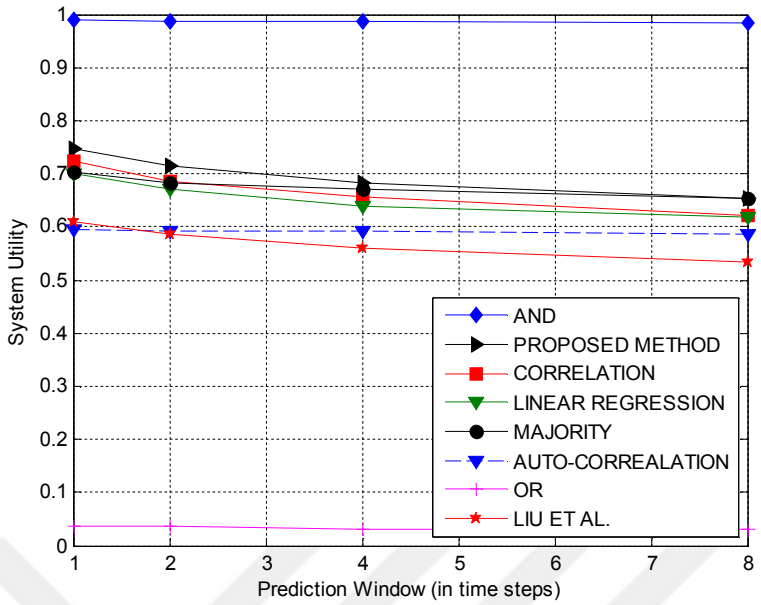

(a)

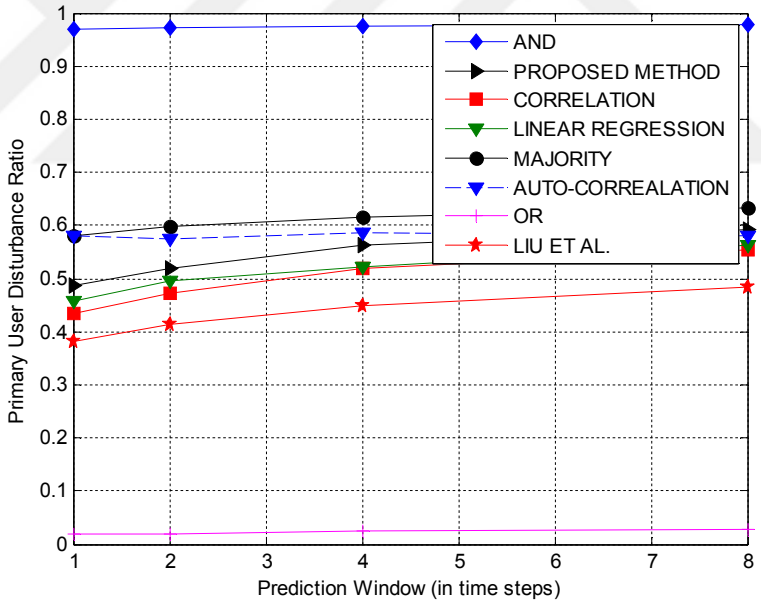

(b)

Figure 5.22 Performances of algorithms with varying prediction window sizes $|W_P|$. (a) System utility, (b) Primary user disturbance ratio.

CHAPTER SIX
CONCLUSIONS AND FUTURE WORK POSSIBILITIES

Spectrum sensing is considered as one of the most crucial operations fulfilled by a CR. Motivated by this fact, several spectrum sensing techniques have been proposed in the CR literature. It is still a popular research topic since a robust method has yet to be proposed although there are already some techniques that show optimality under different assumptions. Furthermore, traditional spectrum sensing techniques generally assume that the PU does not change its status within the sensing period and their detection performances are evaluated under this assumption. However, performance degradation is observed for all the previously proposed techniques when the PU is more realistically assumed to be dynamic or there are PU status changes within the sensing period. In this dissertation, dynamic spectrum management in CR has been considered by aiming to propose new spectrum sensing and channel status prediction schemes particularly under the existence of dynamic PUs in the channel.

A change point estimation based spectrum sensing scheme has been introduced as our first study on detection of dynamic PUs. Motivated by the fact that the noise-only samples under H_1 and signal+noise samples under H_0 have degrading effects on detection performance, the LSCP of the PU has been estimated and the signal samples after the LSCP have been used for calculation of the test statistics. In this way, it has been aimed to lessen the performance degradation for the previously proposed sensing techniques under PU traffic. A CuSum based weighting scheme has also been embedded to change point estimation algorithm motivated by the following observations. First, LSCP is generally estimated inaccurately at low SNR levels and undesired signal samples are automatically involved in the decision process. To compensate for the error caused by the inaccurate estimation of the LSCP, the weights of the latter samples in the sensing period are increased using CuSum weighting scheme. Second, the status of the PU in the next sensing period is highly correlated with its status at the end of the current sensing period. Therefore, it

is intuitive to increase the weight of the latter samples in order to increase the effect of the last status of the PU on the decision process.

Estimation of the LSCP brings an additional computational load for spectrum sensing process. To reduce the time spent for estimation of LSCP, DP approach has been adopted. Also, exploring only one PU status change point accelerates the computation, and in this way, computational load of the proposed algorithm is reduced.

The proposed sensing scheme has been used for detection of dynamic PUs that use DC signalling scheme. Since the sample mean detector is the optimal method for detection of DC signals (when there is no change in the data), it has been embedded to our proposed sensing scheme. Theoretical derivations for probability of detection, P_D, and probability of false alarm, P_{FA}, of CuSum based weighted sample mean detector are also presented and verified with the simulation results. It is shown in the simulations that the proposed sensing scheme outperforms other considered techniques in terms of P_D. Besides that, the performed simulations also indicate that estimation of LSCP provides a performance enhancement for all the methods to which it is applied.

For further analysis of the proposed sensing scheme, CuSum based weighting and estimation of LSCP have also been applied to ED, which is the optimal sensing technique when the PU signal is unknown. For this case, the PU signal is assumed to be Gaussian distributed and LSCP estimation is adapted to variance change estimation problem. As in the sample mean detector, it is assumed that one or at most two PU status changes occur within the sensing period and the theoretical derivations for CuS-WED are verified by simulations. According to simulation results, when Cus-WED is used, higher detection performance could be obtained particularly at low P_{FA} values compared to other considered techniques.

In summary, it is possible to say that estimation of LSCP together with CuSum based weighting scheme provides a noticeable performance enhancement in terms of

P_D for all the techniques it is applied to. However, environmental parameters such as high noise power, high PU traffic density etc. can be considered as the factors that reduce the performance enhancement provided by the proposed sensing scheme.

As another open research area in the CR literature, GOF tests have been considered for detection of dynamic PUs. Although there are several studies on GOF test based spectrum sensing, none of them considers the existence of dynamic PUs in the channel. Motivated by the lack of a study on this topic, a novel OS based spectrum sensing technique has been proposed in this dissertation. In addition, most of the previously proposed studies assume that the PU is a DC valued (or constant) signal. However, in this study, detection performances of the considered methods have been evaluated assuming that the PU has various signalling schemes contrary to the previously proposed studies.

It is shown via simulations that GOF tests show better performance than ED when the PU signal is constant. However, if the PU signal is not constant, performances of all the GOF based techniques significantly decrease. A possible solution to prevent this degradation is increasing the length of the sensing period. However, this also leads to existence of dynamic PUs in the channel. Therefore, a new algorithm based on OS has been proposed for detection of dynamic PUs in this study. Detection performance of the proposed method is investigated for real and complex valued PU signals. According to simulation results, our proposed algorithm achieves better performance among the considered techniques independent of the fact that the PU signal is real or complex valued. Additional simulations are also carried out to see the performance of the proposed method under various SNR levels. In the considered SNR interval of -20 dB $<$ SNR < 20 dB, our proposed algorithm achieves the highest P_D values among the simulated techniques. As a final comment, it is possible to say that the proposed algorithm in this dissertation can be preferred as a robust detector for detection of unknown PU signals at low SNR values since it shows high detection accuracy even if the channel suffers from PU traffic.

As the final contribution of the dissertation, channel status prediction in channels containing PU traffic has been investigated. By analyzing the previously taken decisions, it has been aimed to predict the future states of the channel as "idle" or "busy". "System Utility (SYSU)" and "Primary User Disturbance Ratio (PUDR)", two metrics introduced by Uyanik et al. (2012), have been used to measure the prediction accuracy of the considered prediction techniques in the simulations. Simulation studies have been carried out separately by assuming that the PU traffic density is either constant or it changes stochastically with time. Poisson process has been used to model the PU traffic under both scenarios. The arrival and departure rates are chosen constant when the PU traffic density is also assumed to be constant. On the other hand, rate values are obtained using two-state Markov process when it is assumed that the traffic density changes stochastically with time.

For the case of constant PU traffic density, a novel prediction algorithm based on empirical arrival and departure rates has been proposed and its performance has been compared with correlation based prediction techniques. According to simulation results, it is possible to state that the proposed algorithm outperforms correlation based techniques in terms of both SYSU and PUDR under various scenarios.

A novel prediction algorithm has also been proposed for the case when the PU traffic density changes stochastically with time. According to the proposed scheme, the transition probabilities among the previously taken decisions are obtained first and then compared against each other. Simulation results demonstrate that the proposed prediction scheme outperforms all other considered techniques in terms of SYSU for varying history and prediction window lengths. Considering PUDR criterion, it is possible to say that our proposed algorithm has better prediction performance than correlation based prediction techniques and displays close performance to Liu et al. (2012) particularly when long history window lengths are used. On the other hand, for varying prediction window lengths, our proposed method has an average performance in terms of PUDR criterion.

Dynamic PU issue in CR has been considered under three titles in this dissertation and the related suggestions for future works are given as follows.

During the studies, CuSum based weighting scheme has been applied to sample mean detector and ED which are, the test statistics showing optimality under different conditions. The sample mean detector needs constant (or DC) PU signal and ED requires high SNR to show optimal detection performance. However, there are also other proposed techniques in the literature that can achieve high detection performance for various signalling schemes at low SNR levels. By applying the proposed change point estimation with CuSum based weighting scheme to these techniques, their performances under PU traffic can be enhanced and more robust sensing methods could possibly be obtained.

The proposed OS based technique outperforms other spectrum sensing methods based on GOF testing in terms of probability of detection. It is worth to note that its computational complexity is comparable to OS based spectrum sensing technique in Rostami et al. (2012). Intuitively, increasing the speed of the currently proposed algorithm or proposing faster methods with high detection performance can be considered as future works.

When it is assumed that the traffic density changes stochastically with time, it is observed that the proposed algorithm shows a mediocre performance in terms of PUDR, particularly when long prediction window lengths are used. This means that the proposed algorithm is inadequate to predict the channel status for sensing periods in the far future. This requires design of more intelligent algorithms that can forecast the channel status in the far future. Investigation of such algorithms is left as a future research direction.

REFERENCES

Akyildiz, I. F., Lee, W. Y., & Chowdhury, K. R. (2009). CRAHNs: Cognitive radio ad hoc networks. *AD Hoc Networks*, *7* (5), 810-836.

Akyildiz, I. F., Lee, W. Y., Vuran, M. C., & Mohanty, S. (2006). NeXt generation/dynamic spectrum access/cognitive radio wireless networks: A survey. *Computer Networks*, *50* (13), 2127-2159.

Arshad, K., & Moessner, K. (2013). Robust spectrum sensing based on statistical tests. *IET Communications*, *7* (9), 808-817.

Axell, E., Leus, G., Larsson, E. G., & Poor, H. V. (2012). Spectrum sensing for cognitive radio: State-of-the-art and recent advances. *IEEE Signal Processing Magazine*, *29* (3), 101-116.

Basu, S., Dassios, A. (1999). A Doubly Stochastic Poisson Process with Log - Normal Intensity. *Technical Report, Department of Statistics, London School of Economics.*

Beaulieu, N. C., & Chen, Y. (2010). Improved energy detectors for cognitive radios with randomly arriving or departing primary users. *IEEE Signal Processing Letters*, *17* (10), 867-870.

Bhargavi, D., & Murthy, C. R. (2010). Performance comparison of energy, matched-filter and cyclostationarity-based spectrum sensing. *IEEE Eleventh International Workshop on Signal Processing Advances in Wireless Communications (SPAWC)*, Marrakech, 1-5.

Black, T., Kerans, B., & Kerans, A. (2012). Implementation of hidden Markov model spectrum prediction algorithm. *International Symposium on Communications and Information Technologies (ISCIT)*, Gold Coast, QLD, Australia, 280-283.

Burnecki, K., & Weron, R. (2005). Modeling of the risk process. In *Statistical Tools for Finance and Insurance* (pp. 319-339). Berlin: Springer.

Cabric, D., Mishra, S. M., & Brodersen, R. W. (2004). Implementation issues in spectrum sensing for cognitive radios. *Conference Record of the Thirty-eighth Asilomar Conference on Signals, Systems and Computers*, *1*, 772-776.

Chang, K., & Senadji, B. (2012). Spectrum sensing optimisation for dynamic primary user signal. *IEEE Transactions on Communications*, *60* (12), 3632-3640.

Chen, Y. (2010). Improved energy detector for random signals in Gaussian noise. *IEEE Transactions on Wireless Communications*, *9* (2), 558-563.

Chen, Y., Wang, C., & Zhao, B. (2011). Performance comparison of feature-based detectors for spectrum sensing in the presence of primary user traffic. *IEEE Signal Processing Letters*, *18* (5), 291-294.

Chen, X., Xia, W., Bao, N., & Shen, L. (2013). Weighted energy detection method for spectrum sensing in cognitive radio. *International Conference on Information Science and Technology (ICIST)*, Yangzhou, China, 1296-1300.

Chiang, T. W., Lin, J. M., & Ma, H. P. (2009). Optimal detector for multitaper spectrum estimator in cognitive radios. *IEEE Global Telecommunications Conference (GLOBECOM)*, Honolulu, USA, 1-6.

Choi, J. K., & Yoo, S. J. (2013). Undetectable primary user transmissions in cognitive radio networks. *IEEE Communications Letters*, *17* (2), 277-280.

Düzenli, T., & Akay, O. (2013). Bilişsel radyolar için birincil kullanıcı trafiği içeren kanallarda dinamik programlama ve ortalama kümülatif toplama dayalı yeni bir test istatistiğinin önerilmesi. *V. İletişim Teknolojileri Ulusal Sempozyumu*, İzmir, Turkey, 1-10.

Düzenli, T., & Akay, O. (2014). Birincil kullanıcı trafiği içeren bilişsel radyolarda kanal durumunun tahmini için yeni bir yöntem. *Elektrik Elektronik-Bilgisayar ve Biyomedikal Mühendisligi Sempozyumu ve Sergisi (ELECO)*, Bursa, Turkey, 513-517.

Düzenli, T., & Akay, O. (2015). Birincil kullanıcı trafik yoğunluğu olasılıksal olarak değişen bilişsel radyolar için kanal durum tahmini. *23th Signal Processing and Communications Applications Conference (SIU)*, Malatya, Turkey, 1232-1235.

Düzenli, T., & Akay, O. (2016). A new spectrum sensing strategy for dynamic primary users in cognitive radio. *IEEE Communications Letters*, *20* (4), 752-755.

Eduardo, A. F., & Caballero, R. G. (2015). Experimental evaluation of performance for spectrum sensing: Matched filter vs. energy detector. *IEEE Colombian Conference on Communications and Computing (COLCOM)*, Popayán, Colombia, 1-6.

Eghbali, Y., Hassani, H., Koohian, A., & Ahmadian-Attari, M. (2014). Improved energy detector for wideband spectrum sensing in cognitive radio networks. *Radioengineering*, *23* (1), 430-434.

Gaaloul, F., Yang, H. C., Radaydeh, R. M., & Alouini, M. S. (2012). Opportunistic spectrum access in cognitive radio based on channel switching. *7th International ICST Conference on Cognitive Radio Oriented Wireless Networks and Communications (CROWNCOM)*, Stockholm, Sweden, 270-274.

Gismalla, E. H., & Alsusa, E. (2011). Performance analysis of the periodogram-based energy detector in fading channels. *IEEE Transactions on Signal Processing*, *59* (8), 3712-3721.

Gismalla, E. H., & Alsusa, E. (2012). On the performance of energy detection using Bartlett's estimate for spectrum sensing in cognitive radio systems. *IEEE Transactions on Signal Processing*, *60* (7), 3394-3404.

Glen, A. G., Leemis, L. M., & Barr, D. R. (2001). Order statistics in goodness-of-fit testing. *IEEE Transactions on Reliability*, *50* (2), 209-213.

Guibene, W., & Hayar, A. (2010). Joint time-frequency spectrum sensing for cognitive radio. *3rd International Symposium on Applied Sciences in Biomedical and Communication Technologies (ISABEL)*, Rome, Italy, 1-4.

Guo, H., Jiang, W., & Luo, W. (2015). A modified energy detector for random signals in Gaussian noise. *IEEE Communications Letters*, *19* (8), 1358-1361.

Haykin, S., Thomson, D. J., & Reed, J. H. (2009). Spectrum sensing for cognitive radio. *Proceedings of the IEEE*, *97* (5), 849-877.

Höyhtyä, M., Pollin, S., & Mämmelä, A. (2010). Classification-based predictive channel selection for cognitive radios. *IEEE International Conference on Communications (ICC)*, Cape Town, South Africa, 1-6.

Javed, F., & Mahmood, A. (2010). The use of time frequency analysis for spectrum sensing in cognitive radios. *4th International Conference on Signal Processing and Communication Systems (ICSPCS)*, Gold Coast, QLD, Australia, 1-7.

Jin, J., & Xu, H. (2011). Exploiting multi-antennas for spectrum sensing. *Journal of Computational Information Systems*, *7* (10), 3406-3414.

Jin, M., Li, Y., & Ryu, H. G. (2012). On the performance of covariance based spectrum sensing for cognitive radio. *IEEE Transactions on Signal Processing*, *60* (7), 3670-3682.

Johnson, N. L., Kotz, S., & Balakrishnan, N. (1994). *Continuous univariate distributions, vol. 1-2* (2nd ed.). New York: Wiley and Sons.

Kababulut, F. Y., Kuntalp, D., & Duzenli, T. (2015). New methods of density estimation for vehicle traffic. *IEEE 9th International Conference on Electrical and Electronics Engineering (ELECO)*, Bursa, Turkey, 223-226.

Kay, S. M. (1998). F*undamentals of statistical signal processing: Detection theory, vol. 2* (1st ed.). New Jersey: Prentice Hall (PTR).

Kortun, A., Ratnarajah, T., Sellathurai, M., & Zhong, C. (2010). On the performance of eigenvalue-based spectrum sensing for cognitive radio. *IEEE Symposium on New Frontiers in Dynamic Spectrum*, Singapore, 1-6.

Kundargi, N., & Tewfik, A. H. (2010). A performance study of novel sequential energy detection methods for spectrum sensing. *IEEE International Conference on Acoustics, Speech and Signal Processing (ICASSP)*, Dallas, TX, USA, 3090-3093.

Lee, Y., Lee, S. R., Yoo, S., Liu, H., & Yoon, S. (2014). Cyclostationarity-based detection of randomly arriving or departing signals. *Journal of Applied Research and Technology*, *12* (6), 1083-1091.

Lei, S., Wang, H., & Shen, L. (2011). Spectrum sensing based on goodness of fit tests. *IEEE International Conference on Electronics, Communications and Control (ICECC)*, Ningbo, China, 485-489.

Lewis, P. A. W., & Shedler, G. S. (1979). Simulation of nonhomogeneous Poisson processes by thinning. *Naval Research Logistics Quarterly*, *26* (3), 403-413.

Li, H., Wang, Y., Chen, Y., & Li, S. (2012). Implementation of spectrum sensing based on covariance in cognitive radio. *Instrumentation, Measurement, Circuits and Systems*, 61-69.

Liang, Y. C., Zeng, Y., Peh, E. C., & Hoang, A. T. (2008). Sensing-throughput tradeoff for cognitive radio networks. *IEEE Transactions on Wireless Communications*, *7* (4), 1326-1337.

Lim, Y., Park, J., & Sung, Y. (2009). Upper bound for the loss of energy detection of signals in multipath fading channels. *IEEE Signal Processing Letters*, *16* (11), 949-952.

Liu, C. H., Gabran, W., & Cabric, D. (2012). Prediction of exponentially distributed primary user traffic for dynamic spectrum access. *IEEE Global Communications Conference (GLOBECOM)*, Anaheim, CA, USA, 1441-1446.

Ma, J., Zhao, G., & Li, Y. (2008). Soft combination and detection for cooperative spectrum sensing in cognitive radio networks. *IEEE Transactions on Wireless Communications*, *7* (11), 4502-4507.

Mitola III, J., & Maguire Jr, G. Q. (1999). Cognitive radio: Making software radios more personal. *IEEE Personal Communications*, *6* (4), 13-18.

Mohamad, M. H., Wen, H. C., & Ismail, M. (2012). Matched filter detection technique for GSM band. *International Symposium on Telecommunication Technologies (ISTT)*, Kuala Lumpur, Malaysia, 271-274.

Moragues, J., Vergara, L., Gosálbez, J., & Bosch, I. (2009). An extended energy detector for non-Gaussian and non-independent noise. *Signal Processing*, *89* (4), 656-661.

Nadler, B., Penna, F., & Garello, R. (2011). Performance of eigenvalue-based signal detectors with known and unknown noise level. *IEEE International Conference on Communications (ICC)*, Kyoto, Japan, 1-5.

N.-Thanh, N., K.-Xuan, T., & Koo, I. (2012). Comments on "Spectrum sensing in cognitive radio using goodness-of-fit testing". *IEEE Transactions on Wireless Communications*, *11* (10), 3409 – 3411.

Pasupathy, R. (2011). Generating homogeneous poisson processes. In *Wiley Encyclopedia of Operations Research and Management Science* (1st ed.). New York: Wiley and Sons.

Penna, F., & Garello, R. (2011). Detection of discontinuous signals for cognitive radio applications. *IET Communications*, *5* (10), 1453-1461.

Rao, A., Ma, H., Alouini, M. S., & Chen, Y. (2013). Impact of primary user traffic on adaptive transmission for cognitive radio with partial relay selection. *IEEE Transactions on Wireless Communications*, *12* (3), 1162-1172.

Rostami, S., Arshad, K., & Moessner, K. (2012). Order-statistic based spectrum sensing for cognitive radio. *IEEE Communications Letters*, *16* (5), 592-595.

Sadough, S. S., & Ivrigh, S. S. (2012). Spectrum sensing for cognitive radio systems through primary user activity prediction. *Radioengineering*, *21* (4), 1092-1100.

Sahai, A., Hoven, N., & Tandra, R. (2004). Some fundamental limits on cognitive radio. In *Forty-second Allerton Conference on Communication, Control, and Computing*. 1-11.

Satheesh, A., Aswini, S. H., Lekshmi, S. G., Sagar, S., & Hareesh Kumar, M. (2013). Spectrum sensing techniques: A comparison between energy detector and cyclostationarity detector. *International Conference on Control Communication and Computing (ICCC)*, Thiruvananthapuram, India, 388-393.

Senadji, B., & Chang, K. P. (2013). Detection of dynamic primary user with cooperative spectrum sensing. *Proceedings of the 21st IEEE European Signal Processing Conference (EUSIPCO)*, Marrakech, Morocco, 1-5.

Sharma, R. K., & Wallace, J. W. (2009). Improved spectrum sensing by utilizing signal autocorrelation. *IEEE 69th Vehicular Technology Conference – VTC*, Barcelona, Spain, 1-5.

Shim, J., Lee, J., Lee, Y., Lee, Y., & Yoon, S. (2013). A cyclostationary spectrum sensing scheme for high traffic environments. *3rd International Conference on Wireless Communications, Vehicular Technology, Information Theory and Aerospace & Electronic Systems (VITAE)*, Atlantic City, NJ, USA, 1-4.

Stephens, M. A. (1974). EDF statistics for goodness of fit and some comparisons. *Journal of the American Statistical Association*, *69* (347), 730-737.

Sung, K. W., Kim, S. L., & Zander, J. (2010). Temporal spectrum sharing based on primary user activity prediction. *IEEE Transactions on Wireless Communications*, *9* (12), 3848-3855.

Tang, L., Chen, Y., Hines, E. L., & Alouini, M. S. (2011). Effect of primary user traffic on sensing-throughput tradeoff for cognitive radios. *IEEE Transactions on Wireless Communications*, *10* (4), 1063-1068.

Tang, L., Chen, Y., Hines, E. L., & Alouini, M. S. (2012). Performance analysis of spectrum sensing with multiple status changes in primary user traffic. *IEEE Communications Letters*, *16* (6), 874-877.

Teguig, D., Scheers, B., Le Nir, V., & Horlin, F. (2014). Spectrum sensing method based on the likelihood ratio goodness of fit test under noise uncertainty. *International Journal of Engineering Research and Technology*, *3* (9), 488-494.

Teguig, D., Le Nir, V., & Scheers, B. (2015). Spectrum sensing method based on likelihood ratio goodness-of-fit test. *IET Electronics Letters*, *51* (3), 253-255.

Tran, T. T., & Kong, H. Y. (2013). Block-time of arrival/leaving estimation to enhance local spectrum sensing under the practical traffic of primary user. *Journal of Communications and Networks*, *15* (5), 514-526.

Urkowitz, H. (1967). Energy detection of unknown deterministic signals. *Proceedings of the IEEE*, *55* (4), 523-531.

Uyanik, G. S., Canberk, B., & Oktug, S. (2012). Predictive spectrum decision mechanisms in cognitive radio networks. *IEEE Globecom Workshops (GC Wkshps)*, Anaheim, CA, USA, 943-947.

Wang, T., Chen, Y., Hines, E. L., & Zhao, B. (2009). Analysis of effect of primary user traffic on spectrum sensing performance. *Fourth International Conference on Communications and Networking in China (ChinaCOM 2009)*, Xian, China, 1-5.

Wang, H., Yang, E. H., Zhao, Z., & Zhang, W. (2009). Spectrum sensing in cognitive radio using goodness of fit testing. *IEEE Transactions on Wireless Communications*, *8* (11), 5427-5430.

Wang, H., Noh, G., Kim, D., Kim, S., & Hong, D. (2010). Advanced sensing techniques of energy detection in cognitive radios. *Journal of Communications and Networks*, *12* (1), 19-29.

Wang, P., Fang, J., Han, N., & Li, H. (2010). Multiantenna-assisted spectrum sensing for cognitive radio. *IEEE Transactions on Vehicular Technology*, *59* (4), 1791-1800.

Wang, J., & Zhang, Q. T. (2009). A multitaper spectrum based detector for cognitive radio. *IEEE Wireless Communications and Networking Conference (WCNC 2009)*, Budapest, Hungary, 1-5.

Wang, F., Tian, Z., & Sadler, B. M. (2011). Weighted energy detection for noncoherent ultra-wideband receiver design. *IEEE Transactions on Wireless Communications*, *10* (2), 710-720.

Wei, L., & Tirkkonen, O. (2009). Cooperative spectrum sensing of OFDM signals using largest eigenvalue distributions. *IEEE 20th International Symposium on Personal, Indoor and Mobile Radio Communications*, Tokyo, Japan, 2295-2299.

Wei, L., & Tirkkonen, O. (2012). Spectrum sensing in the presence of multiple primary users. *IEEE Transactions on Communications*, *60* (5), 1268-1277.

Wei, L., Dharmawansa, P., & Tirkkonen, O. (2012). Locally best invariant test for multiple primary user spectrum sensing. *7th International ICST Conference on Cognitive Radio Oriented Wireless Networks and Communications (CROWNCOM)*, Stockholm, Sweden, 367-372.

Wu, J. Y., Huang, P. H., Wang, T. Y., & Wong, V. W. (2013). Energy detection based spectrum sensing with random arrival and departure of primary user's signal. *IEEE Globecom Workshops (GC Wkshps)*, Atlanta, GA, USA, 380-384.

Xie, X., & Hu, X. (2014). Improved energy detector with weights for primary user status changes in cognitive radios networks. *IEEE 11th Consumer Communications and Networking Conference (CCNC)*, Las Vegas, Nevada, USA, 53-58.

Yao, Y., Ngoga, S. R., & Popescu, A. (2012). Cognitive radio spectrum decision based on channel usage prediction. *8th EURO-NGI Conference on Next Generation Internet (NGI)*, Karlskrona, Sweden, 41-48.

Yarkan, S., & Arslan, H. (2007). Binary time series approach to spectrum prediction for cognitive radio. *IEEE 66th Vehicular Technology Conference, (VTC-2007 Fall)*, Baltimore, MD, USA, 1563-1567.

Yücek, T., & Arslan, H. (2009). A survey of spectrum sensing algorithms for cognitive radio applications. *IEEE Communications Survey & Tutorials*, *11* (1), 116-130.

Zeng, Y., Koh, C. L., & Liang, Y. C. (2008). Maximum eigenvalue detection: Theory and application. *IEEE International Conference on Communications (ICC'08)*, Beijing, 4160-4164.

Zeng, Y., & Liang, Y. C. (2009). Eigenvalue-based spectrum sensing algorithms for cognitive radio. *IEEE Transactions on Communications*, *57* (6), 1784-1793.

Zhang, J. (2002). Powerful goodness-of-fit tests based on the likelihood ratio. *Journal of the Royal Statistical Society: Series B (Statistical Methodology)*, *64* (2), 281-294.

Zhang, W., Mallik, R. K., & Letaief, K. B. (2009). Optimization of cooperative spectrum sensing with energy detection in cognitive radio networks. *IEEE Transactions on Wireless Communications*, *8* (12), 5761-5766.

Zhang, R., Lim, T. J., Liang, Y. C., & Zeng, Y. (2010). Multi-antenna based spectrum sensing for cognitive radios: A GLRT approach. *IEEE Transactions on Communications*, *58* (1), 84-88.

Zhang, F., Wang, W., & Zhang, Z. (2011). A primary traffic aware opportunistic spectrum sensing for cognitive radio networks. *IEEE 22nd International Symposium on Personal Indoor and Mobile Radio Communications (PIMRC)*, Toronto, ON, Canada, 700-704.

Zhao, B., Chen, Y., He, C., & Jiang, L. (2012). Performance analysis of spectrum sensing with multiple primary users. *IEEE Transactions on Vehicular Technology*, *61* (2), 914-918.

APPENDIX

DERIVATIONS FOR APPROXIMATE PDFs OF CuS-WED TEST STATISTIC UNDER HYPOTHESES H_0 AND H_1

Under hypothesis H_0, the observed signal vector $\boldsymbol{x}$ contains the noise-only samples. In this case, CuS-WED takes the following form;

$$T(\boldsymbol{x}) = \frac{1}{N}\sum_{n=1}^{N}(N-n+1)w^2(N-n+1) \tag{A.1}$$

where $w(N-n+1) \sim \mathcal{N}(0,\sigma_w^2)$. The mean of CuS-WED under H_0 can be found as

$$E[T(\boldsymbol{x});H_0] = \frac{1}{N}\sum_{n=1}^{N}(N-n+1)E[w^2(N-n+1)]$$

$$= \frac{1}{N}\sigma_w^2\left(N(N+1) - \frac{N(N+1)}{2}\right) = \frac{N+1}{2}\sigma_w^2. \tag{A.2}$$

In Equation (A.2), $E[\cdot]$ denotes the expectation operator.

The variance of CuS-WED under H_0 can be found as

$$\mathrm{var}[T(\boldsymbol{x});H_0] = \frac{1}{N^2}\sum_{n=1}^{N}(N-n+1)^2\,\mathrm{var}[w^2(N-n+1)]$$

$$= \frac{1}{N^2}\left[\sum_{n=1}^{N}(N-n+1)^2\underbrace{\mathrm{var}[w^2(N-n+1)]}_{2\sigma_w^4}\right]$$

$$+2\sum_{\substack{n=1\\n\neq m}}^{N}\sum_{m=1}^{N}(N-n+1)(N-m+1)\underbrace{\mathrm{cov}(w^2(N-n+1),w^2(N-m+1))}_{=0}. \tag{A.3}$$

In Equation (A.3), the term $\operatorname{cov}\left(w^2\left(N-n+1\right), w^2\left(N-m+1\right)\right)$ is equal to zero since $w^2\left(N-n+1\right)$ and $w^2\left(N-m+1\right)$ are uncorrelated for $n \neq m$. Then, the variance can be calculated using the first term in Equation (A.3) as

$$\operatorname{var}\left[\frac{1}{N}\sum_{n=1}^{N}\left(N-n+1\right)w^2\left(N-n+1\right)\right] = \frac{2\sigma_w^4}{N^2}\left(\sum_{n=1}^{N}\left(N+1\right)^2 + n^2 - 2\left(N+1\right)n\right)$$

$$= \frac{\left(N+1\right)\left(2N+1\right)}{3N}\sigma_w^4. \tag{A.4}$$

Thus, by invoking CLT, the PDF of CuS-WED under H_0 can be obtained as

$$T\left(\boldsymbol{x}\right) \sim \mathcal{N}\left(\frac{N+1}{2}\sigma_w^2, \frac{\left(N+1\right)\left(N+1\right)}{3N}\sigma_w^4\right). \tag{A.5}$$

Under hypothesis H_1, CuS-WED takes the following form;

$$T\left(\boldsymbol{x}\right) = \frac{1}{N}\sum_{n=1}^{N}\left(N-n+1\right)\left(s\left(N-n+1\right)+w\left(N-n+1\right)\right)^2 \tag{A.6}$$

where $w\left(N-n+1\right) \sim N\left(0,\sigma_w^2\right)$ and $s\left(N-n+1\right) \sim N\left(0,\sigma_s^2\right)$. The mean of CuS-WED under H_1 can be found as

$$E\left[T\left(\boldsymbol{x}\right);H_1\right] = \frac{1}{N}\sum_{n=1}^{N}\left(N-n+1\right)\underbrace{E\left[\left(s\left(N-n+1\right)+w\left(N-n+1\right)\right)^2\right]}_{\sigma_s^2+\sigma_w^2}$$

$$= \frac{\left(N+1\right)}{2}\left(\sigma_s^2+\sigma_w^2\right). \tag{A.7}$$

To find the variance of CuS-WED under H_1, the following calculation should be performed

$$\mathrm{var}\left[T(\boldsymbol{x});H_1\right]=\mathrm{var}\left[\frac{1}{N}\sum_{n=1}^{N}(N-n+1)\left(\mathrm{s}(N-n+1)+w(N-n+1)\right)^2\right]. \quad \text{(A.8)}$$

First, Equation (A.8) can be written as

$$\mathrm{var}\left[T(\boldsymbol{x});H_1\right]=\frac{1}{N^2}\sum_{n=1}^{N}(N-n+1)^2\underbrace{\mathrm{var}\left[\left(\mathrm{s}(N-n+1)+w(N-n+1)\right)^2\right]}_{2\left(\sigma_s^2+\sigma_w^2\right)}$$

$$+\frac{2}{N^2}\sum_{\substack{n=1\\n\neq m}}^{N}\sum_{m=1}^{N}(N-n+1)(N-m+1)\underbrace{\mathrm{cov}\left(\left(s(N-n+1)+w(N-n+1)\right)^2,\left(s(N-m+1)+w(N-m+1)\right)^2\right)}_{=0}. \quad \text{(A.9)}$$

In Equation (A.9), the PU signal and noise samples are uncorrelated with each other. Moreover, the samples in both the PU signal and noise vector are identically distributed in themselves. Therefore, the covariance term is equal to zero in Equation (A.9) as in Equation (A.3). Accordingly, the variance of the CuS-WED under H_1 can be found as

$$\mathrm{var}\left[T(\boldsymbol{x});H_1\right]=\frac{1}{N^2}\sum_{n=1}^{N}(N-n+1)^2 2\left(\sigma_s^2+\sigma_w^2\right)^2=\frac{(N+1)(2N+1)}{3N}\left(\sigma_s^2+\sigma_w^2\right)^2. \quad \text{(A.10)}$$

Finally, the PDF of CuS-WED under H_1 can be written using Equations (A.7) and (A.8) as

$$T(\boldsymbol{x})\sim\mathcal{N}\left(\frac{N+1}{2}\left(\sigma_s^2+\sigma_w^2\right),\frac{(N+1)(2N+1)}{3N}\left(\sigma_s^2+\sigma_w^2\right)^2\right). \quad \text{(A.11)}$$